



Università degli Studi di Padova

DIPARTIMENTO DI INGEGNERIA INDUSTRIALE

Corso di Laurea Magistrale in Ingegneria dell'Energia Elettrica

TESI DI LAUREA

**ECO-FRIENDLY ALTERNATIVES TO
REPLACE SF₆ IN HIGH VOLTAGE
GAS-INSULATED TRANSMISSION
LINES: A COMPARATIVE STUDY**

Relatori:

Prof. A. Haddad

School of Engineering, Cardiff University

Prof. R. Turri

Dipartimento di Ingegneria Industriale, Università di Padova

Laureando:

Andrea Manganella

Matricola 1197570

A.A. 2019/2020

Abstract

This project focuses on the research of an eco-friendly alternative that could replace SF₆, which is a strong greenhouse gas, in high voltage Gas-Insulated Transmission Lines, reducing the environmental impact but at the same time maintaining the excellent dielectric properties that make GIL the most reliable power transmission line. In order to achieve this goal several gases are considered, including NOVECTM 4710 and 5110, CF₃I, R12, R134, R410A and their mixtures with some buffer gases like dry air, N₂ or CO₂; different working conditions are also studied to find the most suitable for each candidate. This work is conceived as a parametric study, with the aim to compare the most influencing characteristics of each type of gas analyzing their physicochemical, environmental and dielectric properties. In the first case the main parameters are the liquefaction temperature, which is fundamental as the dielectric medium must always remain in the gaseous state to guarantee the insulation, and others that affect the functionality of the structure, such as chemical and thermal stability or flammability; the toxicity is also considered as connected to personnel safety. As regards the environmental impact, global warming potential, ozone depletion potential and atmospheric lifetime are compared. Finally, concerning the dielectric properties, several parameters are analyzed and these are AC, DC, lightning impulse dielectric strength and partial discharge inception voltage. A very simplified GIL design is also reported, resulting in the definition of an optimum combination, for each mixture, of pressure, mixing ratio and geometrical dimensions. This document is based on the use of three softwares: MATLAB for the data reworking and plotting, BOLSIG+, an electron collisions simulator, to obtain and compare the gases ionization coefficients and COMSOL Multiphysics 5.4a, a FEM solver, to simulate the 3D GIL model and determine the electric field distribution along the geometry. Data are obtained by recent scientific papers and partly by the LXCat database, due to the impossibility to perform laboratory experimental tests caused by the limitations linked to the COVID-19 outspread.

Acknowledgements

Firstly, I would like to thank my Italian supervisor Prof. Roberto Turri of University of Padua who allowed me to start this project and has always been available to solve any problem both when I was abroad and during the quarantine in Italy.

Special thanks to my supervisor Prof. Abderrahmane Haddad of Cardiff University who made all possible effort to guarantee me a good thesis work, despite all the obstacles caused by the COVID-19 emergence which forced me to modify the approach from experimental to computational and to interrupt my experience in Cardiff that lasted only a month.

It is always thanks to him that I had the possibility to enter the Cardiff Advanced High Voltage Engineering Research Group, and, although only telematically, getting in touch with very professional people that thought me a lot and whom I also sincerely thank.

Finally I would like to thank my family, my girlfriend and my friends for the constant support they daily show me and which gave me the strength to face up to the disappointment for not having been able to live the experience I have dreamed of for years, and at the same time enthusiasm to reach one of the most important milestones of my life.

Contents

Introduction	1
1 Gas-Insulated Transmission Lines	3
1.1 Benefits	4
1.2 Technology	6
1.2.1 Structure	6
1.2.2 Layout techniques	10
1.3 History	13
1.3.1 First generation	13
1.3.2 Second generation	14
2 Gas insulation overview	16
2.1 Gas discharge theory	16
2.1.1 Space-charge-free discharge	19
2.1.2 Space-charge-dominated discharge	25
2.1.3 Discharges in non-uniform fields	27
2.2 Sulphur hexafluoride (SF ₆)	29
2.2.1 Physicochemical properties	30
2.2.2 Dielectric properties	33
2.2.3 Environmental properties	34
2.3 Alternative gases	36
2.3.1 Natural gases	41
2.3.2 SF ₆ mixtures	42

2.3.3	Perfluorocarbons (PFCs)	46
2.3.4	Tetrafluoropropene (HFO-1234ze)	48
3	Target gases analysis	50
3.1	Perfluoronitrile (C_4F_7N)	50
3.1.1	Physicochemical properties	50
3.1.2	Environmental properties	52
3.1.3	Dielectric properties	53
3.1.4	C_4F_7N mixtures	55
3.2	Perfluoropentanone ($C_5F_{10}O$)	67
3.2.1	Physicochemical properties	67
3.2.2	Environmental properties	70
3.2.3	Dielectric properties	71
3.2.4	$C_5F_{10}O$ mixtures	71
3.3	Trifluoroiodomethane (CF_3I)	79
3.3.1	Physicochemical properties	79
3.3.2	Environmental properties	82
3.3.3	Dielectric properties	83
3.3.4	CF_3I mixtures	83
3.4	R12 (CCl_2F_2)	96
3.4.1	Physicochemical properties	96
3.4.2	Environmental properties	98
3.4.3	Dielectric properties	98
3.4.4	R12 mixtures	99
3.5	R134a ($C_2H_2F_4$)	107
3.5.1	Physicochemical properties	107
3.5.2	Environmental properties	109
3.5.3	Dielectric properties	110
3.5.4	R134a mixtures	110
3.6	R410A (50% CH_2F_2 / 50% C_2HF_5)	117
3.6.1	Physicochemical properties	117

3.6.2	Environmental properties	119
3.6.3	Dielectric properties	119
3.6.4	R410A mixtures	120
4	Gas-Insulated Line design	128
4.1	Insulating mixture choice	128
4.1.1	Environmental impact	128
4.1.2	Liquefaction temperature	131
4.1.3	Insulation properties	133
4.1.4	The best compromise	140
4.2	GIL dimensioning	141
	Conclusions	148
	Bibliography	151

List of Figures

1.1	GIL straight section module	7
2.1	Example of a V - I gas discharge characteristic	17
2.2	Different types of gas discharges	19
2.3	Ionization, attachment and effective ionization reduced coefficients . .	23
2.4	Representation of electron ionizing collisions	24
2.5	Paschen's law representation as analytical and real curve	25
2.6	A physical model describing the streamer discharge	26
2.7	Dependence of pre-discharges and breakdown on field efficiency factor	28
2.8	SF ₆ molecular structure	30
2.9	SF ₆ decomposition byproducts toxicity	33
2.10	Normalized properties of N ₂ / SF ₆ gas mixtures	45
3.1	Molecular structure of perfluoroketone C ₄ F ₇ N	50
3.2	AC breakdown voltage of C ₄ F ₇ N and SF ₆ with different field utilization factors	53
3.3	Positive lightning impulse breakdown voltage of C ₄ F ₇ N and SF ₆ with different field utilization factors	54
3.4	GWP (ITH = 100) of C ₄ F ₇ N / CO ₂ mixture	56
3.5	AC dielectric strength of C ₄ F ₇ N / CO ₂ mixture	57
3.6	AC breakdown voltage of C ₄ F ₇ N / CO ₂ mixture compared to SF ₆ . .	58
3.7	Liquefaction temperature of C ₄ F ₇ N / CO ₂ mixture	59

3.8	Lightning impulse breakdown voltage of 3.7% C ₄ F ₇ N / 96.3% CO ₂ mixture compared to SF ₆	60
3.9	Partial discharge inception voltage of 3.7% C ₄ F ₇ N / 96.3% CO ₂ mixture compared to SF ₆	61
3.10	GWP (ITH = 100) of C ₄ F ₇ N / N ₂ mixture	62
3.11	AC dielectric strength of C ₄ F ₇ N / N ₂ mixture	63
3.12	Liquefaction temperature of C ₄ F ₇ N / N ₂ mixture	64
3.13	PDIV+ of C ₄ F ₇ N / N ₂ mixture in relation to SF ₆	65
3.14	PDIV- of C ₄ F ₇ N / N ₂ mixture in relation to SF ₆	66
3.15	Molecular structure of perfluoropentanone C ₅ F ₁₀ O	67
3.16	Saturated vapor pressure of C ₅ F ₁₀ O and SF ₆	69
3.17	Liquefaction temperature at 0.1 MPa of perfluoroketones	69
3.18	GWP (ITH = 100) of C ₅ F ₁₀ O / air mixture	72
3.19	AC dielectric strength of C ₅ F ₁₀ O / air mixture compared to SF ₆ and pure air	73
3.20	AC dielectric strength of C ₅ F ₁₀ O / N ₂ mixture compared to SF ₆ and pure N ₂	75
3.21	Lightning impulse and AC dielectric strength of C ₅ F ₁₀ O / CO ₂ / O ₂ mixture and SF ₆ under uniform electric field	76
3.22	Lightning impulse and AC breakdown voltage of C ₅ F ₁₀ O / CO ₂ / O ₂ mixture and SF ₆ under particle-like field	77
3.23	AC dielectric strength of C ₅ F ₁₀ O / N ₂ / O ₂ mixture in dependence on oxygen concentration	78
3.24	Molecular structure of trifluoroiodomethane CF ₃ I	79
3.25	CF ₃ I and SF ₆ saturated vapor pressure	81
3.26	Saturated vapor pressure of CF ₃ I and SF ₆	84
3.27	Effective ionization coefficients of CF ₃ I mixtures compared to pure gases	85
3.28	AC dielectric strength of 30% CF ₃ I / 70% CO ₂ mixture in comparison with 20% SF ₆ / 80% N ₂ mixture	86

3.29	U_{50} of a 30% CF_3I / 70% CO_2 mixture in a rod-plane electrode configuration under lightning impulses and field utilization factor	86
3.30	A rod-plane electrode configuration	87
3.31	E_{max} of a 30% CF_3I / 70% CO_2 mixture in a rod-plane electrode configuration under lightning impulses	88
3.32	A plane-plane electrode configuration	89
3.33	U_{50} of a 30% CF_3I / 70% CO_2 mixture in a plane-plane electrode configuration under lightning impulses and field utilization factor	89
3.34	E_{max} of a 30% CF_3I / 70% CO_2 mixture in a plane-plane electrode configuration under lightning impulses	90
3.35	U_{50} and E_{max} of a 30% CF_3I / 70% CO_2 mixture in a coaxial cylindrical electrodes configuration under positive lightning impulses	91
3.36	GWP (ITH = 100) of CF_3I / N_2 mixture	92
3.37	Net ionization coefficients of CF_3I / N_2 mixtures in comparison with SF_6 , pure CF_3I and air	93
3.38	AC dielectric strength of 30% CF_3I / 70% N_2 mixture in comparison with 20% SF_6 / 80% N_2 mixture	94
3.39	Lightning impulse breakdown voltage of CF_3I / N_2 mixtures	94
3.40	Maximum normalized dielectric strength of CF_3I / N_2 mixtures	95
3.41	Molecular structure of dichlorodifluoromethane CCl_2F_2	96
3.42	Liquefaction temperatures of SF_6 , R12 and N_2 / air in dependence on pressure	97
3.43	Dielectric strength of R12 compared with that of SF_6	99
3.44	Liquefaction temperatures of R12 / N_2 or air mixture in dependence on mixing ratio	100
3.45	AC dielectric strength of R12 / air mixture in dependence on pressure and mixing ratio	102
3.46	Paschen's curve of R12 / air mixture	103
3.47	DC dielectric strength of R12 / air mixture in dependence on pressure and mixing ratio	103

3.48	Positive impulse dielectric strength of R12 / air mixture in dependence on pressure and mixing ratio	104
3.49	AC dielectric strength of R12 / N ₂ mixture in dependence on pressure and mixing ratio	106
3.50	Paschen's curve of R12 / N ₂ mixture	106
3.51	Molecular structure of tetrafluoroethane C ₂ H ₂ F ₄	108
3.52	Liquefaction temperature of SF ₆ , R134a and N ₂ / air in dependence on pressure	109
3.53	Dielectric strength of R134a compared to that of SF ₆	110
3.54	Liquefaction temperature of R134a / N ₂ or air mixture in dependence on mixing ratio	111
3.55	AC dielectric strength of R134a / air mixture in dependence on pressure and mixing ratio	112
3.56	Paschen's curve of R134a / air mixture	113
3.57	AC dielectric strength of R134a / N ₂ mixture in dependence on pressure and mixing ratio	115
3.58	Paschen's curve of R134a / N ₂ mixture	116
3.59	Molecular structure of difluoromethane CH ₂ F ₂ and pentafluoroethane C ₂ HF ₅	117
3.60	Liquefaction temperatures of SF ₆ , R410A and CO ₂ in dependence on pressure	118
3.61	Dielectric strength of R410A compared to that of SF ₆	120
3.62	Liquefaction temperatures of R410A / CO ₂ mixture in dependence on mixing ratio	121
3.63	AC dielectric strength of R410A / air mixture in dependence on pressure and mixing ratio	122
3.64	DC dielectric strength of R410A / air mixture in dependence on pressure and mixing ratio	123
3.65	Paschen's curve of R410A / air mixture	124

3.66	AC dielectric strength of R410A / CO ₂ mixture in dependence on pressure and mixing ratio	126
3.67	DC dielectric strength of R410A / CO ₂ mixture in dependence on pressure and mixing ratio	126
3.68	Paschen's curve of R410A / CO ₂ mixture	127
4.1	SF ₆ mixtures GWP compared to that of alternative mixtures	129
4.2	Alternative mixtures GWP in dependence on mixing ratio	129
4.3	A detail of the figure 4.2	130
4.4	Atmospheric lifetime of some pure alternative gases	131
4.5	Liquefaction temperature of some pure alternative gases in dependence on pressure	132
4.6	Liquefaction temperature of C ₄ F ₇ N / CO ₂ mixtures in dependence on pressure	133
4.7	Intrinsic dielectric strength of some pure gases	134
4.8	Reduced Townsend coefficient of some pure gases	135
4.9	Rate coefficient of some C ₄ F ₇ N / CO ₂ mixtures	135
4.10	Rate coefficient of some C ₄ F ₇ N / N ₂ mixtures	136
4.11	Rate coefficient of some C ₅ F ₁₀ O / CO ₂ mixtures	137
4.12	Rate coefficient of some C ₅ F ₁₀ O / N ₂ mixtures	137
4.13	Comparison between the rate coefficients of some NOVEC 4710 and 5110 mixtures	138
4.14	Rate coefficient of some C ₄ and C ₅ mixtures also including O ₂	138
4.15	Reduced Townsend coefficient of C ₅ / air mixtures compared to 20% SF ₆ / 80% N ₂ mixture	139
4.16	GIL 3D model representation	144
4.17	GIL 3D model mesh	145
4.18	Elbow's area electric field distribution	146

List of Tables

2.1	Physicochemical properties of SF ₆	31
2.2	Environmental properties of SF ₆	35
3.1	Physicochemical properties of C ₄ F ₇ N	51
3.2	Toxicity of C ₄ F ₇ N	52
3.3	Environmental properties of C ₄ F ₇ N	52
3.4	Physicochemical properties of C ₅ F ₁₀ O	68
3.5	Toxicity of C ₅ F ₁₀ O	70
3.6	Environmental properties of C ₅ F ₁₀ O	70
3.7	Physicochemical properties of CF ₃ I	80
3.8	Environmental properties of CF ₃ I	82
3.9	Physicochemical properties of R12	97
3.10	Environmental properties of R12	98
3.11	Synergistic effect of R12 / air mixture	105
3.12	Synergistic effect of R12 / N ₂ mixture	107
3.13	Physicochemical properties of R134a	108
3.14	Environmental properties of R134a	109
3.15	Synergistic effect of R134a / air mixture	114
3.16	Synergistic effect of R134a / N ₂ mixture	116
3.17	Physicochemical properties of R410	118
3.18	Environmental properties of R410A	119
3.19	Synergistic effect of R410A / air mixture	124
3.20	Synergistic effect of R410A / CO ₂ mixture	127

4.1	ODP of some pure alternative gases	130
4.2	GIL voltage levels (kV)	142
4.3	Technical parameters of 420 kV and 550kV gas insulated lines	143

Introduction

Governments worldwide, in response to the Kyoto Protocol on climate change, have set ambitious targets to reduce greenhouse gas emissions.

In high-voltage equipment, such as Gas-Insulated Transmission Lines, sulphur hexafluoride (SF_6) is the most commonly used dielectric gas medium thanks to the fact that it is chemically stable and has a dielectric strength three times that of air at atmospheric pressure.

SF_6 , however, is one of the six restricted greenhouse gases identified by the Kyoto Protocol as its global warming potential (GWP) for a given time horizon of 100 years is 23500 times the one of CO_2 .

Identifying alternatives to SF_6 for application in high-voltage gas-insulated equipment remains a big problem for researchers.

Most of the gases considered until now exhibit a higher dielectric strength than SF_6 but possess at least one negative characteristic, such as a high GWP, a high liquefaction temperature, harmful byproducts or voltage-withstand limitations.

This project has the goal to compare and analyze some new gases, including perfluoronitrile $\text{C}_4\text{F}_7\text{N}$, perfluoropentanone $\text{C}_5\text{F}_{10}\text{O}$, trifluoroiodomethane CF_3I , dichlorodifluoromethane CCl_2F_2 (R12), tetrafluoroethane $\text{C}_2\text{H}_2\text{F}_4$ (R134a) and a mixture of 50% CH_2F_2 / 50% C_2HF_5 (R410A), which could be attractive eco-friendly alternatives to SF_6 .

All these emerging candidates present great physicochemical properties, an high dielectric strength and a low GWP.

In some cases however some limitations, like an high boiling point, are shown and therefore these gases have to be used in low proportions as part of a binary mixture

with CO₂, N₂ or other buffer gases in order to reduce the overall liquefaction temperature.

These considerations are collocated in a scenario characterized by the increase of power demand in large metropolitan areas, combined with the fact that new exploitable energy sources are often situated far from load centres, which has led to the need for new high capacity transmission systems.

The construction of new overhead lines (OHLs) introduces challenges in terms of routing and public acceptance: there is, therefore, an interest in developing an affordable alternative transmission technology that has less visual impact while being more eco-friendly.

The distance over which power may be transferred using traditional AC cables is limited, since there is a need to supply large capacitive charging currents.

In addition, there is an environmental cost for the materials used to construct cables. GILs, in comparison, have a much lower capacity and the ability to transfer large amounts of power over longer distances than with AC cables.

The solutions proposed in this work appear to be very attractive options that can be implemented as a replacement of SF₆ in GILs, solving the environmental impact problem, yet maintaining at the same time all the great properties of sulphur hexafluoride.

An exceptional potential for a new form of environmentally friendly power transmission system is highlighted.

Chapter 1

Gas-Insulated Transmission Lines

The impact of global warming affects the structure of electric power generation.

This appears clear considering that regenerative energy sources like onshore and offshore wind, solar thermal, photovoltaic, biomass, hydropower, geothermal and sea-based power generation are becoming increasingly diffused in the current power network.

Generation locations are usually far away from the load centres, therefore they need to be connected through the electric power grid: that is why a so called smart grid, able to control the power flow, becomes necessary.

Smart energy consumption based on prices traded on the electricity market and variable flows caused by the availability of regenerative power sources need a power flow control and a long distance power transmission, always taking into account the fundamental role of energy storage in a scenario in which the fluctuating regenerative energy has to be used efficiently.

Most of these long distance power transmission lines consist of overhead lines which guarantee high reliability, high efficiency and several possible rated voltage levels.

However, such large overhead lines can't be built everywhere and underground solutions for at least some sections of the transmission line are necessary.

The need for high-power transmission and the possibility of combining overhead transmission lines with underground solutions make GIL a good candidate for an overall or at least a partial solution.

When overhead lines are not suitable, GIL offers an interesting alternative being able to go underground with the same amount of energy that an overhead line can transmit, for example 2000 MVA of transmitted power at 400 kV [1].

1.1 Benefits

A Gas-Insulated Transmission Line presents several benefits in comparison with other power transmission lines like overhead lines or cables, which justify its increasing diffusion.

A brief description of the most important of them is given [1, 5].

POWER RATING LIKE AN OVERHEAD LINE

A GIL is characterized by an high power transmission capability which allows to go underground in series with an overhead line without any power reduction, moreover the use of protection and control systems is possible as with an OHL.

GIL has a low capacity therefore the inrush current is low; in addition, if a GIL is combined with an OHL no differential protection is necessary for failure location.

LOW TRANSMISSION LOSSES

The large cross-section of the conductor and the enclosure pipe determines low resistive losses (typical GIL resistances are 6-8 m Ω /km depending on the outer diameter and the wall thickness of the enclosure and the conductor pipe).

The effect of low transmission losses is high when the current rating is high (3000 A for a GIL), as shown by the relation

$$P_{TL} = I^2 \cdot R$$

where P_{TL} are the transmission losses, I is the current rating and R is the overall resistance.

Losses through the insulating gas are negligible.

LOW CAPACITIVE LOAD

The capacity of a GIL is low, typically of $55 \mu\text{F}/\text{km}$, thus electric phase-angle compensation is needed only at very long lengths and compensation coils are not necessary for transmission lines up to 100 km.

As a result thermal operation losses are also reduced.

HIGH RELIABILITY

A GIL can be seen as a passive high-voltage gas-insulated system with no active parts and this is due to the fact that the only purpose of GILs is the electric power transmission therefore no internal switching or breaking capability is needed.

GIL is, moreover, the most reliable power transmission system known considering that no major failure (arc fault) has been reported so far.

HIGH LEVEL OF PERSONNEL SAFETY

Personnel safety is always guaranteed by the fact that the outer enclosure pipe is solid grounded and no access to high-voltage parts is possible (thanks to the gas-tight enclosure).

In addition, it has been demonstrated that no external impact can occur on the surroundings not even in case of short-circuit GIL operation, internal failure or arc between the enclosure and the conductor pipe.

NO ELECTRIC AGEING

Gas insulation doesn't age thanks to the fact that the electric field strength of the insulators and the maximum GIL temperature are too low to start the process of electrical ageing.

NO THERMAL AGEING

No practical system thermal ageing can be expected because in all cases the maximum allowed conductor temperature of 100 to 120 °C is not reached by far and a GIL is designed for maximum operational temperatures given by the surrounding conditions (maximum 60 or 70 °C of touching temperature in a tunnel, 40 or 50 °C if directly buried).

OPERATION LIKE AN OVERHEAD LINE

Like OHLs, also GILs are operated with the so called autoreclosure function which means that in case of a ground fault detected on the line, the circuit breaker automatically breaks the line, waits some seconds depending on the network condition and switches on again: often the reason for the fault current detection is gone and the transmission line goes back to the normal operation.

ELECTROMAGNETIC FIELDS

GILs are operated as solid grounded installations, the inductive loop is closed through the ground connection and the coupling factor is about 95%, meaning that the superposition of the two reverse currents reduces the outside magnetic field by 95% and only 5% of the magnetic field of the conductor current is effective outside the GIL.

The current in the conductor induces, due to the induction law, a current into the external enclosure of the same size and with 180° phase shift thus the superposition of both electromagnetic fields is close to zero.

In case of magnetic field limitations in the surroundings, a GIL can fulfill even very low magnetic field requirements (within a few metres of distance a magnetic field strength of 1 μT , as required in some countries, can be reached with a current rating of 3000 A).

1.2 Technology

1.2.1 Structure

The fundamental structure of a Gas-Insulated Transmission Line is characterized by a coaxial configuration consisting of an aluminum conductor pipe at high voltage placed inside an other earthed aluminum enclosure pipe, with the insulation achieved by means of pressurized gas and solid support insulators which also guarantee the internal conductor position maintenance.

Thermal expansion is also considered by adopting sliding contacts since a bending

radius up to 400 m allows the adaption to bends (not excessive) along the route. Angle units are used in order to change direction (with variations from 4° to 90°) and disconnecting units are adopted to separate gas compartments and connect monitoring or testing equipment for the GIL commissioning.

A more detailed description of each part is then reported and the figure 1.1 gives an illustration of them [1, 5].

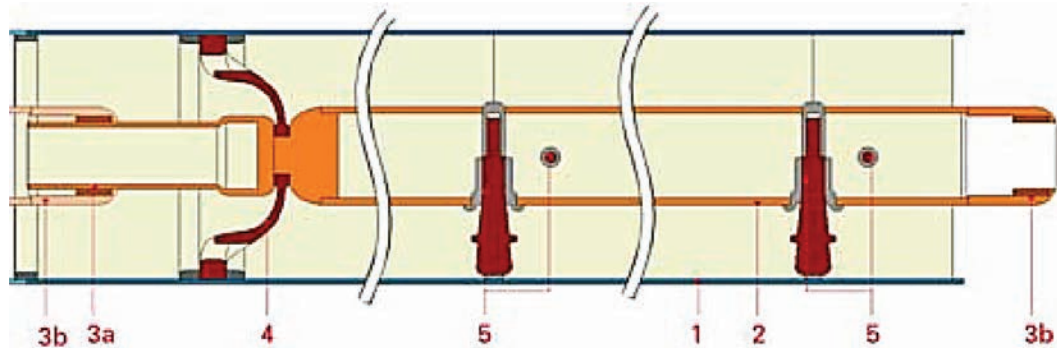


Figure 1.1: GIL straight section module [3]

1- Enclosure; 2- Inner conductor; 3a- Male sliding contact; 3b- Female sliding contacts; 4- Conical insulator; 5- Support insulators

INNER CONDUCTOR

The inner conductor is made of aluminum with high conductivity in order to minimize the electric transmission losses and is characterized by a tubular shape to exploit the skin effect.

Particular attention is given to the surface roughness that can be at most $10\text{-}20\ \mu\text{m}$.

GAS-TIGHT ENCLOSURE

The gas-tight enclosure is the most important part of the structure, mainly for two reasons.

Firstly, there must be no loss of gas in the system because it is necessary to keep the insulation and to guarantee the GIL operation.

Secondly, without gas losses there is also no impact on the environment and, if nothing comes out, nothing can go in.

Besides dust and all kinds of particles, the low level of moisture is important for the high-voltage insulation.

Insulating gases need dew points of $-20\text{ }^{\circ}\text{C}$ and below at atmospheric pressure, in fact a dew point of $-20\text{ }^{\circ}\text{C}$ makes the insulating gas very dry thus moisture would manage to enter the gas compartment even if there is an overpressure in the GIL.

Moisture in the gas would decrease the insulation capability and an internal discharge would be the consequence.

Therefore, high gas-tightness is required over the 50-year expected lifetime and is reached with O-ring sealings and welded joints.

On-site welding is tested by ultrasonic weld control, which proves the gas-tightness and automated orbital-welding machines produce multilevel welds to joint the enclosure pipes.

Depending on the wall thickness, 5 to 10 layers of welds form the joint and avoid voids in the aluminum which could cause gas leakage.

The enclosure material is sheet or extruded aluminum, both gas-tight thanks to their molecular structure and aluminum alloys are used in order to increase the mechanical stability.

The sheet aluminum is produced by milling under high pressure from high material thickness to sheet strengths of typically 5-10 mm, forming an homogeneous and gas-tight structure.

Sheet aluminum is formed into pipes by milling and plates or coils are connected by longitudinal welding or by spiral welding.

The extruded pipes are pressured from a block of aluminum through a pressure tool into a seamless pipe.

The material structure is longitudinal and homogeneous and delivers gas-tight pipes.

INSULATORS

The conductor needs to be held in the centre of the enclosure so that the electric field distributes equally in the concentric pipe system: this is one of the insulators functions.

These are typically made of epoxy resins with filler material, of which two types are

used today: silicium (fine sand) and aluminum oxide (AlO_3).

Both have the task of giving the insulator the necessary mechanical strength when moulded with epoxy resin.

Several formulas for epoxy resin are used today in high voltage gas-insulated equipment and the requirements come from features such as mechanical strength, maximum allowed temperature, electric insulation behavior, surface discharge sensitivity and surface tracking withstandability.

For applications in GIL, the maximum temperature and the discharge tracking withstandability are the main features, where mechanical strength and electric insulation are of minor importance.

The electrical insulation capability of dielectric material is not fully used because the dimensioning (enclosure diameter) is given by the free gas space design of the insulating gas.

The insulating capability of epoxy resin used in a GIL is in the range of $\epsilon_r = 3 - 5$ compared to gases.

This means that the insulator is operated 3 - 5 times below its physical insulation capability which is a high safety margin.

This GIL design feature is an other reason for the high reliability in operation.

Today, three types of insulator are in use:

- POST-TYPE INSULATOR

It can be with one, two or three legs and holds the conductor in the centre of the enclosure;

- CONICAL INSULATOR

It is concentric around the conductor, has holes and fixes the conductor towards the enclosure;

- GAS-TIGHT CONICAL INSULATOR

It is concentric around the conductor and the enclosure but doesn't own holes in order to separate gas compartments and to fix the conductor towards the enclosure.

SLIDING CONTACTS

Sliding contacts, which can be of male or female type, are fundamental to compensate the conductor thermal expansion.

They consist of a sort of plug which a multi-contact system can slide on, guaranteeing high system reliability.

As regards the GIL overall structure, a further distinction between different units can be made:

- **STRAIGHT UNIT**

This unit has a length up to 120 m, it can be bended up to a radius of 400 m and it is composed of small units 12 - 18 m long;

- **ANGLE UNIT**

This unit can face up to angles from 4° to 90° and is used when the elastic bending radius of the straight unit is not enough;

- **DISCONNECTING UNIT**

This unit has the function to create independent gas compartments when it is necessary and it is installed every 1000 or 1500 m;

- **COMPENSATOR UNIT**

This unit is adopted to compensate the structure movement due to thermal expansion and it can manage around 400 m of enclosure pipe.

1.2.2 Layout techniques

The application which a GIL is adopted for directly affects the installation methods. The most common solutions are reported [1].

DIRECTLY BURIED INSTALLATION

This is the fastest and most economical method, very attractive for an use in substations or to connect different countries.

GIL takes the form of an electrical pipeline with a laying technique very similar to that used for gas or oil, thus representing a reliable option for long distance transmission. Installation is achieved in a very simple way, with GIL that lays into a trench and the welding process which is performed in a welding tent, with 1 metre (as minimum) of soil used to cover the structure, allowing the agriculture of the above area.

Soil has fundamental functions of maintaining GIL in a fixed position and compensating the thermal expansion, reducing installation time and costs; on the other hand, this direct contact makes a corrosion protection necessary.

There are two different corrosion protection methods:

- **PASSIVE CORROSION PROTECTION**

A layer of polymeric coating (polyethylene or polypropylene) and an anti-corrosion layer avoid any contact between the aluminum enclosure and oxygen.

- **ACTIVE CORROSION PROTECTION**

A sacrificial electrode provides an alternative path which the current can follow and corrode instead of the aluminum enclosure.

External magnetic fields are also marginal in this configuration.

ABOVE GROUND INSTALLATION

This is a trouble-free and very diffused option considering that it also works in extreme environmental conditions since a GIL is not affected by high ambient temperatures, intense solar radiation, dust, pollution, sand or moisture.

This method is often adopted, by using steel structures (typically with an height of 5-8 metres) in power plants or inside substations to connect different parts avoiding a lot of crossed overhead lines and allowing to have some exploitable space below.

A corrosion protection is optional thanks to the thin oxide layer which forms under atmospheric conditions.

TRENCH INSTALLATION

This is a trade-off, as regards the expansion, between the above ground and the tunnel solution and it is frequently adopted in substations and power plants for practical

reasons.

The trench is made of concrete and is covered by a block of the same material.

The corrosion protection is optional in this case also thanks to the oxide film on the aluminum pipe but a drainage system is necessary in order to maintain the GIL dry.

TUNNEL INSTALLATION

This method, very diffused in hydropower plants, adopts prefabricated elements and allows to obtain an high power transmission without being visible from the outside, with overall costs dependent on cases (water tight, deep underground and others).

In this way the influence on the land near the tunnel is negligible and agriculture of the soil above is not affected; moreover, the system is easily accessible for inspections.

Natural ventilation is used to dissipate the heat produced by the current flowing into the conductor but in some situation a forced ventilation could be required.

In this case a corrosion protection is again not required but any contact of GIL with water must be avoided.

Tunnel installations can be of two types:

- OPEN TRENCH-LAID TUNNEL

This is a trench dug with concrete tunnel segments placed inside it, normally covered with 1 or 2 meters of soil.

Such tunnels can be built in densely populated areas under or beside streets and highways;

- BORED TUNNEL

This is a structure characterized by a minimum depth of three times its diameter, typically of 3-4 metres depending on space requirements, reaching also 30 metres under cities; in this case inspections are favored by the fact that GILs are fixed to the tunnel walls.

VERTICAL INSTALLATION

This solution is really suitable for cavern hydropower plants applications where a lot of energy has to be transmitted from the underground to the surface, thanks to the fact that gas-insulated tubular conductors can be installed at any gradient.

SHARED STRUCTURE

This is an option characterized by sharing of structures like bridges or tunnels between GIL and a railway, a motorway or other pipelines, resulting in an higher structure efficiency, a reduction of the overall costs and less territory disfigurement.

The GIL shielding effect determines a very high electromagnetic compatibility, in particular in comparison with cables and overhead lines; moreover, a Gas-Insulated Transmission Line presents no risks in case of failure, an high reliability and an insulating medium which doesn't age resulting in the perfect suitability for sharing a structure.

1.3 History

The gas insulation technology was designed in 1920s and its exceptional electrical properties led to the development of high-voltage and high-current rating systems.

The history of Gas-Insulated Transmission Lines can be divided in two phases regarding respectively the first and the second GIL generation, mainly on the basis of the development of the gas insulation medium [1].

1.3.1 First generation

The first generation of GILs is characterized by the use of pure SF₆ as insulation medium without the possibility of bending aluminum pipes.

First high-voltage experimental tests started in 1960s and were carried out using pure SF₆ in a closed compartment, under both DC and AC voltages.

The great results obtained with AC voltage especially regarding the electrical stability led to a focalization on the AC case.

In 1968, the first complete SF₆ system was introduced including a bus bar, a switch-gear circuit breaker and a ground switch leading to the development of a very attractive electrical system (GIS).

Meanwhile an important role was played by the development of other technology for jointing, monitoring, and installing GILs.

Many names were created, each linked to a different design: gas-insulated bus duct, compressed gas-insulated bus duct, bus bar, gas-insulated transmission line (GITL) or gas-insulated line (GIL).

In 1998, the international standardization organization (IEC-61640) introduced the name *Gas-Insulated Transmission Line* which can be compressed into the universally adopted abbreviation *GIL*.

In 1974, the first application of a first generation GIL were built at the cavern hydropower plant of Schluchseewerke in the Black Forest in Germany at a voltage level of 400 kV, being in a full operation for about 40 years, which proved the high reliability of GIL technology as a power transmission system.

This first case demonstrated GIL reliability for a long time without any sign of aging. In addition it has been shown that no gas leakage is detected when pipe joints are welded and that usually GIL gas-tightness doesn't require any gas refill during the 40 years of operation, a consequence of the high reliability of GIL on-set welding technology.

Although the GIL first generation showed very high reliability and high transmission capability, it was not widely used due to the environmental and economical drawbacks connected to the use of pure SF₆.

1.3.2 Second generation

GILs of second generation are filled with a gas insulating mixture of 20% SF₆ and 80% N₂ with the possibility of being welded or flanged and an elastic bending which can reach a radius of 400 m.

Since 1970s, many research studies have been carried out to find a gas to replace SF₆. Some gases with higher insulation capabilities than SF₆ were found but unfortunately all of them were more critical in terms of toxicity or greenhouse effect.

Therefore an attractive alternative to SF₆ wasn't found, however research showed that mixing SF₆ with other gases and reducing its content percentage good insulation properties can be achieved.

It was found that N₂ is able to form a great insulating gas in combination with SF₆ as

it can be seen from the fact that with an SF₆ content of less than 20%, an insulating capability of 70-80% the one of pure SF₆ is achieved at the same gas pressure.

In 1994, EDF carried out a feasibility study to develop a technical solution for a GIL future generation, specifying some technical data as a target for the new GIL design. Three GIL design groups (ABB, Alstom, Siemens) worked on the development of the second generation of GIL, focusing on two basic designs: the three-phase and the single-phase insulation design.

The three-phase insulation design was based on three aluminum conductors placed inside an enclosure of steel with an aluminum inlay acting as a high-pressure vessel.

The enclosure made of steel was a consequence of the need to withstand the required 1.5-2.0 MPa gas pressure; the diameter of the three-phase design was about 1.5 m.

The single-phase design was based on one aluminum conductor in one aluminum enclosure, with a gas pressure of 0.8 MPa and a diameter of 0.5 m.

The insulation gas for both designs was a mixture of 80-98% of N₂ and 20-2% of SF₆ depending on gas pressure and the dimensions of conductor and enclosure.

After many additional studies on different aspects it has been concluded that, at least from a technical point of view, both designs were possible.

The single phase GIL design required more space for laying but jointing and laying process were simpler than those of the three-phase design: that is the reason why the single-phase design was chosen for the second stage of investigation.

In this phase two prototypes of GIL were built to simulate the lifetime of the equipment of a directly buried 100 metres long GIL system.

The first one was built at the EDF test field in France according to the ABB design since the other one was built at the IPH test field in Germany according to the Siemens design.

The first application of a second generation GIL was built in 2001 in Palexpo Geneva, Switzerland, laid in an underground tunnel, with a gas mixture of 20% SF₆ / 80% N₂, at 0.7 MPa and with a length of 420 metres; it has been in operation since 2001. Results demonstrated excellent power transmission capability and reliability, with minimum negative impact.

Chapter 2

Gas insulation overview

2.1 Gas discharge theory

Generally gases are exceptional insulating mediums at low fields in comparison with other dielectric types thanks to their low conductivity, low losses and nearly constant relative permittivity $\epsilon \approx 1$ with frequency variation.

However, gases usually have a much lower dielectric strength than liquids and solids and under some typical stress conditions voltage and current can result linked by a non-linear relationship, determining a specific gas discharge mechanism.

A first distinction in gas discharges can be done between *non-self-sustaining* and *self-sustaining* discharges.

The first one occurs when, typically at low electric field strengths, electron generation due to photoionization or thermal ionization and recombination due to the attachment of electrons to molecules are nearly in equilibrium: in this case the current flowing through the dielectric is negligible and there's not a generation of additional charge carriers.

The second one appears at higher electric field strengths when all generated electrons are extracted by the electric field before they recombine, reaching the saturation current density (very small value, $\approx 10^{-18}$ A/cm²): by further rising up the voltage, electrons are accelerated by the electric field and, gaining kinetic energy, become able to generate other charge carriers by ionization collisions.

A central parameter to be considered in gas discharges is the electric field uniformity. In a uniform field, when the so called *ignition voltage* is reached the current increases suddenly due to the additional charge carriers generated by ionization resulting in a voltage breakdown: in this case the breakdown voltage is equal to the ignition voltage. In a non-uniform field, when the ignition voltage is reached some stable pre-discharges or partial discharges, known as *glow* or *corona discharges*, appear without the voltage breakdown: in this case the partial discharges inception voltage is equal to the ignition voltage.

If the electric field strength in a uniform field is not influenced by the generated space charges, typical at the beginning of the discharge, it's the case of a *space-charge-free discharge*, known also as a *Townsend discharge*.

When the electric field is instead strongly distorted by the generated space charges, generally due to a strong increase of the current, the phenomenon is named *space-charge-dominated discharge* or *glow/corona discharge* because of the visible light emitted in this process.

A third situation can occur at very high currents, when the space charges are generated by thermal ionization resulting in a very conductive gas plasma: this case is known as *arc discharge*.

In the figure 2.1 an example of a gas discharge characteristic is shown.

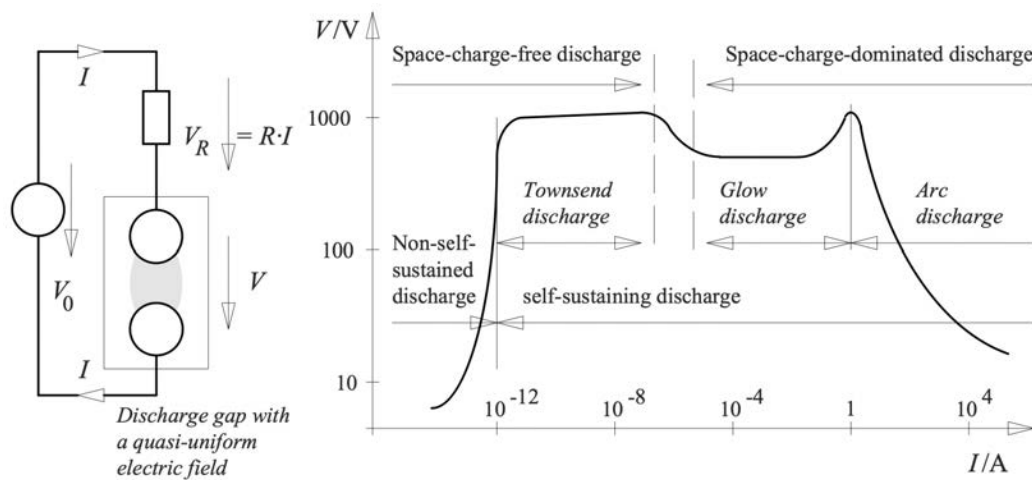


Figure 2.1: Example of a V - I gas discharge characteristic [4]

A logarithmic scale is adopted due to the huge range of possible voltage and current values.

Shortly, gas discharges can be of two types: *breakdowns* or *flashovers* if they cause a conductive channel which goes across the whole insulation gap, *partial discharges* if they don't determine the direct breakdown of the insulation.

In uniform or weakly non-uniform fields partial discharges are not possible, with the exception of stable glow discharges in case of an high series resistance limiting the discharge current; the voltage breakdown occurs suddenly at the ignition voltage achievement.

Regarding the arc discharges, they are characterized by high current, low voltage, stationary thermal equilibrium and a source of constant power; when the source has a limited energy it's the case of the *spark discharge*, associated to a transient current impulse.

In strongly non-uniform fields the gas discharges occur, verifying the ignition condition, firstly in a small and highly stressed gas volume, in particular near to the curved electrode contour, not propagating across the entire insulating gas as in the uniform field case.

The process can start for example with a corona discharge around a tip: the initial glow discharge turns, with the voltage rise, to streamers and leaders, finally resulting in the whole insulation breakdown thanks to an arc or spark discharge.

Partial discharges can appear also in the interfaces between the gas and the solid insulation (*surface* or *creeping discharges*) or in gas-filled cavities in solid and liquid insulating mediums (*internal partial discharges*).

A summary of all the possible gas discharge manifestations is reported in the figure 2.2.

A focus on space-charge-free discharge theory, in particular on Townsend discharge mechanism and Paschen's law, is reported in order to fully understand the concepts which this document is based on.

Informations about space-charge dominated discharge theory and discharges in non-uniform fields are also given in order to comprehend the computational results which,

referring to a Gas-Insulated Transmission Line model, are related to a non-uniform field [4].

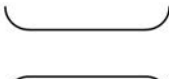

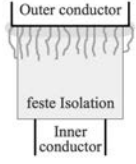
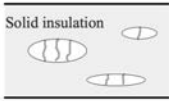
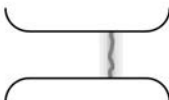
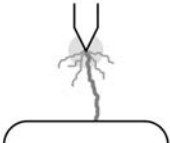
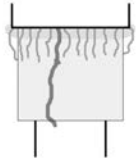

	Uniform and weakly non-uniform fields	Non-uniform fields	Interfaces	Voids
<p>Pre-discharges <i>(partial discharges)</i></p> <p>Discharges that do not cause a direct breakdown of the voltage.</p>	 <p><i>do not occur, discharge inception directly results in breakdown</i></p>	 <p>Corona discharges</p> <p>External partial discharges (PD) Glow discharges Streamer and leader discharges</p>	 <p>Surface discharges Creeping discharge</p>	 <p>Cavity discharge</p> <p>Internal PD ("Glow")</p>
<p>Breakdown, flashover</p> <p>Discharges that cause a very conductive channel between the electrodes resulting in a direct breakdown of the voltage.</p>	 <p>Breakdown</p> <p><i>Lightning discharges</i> <i>(very long sparks during atmospheric disch.)</i></p>	 <p>Breakdown</p> <p><i>Electric arc, arc discharge (in the case of a thermal equilibrium)</i> <i>Spark (in the case of a limited energy content of the source)</i></p>	 <p>Flashover</p> <p><i>Creeping spark</i></p>	 <p>Breakdown</p> <p><i>Erosion breakdown</i> <i>PD breakdown</i></p>

Figure 2.2: Different types of gas discharges [4]

2.1.1 Space-charge-free discharge

Gas discharge in a nearly uniform field under the hypothesis of neglecting space charges is ruled by two main factors: ignition condition, described by Townsend's mechanism, and breakdown voltage dependence on pressure, temperature and electrodes distance, represented by the Paschen's law.

Gas discharge is directly linked to the development of an electron avalanche, started by a free primary electron released from the cathode by some possible causes such as photoelectric emission (UV light, cosmic radiation), ion impacts (in an electric field), thermionic emission (at high temperatures) and field emission (at very high local field strengths).

Initially this free electron follows casual thermal movements, colliding with gas molecules but not ionizing them due to a kinetic energy lower than the ionization one; meanwhile, the electron is accelerated by the electric field resulting in an electron drift into the electric field direction.

The electron doesn't lose appreciable energy in the collisions thanks to the momentum conservation and thus its energy rises up until ionization energy is achieved and a ionization collision happens.

At this point electrons generated by these ionizing collisions are also accelerated and produce other electrons by ionization, resulting in an electron avalanche.

In this process also positive ions are generated: they drift towards the cathode causing the emission of other secondary electrons.

This means that there are feedback processes responsible for the electrons generation in addition to the ionizing collisions: the recombination acts an other important role considering that causes the emission of photons which are able to release other secondary electrons from the cathode by photoionization.

The ignition condition is defined in this way:

A single primary electron that is released from the cathode (for example by an external ionization source) has to generate at least one secondary electron at the cathode by avalanche growth and feedback process, in order to provide at least one new primary electron for the next avalanche.

This means that every avalanche causes at least one subsequent avalanche.

In this way a conductive discharge channel is generated and voltage across the electrodes breaks down.

In order to characterize this process through a parameter, a ionization coefficient α named also *Townsend's first ionization coefficient* is defined: it represents the number of electrons generated per unit length by a single electron by ionizing collisions.

This parameter can be reduced to an even more representative one known as *effective ionization coefficient*:

$$\alpha_{eff} = \alpha - \eta$$

where η is the *attachment coefficient* which defines the decrease in free electrons number per unit length caused by their attachment to gas molecules: this process, very important in gases with an high electron affinity, greatly increases the breakdown strength.

Avalanche growth can only occur if the effective ionization coefficient α_{eff} is greater than zero.

Considering a generic avalanche it results:

$$dN = N \cdot \alpha_{eff} \cdot dx$$

where dN is the electron number N increase along the length dx .

This relation can be turned in

$$\ln(N/N_1) = \alpha_{eff} \cdot x$$

where N_1 is the primary electrons number and α_{eff} is considered constant in a uniform field.

The result is an electron avalanche which grows exponentially:

$$N = N_1 \cdot e^{\alpha_{eff} \cdot x}$$

In addition, there's an other ionization coefficient β representing the electrons generated per unit length by a positive ion: however, being $\beta \ll \alpha$, it can be neglected.

Finally the *surface ionization coefficient* γ , also known as *feedback* or *Townsend's second ionization coefficient*, defines the number of secondary electrons generated by a single positive ion.

These parameters take into account several possible causes of electron generation from the cathode as positive ions or neutral atoms impact, photo effect, field emission, photo emission in the volume and ion emission of the anode, all dependent on electrode material, gas type, pressure and field strength.

It results:

$$\gamma = f(E/p)$$

In an electron avalanche the initial electrons number can be calculated as

$$N_n = \gamma^{n-1} \cdot (e^{\alpha_{eff}} - 1)^{n-1}$$

The sum of all initial electrons at the cathode is defined by a geometric series, in particular

$$N_c = \frac{1}{1 - \gamma \cdot (e^{\alpha_{eff} \cdot d} - 1)}$$

from which the divergence condition clearly appears to be

$$\gamma \cdot (e^{\alpha_{eff} \cdot d} - 1) \geq 1$$

This represents the case of an infinite number of initial electrons resulting in the formation of a conductive channel between cathode and anode and thus in the voltage breakdown: the ignition condition.

These concepts are valid for low pressures or small electrode distances.

The effective ionization coefficient can be defined as

$$\alpha_{eff} = p \cdot f(E/p)$$

where it can be noted its dependence on pressure and electric field strength.

In particular, ionization and attachment coefficients are defined as follows:

$$\alpha = A \cdot p \cdot e^{-\frac{B}{(E/p)}}$$

$$\eta = a \cdot p \cdot \{1 - e^{-\frac{b}{(E/P)}}\}$$

where A, B, a, b are empirical constants.

A reduced form of these coefficients is reported in the figure 2.3 where the dependence on the E/p ratio is highlighted.

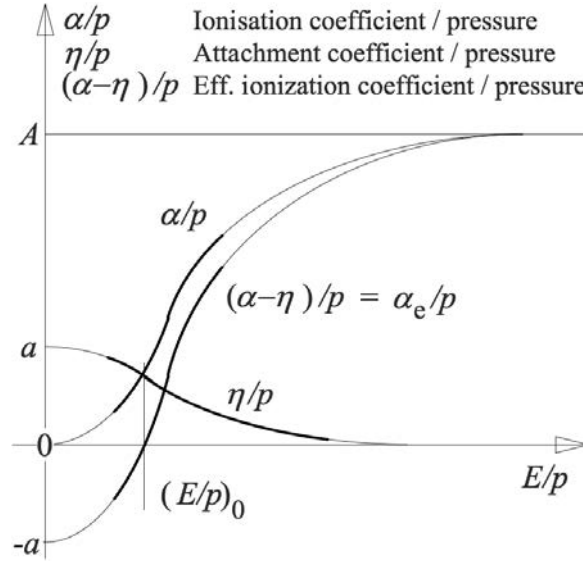


Figure 2.3: Ionization, attachment and effective ionization reduced coefficients [4]

In relation to the electron distribution along the electrodes gap, it is described by the *Clausius law*:

$$N(x) = N(0) \cdot e^{-x/\lambda_m}$$

where $N(x)$ is the number of electrons at a generic distance from the cathode, $N(0)$ is the number of electrons at the cathode and λ_m is the electron mean free path length.

In the figure 2.4 a simplistic representation of the electrons behavior is given.

In order to achieve an high dielectric strength, gases have to be characterized by an high electron affinity, which is the energy released as a photon or as kinetic energy during the electron attachment process.

These have been always denominated electronegative gases even though the electronegativity actually describes the contributions of the elements to the binding conditions within a molecule defining energy levels together with the isometric molecular structure and the spatial atoms arrangement.

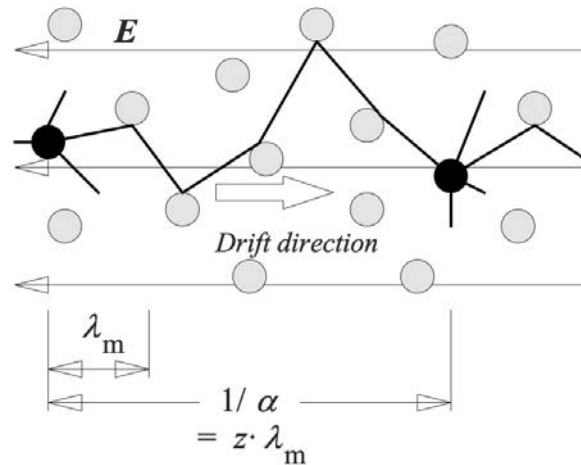


Figure 2.4: Representation of electron ionizing collisions [4]

As regards the breakdown field strength, the *similarity law* has to be considered:

$$\frac{E_{bd}}{p} = f_1(pd)$$

where it can be noted the dependence of the E/p ratio on the product of gap distance and pressure.

Considering that $V_{bd} = E_{bd} \cdot d$ the breakdown voltage is found:

$$V_{bd} = pd \cdot f_1(pd) = f_2(pd)$$

This is the so called *Paschen's law* which states that the ignition voltage is a function of the product of electrode distance and pressure, if the Townsend conditions (uniform field and negligible space charges) are fulfilled.

Considering the temperature influence:

$$V_{bd} = f\left(\frac{pd}{T}\right)$$

Paschen's law can be written in its analytical form as follows:

$$V_{bd} = \frac{B \cdot pd}{\ln \frac{A \cdot pd}{\ln(1+1/\gamma)}}$$

In the figure 2.5 the analytical and real forms of Paschen's law are reported.

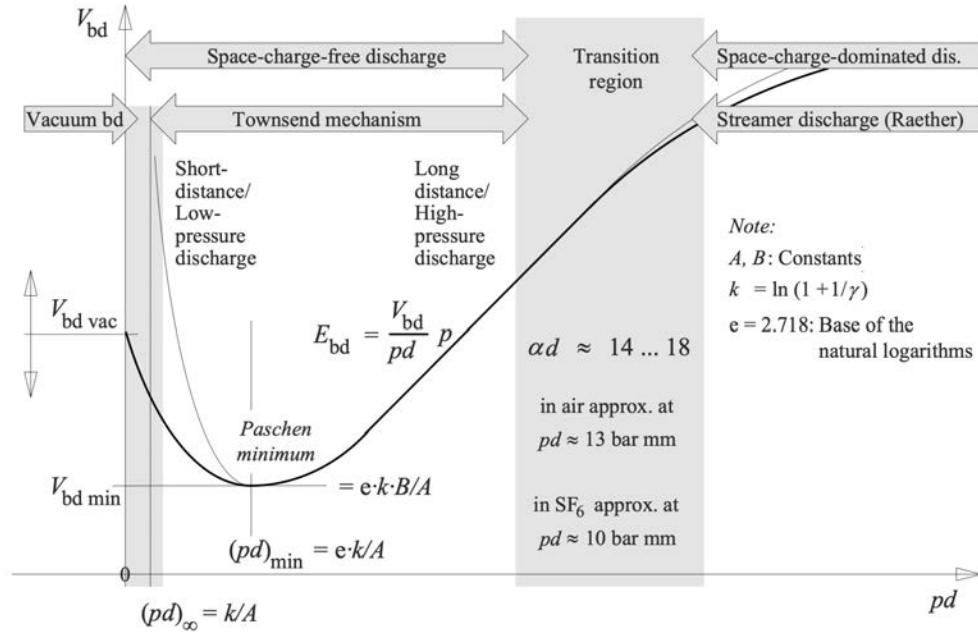


Figure 2.5: Paschen's law representation as analytical (thinner) and real (thicker) curve [4]

Paschen's curve presents high breakdown voltage values at very low and high values of the pd product, with a minimum in between.

Below the minimum breakdown voltage gas breakdown is not possible.

Breakdown voltage is high at low pd values (short distance-low pressure) because of the low number of gas molecules available for ionizing collisions.

On the other hand breakdown voltage is also high at high pd values (long distance-high pressure) due to the fact that long distances are associated to a field strength reduction and high pressures reduce the free path length available for the electron acceleration. In both these cases a reduction of the ionization coefficient α occurs.

2.1.2 Space-charge-dominated discharge

When an avalanche, triggered by an initial electron, grows up to 10^6 to 10^8 electrons, the electric field in the avalanche environment is significantly influenced by space charges.

In this process, very slow positive ions remain in the avalanche tail since electrons, more mobile, form a negative and approximately spherical avalanche head.

A large field strength enhancement is caused by space charges at the front of the avalanche head and thus the number of ionizing collisions and photon-emitting recombinations increases.

Emitted photons cause photoionization in the gas volume and generate initial electrons for consecutive avalanches in the area around the first avalanche's head, leading to the instant in which the superposition of all the avalanches generates a conductive streamer.

This mechanism is therefore known as a *streamer mechanism* or *discharge*.

An illustration is given in the figure 2.6.

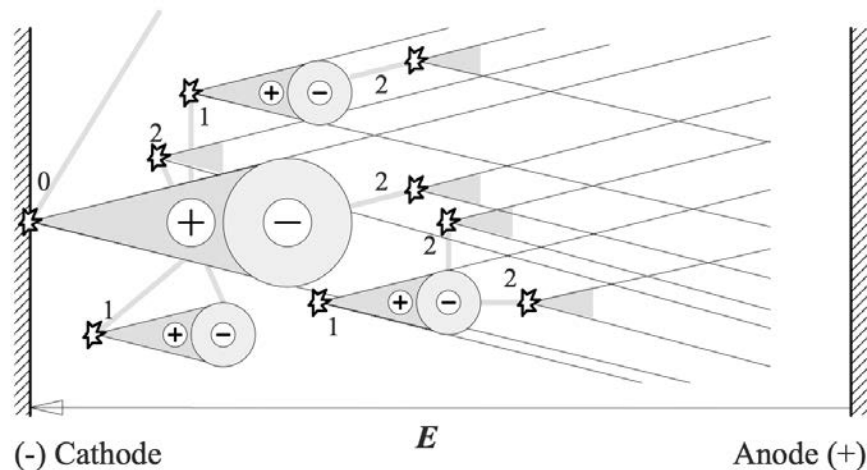


Figure 2.6: A physical model describing the streamer discharge [4]

The streamer, due to the high field strength and the secondary avalanches running ahead, propagates towards the anode with high velocity approximately at $100 \text{ cm}/\mu\text{s}$ in air, at atmospheric pressure and in a uniform field.

Also in this case, a precondition for breakdown is that the generation of electrons by ionizing collision outweighs the attachment of electrons.

More precisely, *Raether's ignition condition* for the streamer mechanism in non-uniform fields is given by analogy with Townsend's ignition condition for the avalanche generation mechanism in uniform fields.

In regions with high field strength, charge carriers generation by ionizing collision is predominant ($\alpha > \eta$) since in regions with low field strength the attachment of electrons predominates ($\alpha < \eta$).

2.1.3 Discharges in non-uniform fields

In case of non-uniform fields, the electron avalanche growth and the ignition condition are strongly affected by the variation of the ionization coefficient with the field strength and the location.

In weakly non-uniform fields breakdown immediately occurs as soon as the ignition condition for the Townsend or the streamer mechanism is fulfilled since pre-discharges don't occur.

In strongly non-uniform fields, favorable ionization conditions only occur close to the curved electrode surface since in the low-field region ionization net coefficient becomes negative due to the predominant electron attachment processes.

If the ignition condition is fulfilled at the curved electrode, pre-discharges (corona discharges) immediately occur causing breakdown.

They begin as glow discharges (Townsend mechanism) at the curved electrode surface in the high field region only; increasing voltage, space-charge dominated streamer discharges start and can propagate into the low-field region as long as the background field is strong enough.

If the background field strength is too low for the streamer growth, the streamer fades away.

The remaining low-field gas volume between discharge head and counter electrode is an ohmic-capacitive impedance stabilizing the pre-discharge.

The inception voltage of pre-discharges decreases with decreasing the field efficiency factor (i.e. with increasing non-uniformity of the field).

Breakdown occurs only at a higher voltage, if the field strength in the low-field region is sufficiently high for the streamer growth to the counter-electrode.

A representation of different types of discharges in dependence on the field efficiency factor is given in figure 2.7.

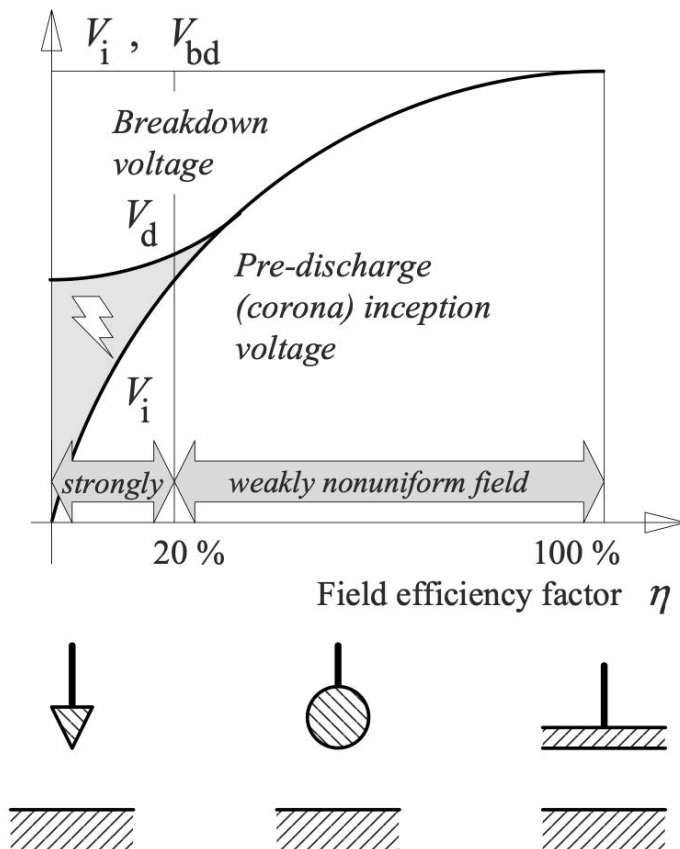


Figure 2.7: Dependence of pre-discharges and breakdown on field efficiency factor [4]

In a non-uniform field, there is a significant difference between the corona inception voltage and the breakdown voltage, both strongly dependent on polarity.

For a negative point electrode, the pre-discharge inception voltage is comparatively low, but breakdown only occurs at comparatively high voltages since for a positive point electrode, the pre-discharge inception voltage is relatively high, but the breakdown occurs at comparatively low voltages: that is the so called *polarity effect*.

The reason for this behavior is the formation of a positive space charge close to the point electrode, which has to be taken into account.

For a positive point electrode, avalanches have to start within the gas volume because of the very low field strength at the cathode since, for a negative point electrode, an initial electron has to be provided on a very small surface on the point electrode.

At the end, many parameters affect the discharge development and the most important

are geometry, pressure, temperature, gas humidity, gas type and field distortions. Electrodes geometry is strongly connected to the field efficiency factor and thus directly influences corona inception voltages and breakdown voltage. The influence of pressure, temperature and humidity can be described by a density correction factor k_1 and by an humidity correction factor k_2 . For example, the real breakdown voltage V_{bd} is deduced from the breakdown voltage V_{bd0} under standard atmospheric conditions in this way:

$$V_{bd} = V_{bd0} \cdot k_1 \cdot k_2$$

Finally, as regards the influence of pressure, for high values it can no longer be described by a linear approach and the discharge behavior in a strongly non-uniform field can significantly change during a pressure increase. At low pressure, a significant difference can exist between inception voltage and breakdown voltage which disappears at high pressures. For a given electrodes configuration, an increase in pressure shifts the discharge behavior from a range with pre-discharges to a range without. The suppression of pre-discharges with increasing pressure can be explained by the decreasing range of photon emission by increasing gas density, which significantly degrades the conditions for secondary avalanches and streamers.

2.2 Sulphur hexafluoride (SF₆)

Sulphur hexafluoride (SF₆) has been used as the most popular insulating gas in Gas-Insulated Transmission Lines since 1947 due to the exceptional combination of physical and chemical properties for high-voltage applications, resulting in the chance to design SF₆ insulated equipment with reduced size, high reliability and economic efficiency.

Its properties were discovered when, after 20 years of studies on many potential insulating gases (1930/40s), halogenated molecules were found to be able to attach free electrons: between them, SF₆ resulted the best one.

Nowadays, unfortunately, after 70 years of industrial applications, SF₆ properties as a

strong greenhouse gas have been known and its use in GILs will be limited more and more: actually it is no longer used in pure form but only admixed with N_2 in order to reduce the environmental impact, which is only one of many steps that will lead to its complete replacement by 2022, according to the EU Regulation No. 517/2014. Moreover, this gas is relatively expensive in comparison with other insulating mixtures, with a cost for kg of 8 US \$ [1, 5, 6, 42].

2.2.1 Physicochemical properties

Sulphur hexafluoride is composed of sulphur (S) and fluorine (F) which are the most active halogen elements, linked by covalent bonds to form a molecular structure similar to an octahedron where six fluorine atoms occupy fix positions around the central sulphur atom, bonded by the sp^3d^2 hybrid orbit.

In the figure 2.8 the SF_6 molecular structure is shown.

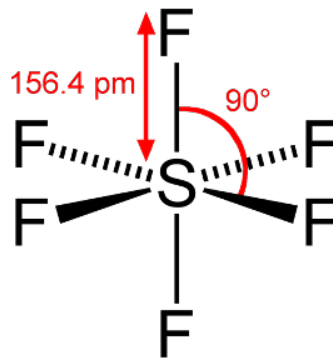


Figure 2.8: SF_6 molecular structure

This is an artificial gas, five times heavier than air, synthesized in 1900 by two French chemists, Lebeau and Moissan, characterized by non-toxicity, non-flammability, non-explosivity, non-corrosivity, chemical inertia, high heat storage capability and thermal stability over the long term.

In the table 2.1 these and other physicochemical parameters are reported.

Table 2.1: Physicochemical properties of SF₆

Parameter	Value	Unit
Molecular weight	146.06	g/mol
Density	6.17	kg/m ³
Number of electrons	77	
Freezing point	- 51	°C
Boiling point at 1 bar	- 63	°C
Saturated vapor pressure at - 30 °C	0.52	MPa
Saturated vapor pressure at 0 °C	1.26	MPa
Saturated vapor pressure at 20 °C	2.11	MPa
Flammability	non-flammable	
Explosiveness	non-explosive	
Chemical stability	inert	
Thermal stability	stable up to 500 °C	
Corrosivity	non-corrosive	
Solubility in water	non-soluble	
Appearance	colourless/odourless	
Toxicity (LC 50 (rat))	> 500000	

There are many properties that make this gas attractive for use in a GIL.

Firstly, it can ensure a long term chemical and thermal stability, with no possibility of chemical reaction with the HV electrode, enclosure or insulators, meaning both reduced maintenance and long life of the structure.

Secondly, it provides an intrinsic safety for the transmission line and for the maintenance staff because no fire, explosion or toxicity risks are taken using this insulation medium.

In addition, the high thermal conductivity allows an easy heat exchange between the inner conductor and the outer enclosure and then the external environment.

This is the reason for which it is possible for this type of transmission line to have a great power capability without high restrictions on the thermal aspect.

Finally, it can be noted that the boiling temperature is low ($-63\text{ }^{\circ}\text{C}$ at atmospheric pressure), a fundamental property which ensures that the insulation medium remains in the gaseous state in most of the practical applications, providing higher dielectric strength.

A characterizing parameter is the pressure-temperature product and, considering that GIL internal pressure is always higher than the atmospheric one, it is clear how much important a low boiling temperature can be.

This choice about the internal pressure is linked to two considerations: firstly, by increasing gas pressure is possible to achieve a better dielectric strength of the gas; secondly, in case of leak, the insulating gas doesn't come out since it is the air that goes inside the enclosure.

SF_6 has a density which is greater than the one of air (6.17 kg/m^3 and 1.20 kg/m^3 respectively), so the insulating gas tends to stay at a lower quote than air and the consequence is a possible risk of suffocation.

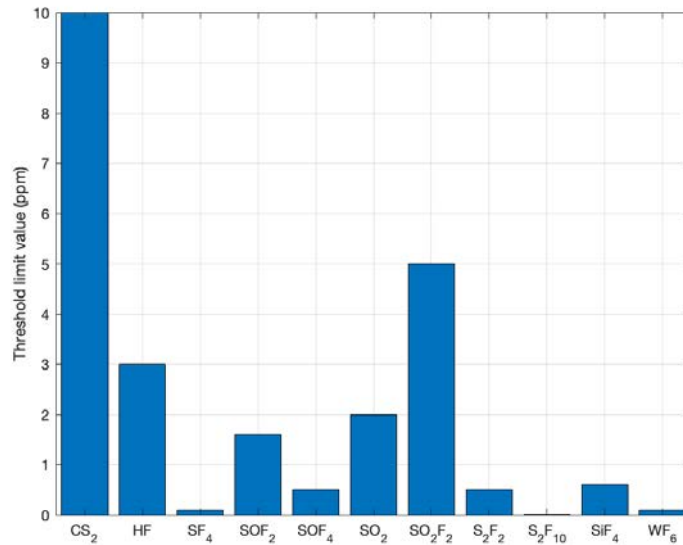
An other important aspect regards SF_6 decomposition byproducts which may appear when an electrical discharge such as an arc, spark, or corona occurs.

Some of these, including disulphur decafluoride (S_2F_{10}), sulphur tetrafluoride (SF_4) and hydrogen fluoride (HF) are known to be highly toxic, reactive, corrosive and thus can affect personnel safety and equipment lifetime.

In the figure 2.9 the threshold limit value (TLV) of all SF_6 byproducts is reported.

An other SF_6 byproduct (not reported in the figure due to graphic concerns) has to be added to the previous list: this is carbon monoxide (CO) which is characterized by a TLV of 50 ppm.

A series of symptoms like dyspnea, hemoptysis and cyanosis can occur when SF_6 decomposition products are accidentally inhaled and they have a direct effect on the alveolar capillary membrane, which can lead to pulmonary edema, hypoxemia, arrhythmia and mild tissue acidosis based on the clinical observation [1, 5, 6].

Figure 2.9: SF₆ decomposition byproducts toxicity

2.2.2 Dielectric properties

Gas insulation technology had its spread thanks to the excellent electrical insulation properties of sulphur hexafluoride: this is characterized by a dielectric strength of 89 kV/cm at atmospheric pressure, almost three times higher than the one of air (30 kV/cm) at the same pressure.

This is a direct consequence of SF₆ strong electronegativity which determines a high electron attachment and thus the molecule ability to capture a large number of free electrons.

The task of stopping and binding free electrons is a point of strength of SF₆, a consequence of the fact that the large molecule of one sulphur and six fluorine atoms blocks the free-moving part of the electron, taking out the kinetic energy, binding the electron and sending out a photon.

The photons we can see form the so called corona, a light shining effect around the high-voltage conductors in high electric field areas.

On the other hand, different behaviors in dependence on the electric field uniformity must be taken into account considering that in the case of a strongly non uniform

field the dielectric performance results to be worse than under a uniform field.

This can be an important aspect because sometimes the inner conductor could have a certain roughness or, in worse conditions, even the presence of conducting particles, therefore a total breakdown between the electrodes or also just a partial discharge around them could happen if not enough attention is paid during the design, construction and maintenance phase [1, 5, 6].

2.2.3 Environmental properties

SF₆ is labeled as a greenhouse gas in the Kyoto Protocol and Paris Agreements considering its excessive size, radiative effect and atmospheric lifetime.

It was also defined as one of the most harmful non eco-friendly gas in the 3rd Conference of the Parties to the United Nations Framework Convention on Climate Change (COP3) in 1992.

The global warming potential (GWP) is 23500 times the one of carbon dioxide over a 100-year time horizon which means that 1 kg of SF₆ released into the atmosphere has the equivalent global warming impact as 23.5 tons of CO₂.

Considering instead a 500-year time horizon, the GWP is 32600 times that of CO₂.

The atmospheric lifetime is 3200 years, whereas the one of CO₂ is only 30-90 years: this is a consequence of the fact that SF₆ is a strong molecule, very resistant to degradation and assault in the atmosphere.

The self-cleansing property of the atmosphere is unable to deal with such super molecules and this is one of the reasons why SF₆ emission and consumption must be controlled by the year 2020 and regulations have been implemented to reduce the environmental impact caused by this artificial gas.

Environmental parameters are summarized in the table 2.2, where the ozone depletion potential (ODP) is also reported.

A specific definition of the three parameters linked to the environmental impact, specifically global warming potential, ozone depletion potential and atmospheric lifetime are given in the following section.

The electrical industry is the principal user of the sulphur hexafluoride since its great

insulating performance has been discovered.

Table 2.2: Environmental properties of SF₆

Parameter	Value	Unit
Ozone depletion potential (ODP)	0	
Global warming potential (GWP)	23500	
Atmospheric lifetime	3200	years

The world total amount of SF₆ stored right now in electrical equipment is in the order of 105 tons and it is still increasing, resulting in the fact that the electrical sector is the main responsible of the large quantity of SF₆ emissions.

Generally, the insulating gas remains inside the structure for all its lifetime (≈ 40 years) and just a negligible part is emitted during this period.

Leakages for new electrical equipments are under 0,5% but after around 30 years there is a considerable increase which outstrips 2%.

Although it is necessary to decrease the leaks during the working life, most of the SF₆ is released during the production, testing, installation and disassembly of the electrical equipments, so in the immediate future, more attention is required during all the above mentioned phases and, furthermore, the adoption of gas collection infrastructures must be necessarily implemented in the worldwide.

If no action is taken, the anthropogenic emission of strong greenhouse gases will change in a permanent way the world climate.

The air samples collected from Antarctic demonstrate that in the pre-industrial period the sulphur hexafluoride present in the atmosphere was less than 6.4 parts per quadrillion (10²⁴) since the current SF₆ content in the air is three orders of magnitude higher.

It can be said that, thanks to the huge GWP and the extremely long atmospheric lifetime, SF₆ is the strongest greenhouse gas known until now [5, 6].

2.3 Alternative gases

The use of a gaseous dielectric in HV equipment is linked to its properties and varies depending on the operating conditions and the application.

Properties inherent to the molecular structure and atomic physics of the gaseous molecule are named *intrinsic* and are independent on the environment where the gas is placed.

A really important characteristic of the gas is the dielectric strength which mainly depends on its capability to reduce the density of generated electrons when it is subjected to an electric field.

Therefore, gas electronegativity is fundamental in order to reduce the number of electrons by attachment, taking into account that the attachment capability depends on gas temperature and its efficiency is high up to a certain electron energy level.

In addition, the gaseous dielectric must be able to slow down electrons so that it can capture them efficiently at lower energies avoiding the generation of other electrons by ionizing impact.

Many other secondary processes have to be considered, including the emission of electrons by impact of photons and ions on the surface of the cathode, linked to the photonic mechanism, ion-molecule reactions, dissociation under the action of collision decomposition, reactions with surfaces and impurities.

When it comes to mixtures, the thermodynamic properties must be suitable for uniformity of composition and separation of the mixtures.

Considering physical and chemical properties, the insulating gas must respect several requirements [5, 20].

HIGH DIELECTRIC STRENGTH

The dielectric strength of a gaseous medium is related to AC, DC and lightning impulse breakdown voltage since breakdown mechanisms of insulation gases can be theoretically explained by Paschen's law and Townsend's theory, according to the brief introduction previously presented.

AC and DC breakdown voltages are tested by raising the voltage applied to the

electrodes at a constant rate until the breakdown occurs.

On the other hand, the lightning impulse breakdown voltage is a fundamental test because defines the basic insulation level of the system; it is represented by 50 % breakdown strength and is determined by the up-and-down method by applying a 1.2/50 s standard lightning pulse voltage.

The breakdown test is repeated multiple times under the same conditions in order to calculate the mean value and the standard deviation of the breakdown voltage and thus evaluate the gas performance.

Several conditions can affect the breakdown voltage, including field uniformity, insulation defects, surface roughness, contamination and free-moving conductive particles. In addition to the breakdown voltage, partial discharge inception voltage (PDIV) is the other criterion for evaluating the dielectric strength.

PD is a localized electrical discharge that only partially bridges the insulation between conductors and it occurs at any point in the insulation medium where the electric field strength exceeds the breakdown strength of gas: this is the reason why PD is regarded as an early stage of breakdown.

Alternative gases are compared from the point of view of their insulation performance also by PD characteristics, considering partial discharge inception voltage, discharge magnitude, and pulse count as a function of gas pressure and insulation distance.

HIGH SATURATED VAPOR PRESSURE AT LOW TEMPERATURE

All gaseous mediums are characterized by their boiling point which represents the temperature at which, for a given pressure, gas turns into liquid.

Wagner equation shows the relation between temperature and saturated vapor pressure for a gas mixture:

$$\ln \frac{p}{p_r} = (a\tau + b\tau^{1.5} + c\tau^3 + d\tau^6) \frac{T}{T_c}$$

where p is the partial pressure and p_r is the critical pressure of the gas mixture, T is the thermodynamic temperature and T_c is the critical temperature of the mixture, τ is a parameter equal to $1 - \frac{T}{T_c}$ and a , b , c , d are constant coefficients.

It is clear that alternative gases must have a low boiling point and therefore an high

vapor pressure at low temperatures in order to ensure that the dielectric remains gaseous within the operational temperature range of the system.

NON-FLAMMABILITY AND NON-EXPLOSIVENESS

Flammability and explosiveness are characteristics which must be strongly avoided in the choice of the insulating gas.

THERMAL STABILITY AT A TEMPERATURE ABOVE 400 K

A good insulating gas has to be stable with the temperature increase at least up to a certain limit (400 K is an accepted standard) in order to guarantee security and good performance.

CHEMICAL STABILITY AND INSENSITIVITY TO CONDUCTIVE AND INSULATING MATERIALS

The gaseous medium must not interact with other materials which GIL is composed of (metals, spacers, insulators) and must not be subjected to possible modification of its molecular structure with the change of operational or environmental conditions, otherwise the serviceable lifetime of the power line could be significantly reduced.

Furthermore, gas must not be subjected to extensive decomposition or polymerization and there must be no formation of carbon or other deposition.

HIGH SPECIFIC HEAT AND HIGH THERMAL CONDUCTIVITY

System cooling is a crucial element in a power line: the inner conductor temperature, due to Joule losses, tends to increase and it's really important to optimize the transmission of the heat to the outer enclosure and thus to the external environment. An high specific heat and an high thermal conductivity are beneficial in this process.

LOW GLOBAL WARMING POTENTIAL (GWP)

GWP is a purely physical index of the climate impact added to the climate system by a greenhouse gas relative to that added by CO₂ (definition by the Intergovernmental Panel on Climate Change (IPCC)).

It was introduced for the first time in 1990 in the First IPCC Assessment that gave the following definition:

GWP index is based on the time-integrated global mean of a pulse emission of 1 kg of some compound relative to that of 1 kg of reference gas CO₂.

It can be expressed by

$$GWP = \frac{\int_0^{ITH} R_x C_{x0} \exp[-t/\tau_x] dt}{\int_0^{ITH} R_{CO_2} C_{CO_2}(t) dt}$$

where R is the radiative forcing per unit mass and C is the atmospheric concentration of the compound, t is the time and x is the compound of interest, τ is the lifetime of the compound.

Numerator is called *absolute global warning potential (AGWP)* of the component gas (x) since denominator is called absolute global warning potential of the reference gas (CO₂).

More precisely, GWP is calculated as the ratio of the time-integrated radiative forcing due to 1 kg of the gas emitted into the atmosphere relative to the one of 1 kg of CO₂ over an integration time horizon (ITH, commonly 20, 100 or 500 years).

This parameter has to be as low as possible in order to prevent the emission of greenhouse gases into the atmosphere.

Concerning gas mixtures, GWP can be calculated as a weighted average, considering the sum of the weight fractions of the individual gas multiplied by their GWP:

$$GWP_{mixture} = \Sigma[(X\% \cdot GWP_X) + (Y\% \cdot GWP_Y) + \dots + (N\% \cdot GWP_N)]$$

where X, Y, N are the contribution by weight of the single gas and GWP is the global warming potential of the single pure gas.

NEGLIGIBLE OZONE DEPLETION POTENTIAL (ODP)

Ozone is a gas normally present in the stratospheric layer of the earth, very useful in order not to let pass the ultraviolet radiation produced by the sun, which can heavily

damage the skin tissue.

Since 1970s, it has been noted that the ozone concentration in the stratospheric layer was decreased, especially near the Earth's polar regions (ozone hole) and the source of the problem was found into the continuous increasing of the ozone-depleting substances (ODS), such as halogen gas, solvents and propellants principally due to anthropogenic activity.

These substances can decrease the amount of ozone in the stratosphere thus their use must be drastically reduced.

Ozone depletion potential is a simple relative index linked to the rate of ozone consumption due to the gas emission into the atmosphere: it has to be near to zero considering that SF₆, which has to be replaced, has an ODP of zero because it doesn't react with other gases in the stratosphere thanks to its chemical inertia and an alternative insulating gas must not adversely affect this parameter.

More specifically, ODP indicates the attitude of the compound to damage the ozone layer relatively to the effects of a reference molecule (CFC-11 or CFCl₃).

An analytic definition of this index is:

$$ODP = \frac{\Delta O_3(h, l, t)_x}{\Delta O_3(h, l, t)_{CFC-11}}$$

where ΔO_3 is the global ozone depletion due to the component x or CFC-11, h is the altitude, l is the latitude and t is the time.

SHORT STAY IN THE ATMOSPHERE

A good gas should not rest in the atmosphere for long periods of time: this parameter is strictly linked to the gas ability to decompose once released into the environment. This is an important parameter when considering the environmental impact of a greenhouse gas and can be defined, adopting the Jacob's one-box model (1999), as the average time τ that a molecule remains inside the box:

$$\tau = \frac{m}{f + l + d}$$

where m is the mass of the substance inside the box (kg), f is the flow of the substance outside the box (kg/year), l is the chemical loss of the substance (kg/year) and d is the substance deposition (kg/year).

LOW TOXICITY

The alternative gas and its byproducts must have a minimum toxicity to ensure that it can be safely handled and is not harmful when released into the atmosphere.

There are important indicators of toxicity like acute toxicity, chronic toxicity and medium/long-term epidemiological effects.

The first one is characterized by a lethal concentration at 50 % mortality (LC50) in 4 h: this parameter is expressed in parts per million (ppm) and a low value corresponds to an high gas toxicity.

Chronic toxicity is presented by a time-weighted average (TWA) and measured in ppm in 8 h.

Medium/long-term toxic effects are carcinogenic, mutagenic and toxic for reproduction: they must be avoided.

2.3.1 Natural gases

Natural gases like CO₂, N₂ or dry air are one of the possible alternatives to SF₆.

They are characterized by a negligible environmental impact and a very low liquefaction temperature.

Drawbacks are that a significant increase in the pressure and size of equipment is required: dielectric strength of natural gases is in fact much lower (0.4 times for CO₂) than the one of SF₆.

In addition, in case of surface defects in the equipment a further remarkable decrease in the dielectric performance occurs [6].

Nitrogen (N₂)

Nitrogen is chemically stable as N₂ molecule.

It is an inert gas, which means it is not a very active molecule to react chemically with other molecules.

N₂ has no electronegativity, meaning that free electrons can't be bound with the molecule, with the only exception for very low energy levels.

This is a widely available gas, it can be easily produced out of air and as a consequence

the price is very low.

Compared to SF₆ the molecule size of N₂ is three times smaller and can't capture electrons as SF₆ which instead has a strong electronegativity.

In case of an inhomogeneous field strength electrons are accelerated through the gas and can hardly be stopped by N₂ due to the fact that the small size leaves much free space in between so that electrons can find the way through the gas and the missing electronegativity can't catch electrons in the gas and send out an photon.

N₂ has had a good partner in SF₆ to design the economical high-voltage power transmission system GIL until now.

The lower electrical insulation capability of nitrogen leads, in practical use at high voltage, to very high gas pressures and this is the reason why N₂-insulated systems are limited to about 100 kV in practical use.

Higher voltage levels of 420 kV or 550 kV would require large diameters of 1.0 m and an high gas pressure of 1.5 to 2.0 MPa compared with a diameter of 0.5 m and a pressure of 0.8 MPa related to the use of a 20% SF₆ / 80% N₂ gas mixture.

These large diameters and high pressures make GIL design costly and for AC applications pure N₂ gas insulation has not been used at these higher voltage levels [1].

2.3.2 SF₆ mixtures

The insulating gas SF₆ offers two basic advantages for use at high voltage [1]:

- high insulating capability because of strong electronegativity;
- high arc-extinction capability because of recombination and arc cooling.

For a GIL, the arc-extinction property is not needed, therefore a mixture with nitrogen is possible without losing too much of the insulation capability.

A 20% SF₆ / 80% N₂ mixture has been chosen in the recent years in order to at least reduce SF₆ use in power transmission industry.

This is the result of much research done since the early 1970s on replacing SF₆.

Some of the tested gas mixtures showed higher insulation capabilities than SF₆, but all of them are more critical in terms of toxicity or degenerating under partial discharge

initiated by high electrical field strength so that the wide use of such gas mixtures in high-voltage GILs is not recommended.

It is shown that a mixture of N_2 with only a small amount of SF_6 added is an interesting alternative to pure SF_6 for insulation purposes.

GIL needs a large amount of gas only for insulation purposes, so this gas mixture of mainly nitrogen with as low as possible a content of SF_6 has been very attractive until now.

To fix the percentage of SF_6 , an optimization process has been necessary to find the best ratio between SF_6 content, gas pressure and enclosure diameter.

Characteristics of N_2 / SF_6 gas mixtures show that with an SF_6 content of less than 20%, an insulating capability of 70 – 80% of pure SF_6 can be reached at the same gas pressure.

Investigations made since 1970s indicate that from this point of view nitrogen and sulphur hexafluoride can be used in high-voltage applications.

The strong increase in voltage withstandability with only a small percentage of SF_6 supports the goal of reducing the total amount of sulphur hexafluoride used in a long-distance GIL.

Regarding the lightning impulse voltage level, it depends on the gas pressure and for different mixing ratio of SF_6 and N_2 it shows a non-linear behavior.

When gas pressure is increased, the non-linear behavior of N_2 / SF_6 gas mixtures is the same as for pure SF_6 .

The withstand voltage for pure SF_6 at 0.3 MPa is reached at 0.5 MPa for gas mixtures of 20% SF_6 and at 0.7 MPa for gas mixtures of 10% SF_6 .

Pure N_2 insulation would require a gas pressure of 2.0 MPa and as a consequence pure N_2 solution is not seen as a practical solution.

Only 5% SF_6 content of the N_2 / SF_6 gas mixture delivers much stable test results, similar to pure SF_6 in behavior.

In 20% $SF_6 / 80%$ N_2 mixture, the absolute insulation capability of 80% of pure SF_6 is reached, meaning that with only 20% of the volume of SF_6 , a GIL can be designed at moderate gas pressure of 0.8 MPa and acceptable diameter of 500 mm for 420 kV.

A small change of SF₆ content at low mixing ratio, for example from 5% to 6%, causes a large change in absolute high-voltage insulation capability and this has to be taken into account.

When SF₆ content reaches the 20% , a small change doesn't cause a large change in the absolute insulation capability of the gas mixture and this is the reason why in practice SF₆ content has always been kept around 20%.

The principle behavior of the N₂ / SF₆ gas mixture follows the good electrical characteristics of pure SF₆, including the corona-stabilizing effect.

In the mixture, a small percentage of SF₆ increases the absolute insulation capability strongly, in fact with an SF₆ content of only 20% in the N₂ / SF₆ gas mixture, more than 70% of the insulation capability of pure SF₆ is reached.

Properties and advantages of N₂ / SF₆ gas insulation have been under investigation for more than 40 years.

The use of N₂ / SF₆ gas mixtures has been restricted to low-temperature applications to avoid liquefaction of SF₆ in operation at temperatures down to - 50 °C.

The first real application came with the second-generation GIL where the main driver was the cost reduction for long-distance applications.

The handling of the N₂ / SF₆ gas mixture needs a normalized evaluation tool which allows to find the right pressure, mixture ratio and volume.

Already at low SF₆ concentrations, the N₂ / SF₆ mixture acquires high dielectric strength due to the unique synergistic physical properties of these two components.

The normalized properties of N₂ and SF₆ gas mixtures are shown in the figure 2.10. This figure gives three curves for the dielectric strength of N₂ / SF₆ gas mixture in relation to the 100% SF₆ value.

In the diagram the following parameters are reported:

- NORMALIZED INTRINSIC DIELECTRIC STRNGTH (E_{cr})
 E_{cr} value for pure N₂ is below 0.4, while a 20% SF₆ content improves it to 0.69; pure SF₆ value is 1.
- NORMALIZED PRESSURE FOR EQUAL DIELECTRIC STRENGTH (p_0)
 p_0 value for a 20% SF₆ content of the gas mixture is 1.45, which means that the

pressure is 45% higher in comparison with pure SF₆.

p_0 curve increases strongly with lower SF₆ content and reaches a factor of about 3 for pure N₂.

- NORMALIZED QUANTITY OF SF₆ (q_0)

The curve of q_0 shows an almost linear increase of the quantity of SF₆ in the gas mixture.

With a 20% SF₆ content a value of 0.29 is obtained, meaning that only 29% of the SF₆ quantity is needed in this gas mixture in comparison with pure SF₆.

Only a moderate pressure increase of 40% is necessary to arrive at the same critical field strength as pure SF₆ but the amount of SF₆ in such a mixture is 70% less.

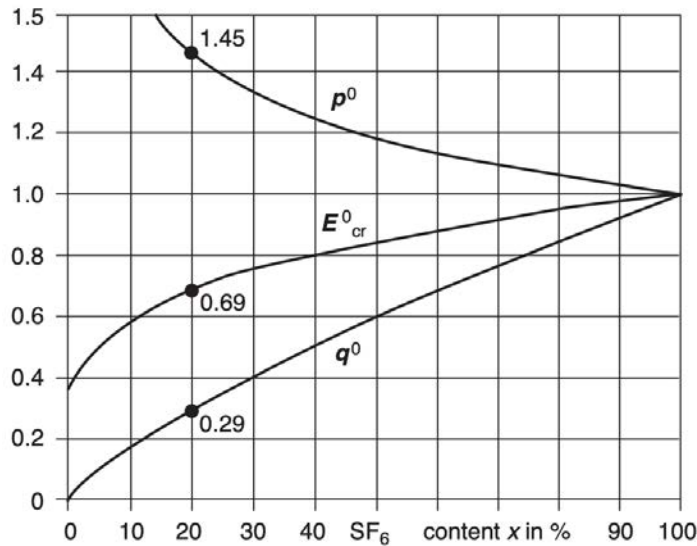


Figure 2.10: Normalized properties of N₂ / SF₆ gas mixtures [1]

N₂ / SF₆ mixtures have been regarded for much time as a potential alternative to pure SF₆ and much relevant research work has been performed.

However, the fundamental limit of this solution is that it doesn't eliminate SF₆ content of GIL insulating mediums but only reduces it: the target of this project is just to find an alternative which totally eliminates the SF₆ use, maintaining the excellent dielectric properties of the mixture 20% SF₆ / 80% N₂ [1].

2.3.3 Perfluorocarbons (PFCs)

PFCs are electronegative gases with better insulating properties and a lower GWP than SF₆.

Typical gases that belong to this family are c-C₄F₈, C₃F₈, C₂F₆ and CF₄.

These are generally admixed with other buffer gases, reducing the cost and lowering the boiling point under the premise of ensuring a good dielectric strength.

It has been demonstrated that, under AC voltage and plate-plate electrodes configuration, a combination with CO₂, N₂ or CF₄ leads to a positive synergistic effect.

When the ambient temperature is above - 20 °C, the insulation performance of the mixed gas can reach 70% of the one of SF₆ and GWP is reduced by 30% [20].

Octafluorocyclobutane (c-C₄F₈)

Octafluorocyclobutane presents an intrinsic dielectric strength of 129.5 kV/cm, a boiling point of - 6.0 °C and a GWP of 8700, much smaller than the one of SF₆.

The insulation performance of c-C₄F₈ gas under a uniform electric field is 1.18-1.25 times that of SF₆ and, although the price of c-C₄F₈ is ten times the one of SF₆, its actual usage is much smaller than that of SF₆.

The use of c-C₄F₈ as an insulating medium may produce, in case of breakdown, carbon particles that affect the insulation properties and adding a buffer gas such as CO₂ or N₂ can ease their formation.

Considering the case of a mixture of c-C₄F₈ / N₂ under a lightning impulse environment, the effect of gas pressure on the synergistic effect is not significant and the polar effect appears in the discharge characteristic.

The breakdown voltage under negative impulse is lower than that under positive impulse and this is because the polarity of the lightning impulses affects the speed and kinetic energy of free electrons: free electrons in a negative lightning strike have an higher velocity, making c-C₄F₈ absorb fewer free electrons, so the breakdown voltage under negative lightning impulses is lower than under positive impulses.

Octafluorocyclobutane has a critical breakdown field strength of 439.5 Td, which is larger than the one of SF₆ (369Td).

Insulating properties of mixtures of $c\text{-C}_4\text{F}_8$ and N_2 are comparable to those of SF_6 / N_2 mixture, but GWP decreases significantly; critical breakdown strength of $c\text{-C}_4\text{F}_8$ and CO_2 mixed gas is instead greater than that of the mixed gas $\text{SF}_6 / \text{CO}_2$.

Critical breakdown field strength of $c\text{-C}_4\text{F}_8 / \text{N}_2$ and $c\text{-C}_4\text{F}_8 / \text{air}$ are similar and significantly higher than other mixed gases.

The insulation performance of $c\text{-C}_4\text{F}_8$ reaches levels of pure SF_6 when the content exceeds 80%.

It has been demonstrated that the ability of $c\text{-C}_4\text{F}_8$ to attach electrons is still weaker than that of SF_6 and its electronegativity coefficient is at least three orders of magnitude lower than that of SF_6 .

As regards the $c\text{-C}_4\text{F}_8$ decomposition products and its mixture with N_2 at 50 Hz AC corona discharge, they mainly include CF_4 , C_2F_4 , C_3F_6 , C_2F_6 , C_3F_8 and $\text{C}_2\text{F}_3\text{N}$ [20].

Octafluoropropane (C_3F_8)

Octafluoropropane has an intrinsic dielectric strength of 78.3 kV/cm, a boiling point of - 36.6 °C and a GWP of 7000, much smaller than the one of SF_6 .

C_3F_8 presents, at both positive and negative impulse voltages, a breakdown voltage of about 2.5 times the one of air with all electrodes configuration.

Mixtures with other buffer gases are adopted.

The synergistic effect of a $\text{C}_3\text{F}_8 / \text{N}_2$ mixture is lower than that of SF_6 / N_2 mixture and the breakdown voltage of the mixed gas is also lower than the one of SF_6 / N_2 .

Under the same mixing ratio, the critical breakdown strength of the $\text{C}_3\text{F}_8 / \text{N}_2$ gas mixture is greater than that of $\text{C}_3\text{F}_8 / \text{CO}_2$ since a $\text{C}_3\text{F}_8 / \text{N}_2$ gas mixture containing 20% C_3F_8 reaches 60% of the dielectric strength of pure C_3F_8 .

With regard to the characteristics of C_3F_8 gas during partial discharge and breakdown, it can be shown that the discharge characteristic of SF_6 is approximately similar in results of discharge capacity, flow propagation time and time interval, which may be related to $(E/N)_{cr}$ and ionization coefficients are closely related.

By calculating breakdown parameters of $\text{C}_3\text{F}_8 / \text{CF}_4$, $\text{C}_3\text{F}_8 / \text{CO}_2$, $\text{C}_3\text{F}_8 / \text{N}_2$, $\text{C}_3\text{F}_8 / \text{O}_2$ and $\text{C}_3\text{F}_8 / \text{Ar}$ in the temperature range 300 - 3500 K, it can be found that

the ionization coefficient of C_3F_8 / N_2 is the highest and the attachment coefficient of C_3F_8 / CF_4 is the largest.

Under standard temperatures, the insulation property of C_3F_8 / N_2 is outstanding; however, the critical breakdown strength of C_3F_8 decreases with the increase in temperature [20].

Hexafluoroethane (C_2F_6)

Hexafluoroethane is characterized by an intrinsic dielectric strength of 70 kV/cm, a boiling temperature of - 78 °C and a GWP of 9200, much smaller than the one of SF_6 .

Also in this case, the pure gas is used to be admixed with some buffer gases.

The synergistic effect of a C_2F_6 / N_2 mixture is lower than that of SF_6 / N_2 since the breakdown voltage of this mixture is lower than the one of C_3F_8 / N_2 and thus also than that of SF_6 [20].

Tetrafluoromethane (CF_4)

Tetrafluoromethane presents an intrinsic dielectric strength of 44.9 kV/cm, a boiling temperature of - 128 °C and a GWP of 6500, much smaller than the one of SF_6 .

This gas is often considered as a buffer gas in mixtures with other perfluorocarbons [20].

2.3.4 Tetrafluoropropene (HFO-1234ze)

Tetrafluoropropene belongs to the family of hydrofluoroolefin and is generally used as a refrigerant, with the property of being non-toxic, non-flammable and non destructive of the ozone layer, with a GWP of less than 0.02 and a lifetime of 1 day.

It has insulation properties very close to SF_6 with a dielectric strength between 0.8 and 0.95 times the one of SF_6 .

Through the application of AC, positive and negative lightning impulse voltage, HFO1234ze shows a dielectric behavior very similar to that of SF_6 .

For the electron swarm parameters of HFO1234ze molecule under partial discharge,

this gas demonstrates a strong electron attachment capacity.

HFO1234ze / N₂ mixture shows excellent dielectric strength in the range of 0.1 to 1 MPa, typical values for GIL applications, even if there is no synergistic effect neither in the HFO1234ze / N₂ mixtures nor in the HFO1234ze / CO₂ ones.

Unfortunately, this gas is characterized by a boiling temperature (-15°C) much higher than that of SF₆ and this strongly affect its potential application range; moreover, HFO-1234ze decomposes when subjected to breakdown, resulting in carbon dust deposition on the electrodes [20].

Chapter 3

Target gases analysis

3.1 Perfluoronitrile (C_4F_7N)

3.1.1 Physicochemical properties

Perfluoronitrile (CF_3)₂CFCN, named also heptafluoro-iso-butyronitrile and commonly known as C_4F_7N , belongs to the fluorinated nitriles family, characterized by a crude formula of the form $C_nF_{2n+1}CN$.

C_4F_7N molecular structure is shown in figure 3.1.

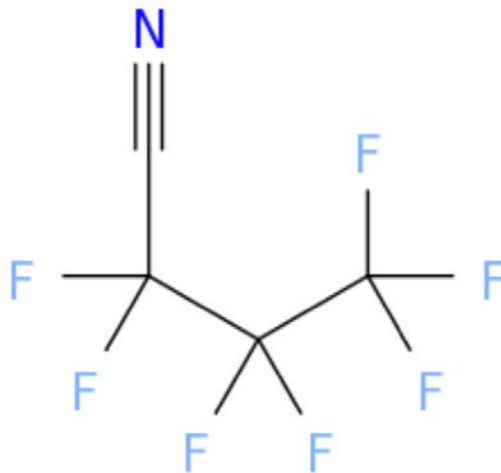


Figure 3.1: Molecular structure of perfluoroketone C_4F_7N

This gas was synthesized and commercialized by 3MTM Company with the name of NOVECTM 4710.

Some physicochemical parameters are reported in the table 2.1.

Table 3.1: Physicochemical properties of C₄F₇N

Parameter	Value	Unit
Molecular weight	195	g/mol
Density	0.0081	g/cm ³
Number of electrons	48	
Freezing point	-118	°C
Boiling point at 1 bar	-4.7	°C
Saturated vapor pressure at -30 °C	0.05	MPa
Saturated vapor pressure at 0 °C	0.15	MPa
Saturated vapor pressure at 20 °C	0.34	MPa
Flammability	non-flammable	
Explosiveness	non-explosive	
Chemical stability	stable	
Thermal stability	stable up to 700 °C	
Corrosivity	non-corrosive	
Appearance	colorless/odorless	

It can be noted the high liquefaction temperature (- 4.7 °C compared to - 63 °C of SF₆), which affects possible pure C₄F₇N applications: this drawback can be solved by mixing fluoronitrile gas to other buffer gases characterized by a low boiling point and a low GWP like CO₂, N₂ or dry air.

C₄F₇N is highly electronegative (beneficial property to improve the electron attachment process), chemically and thermally stable up to 700 °C, temperature at which CO and C₄F₈ begin to form as decomposition products.

Released into the atmosphere, C₄F₇N can react with OH, Cl and O₃ producing COF₂ and CF₃COF.

Other possible byproducts are CF₂HCN, CFH₂CN, CF₃CHF₂CN and CF₃CH₂CN,

characteristic of C_4F_7N reaction with H and OH.

Due to the cyano group ($C\equiv N$) contained in C_4F_7N molecular structure, the free radical may react with other atoms and even the metal in the device during an eventual discharge generating toxic substances such as HCN and CuCN.

The toxicity of the pure gas has not been demonstrated yet with regard to neurotoxicity.

Several tests showed that this gas is not CMR (Carcinogens Mutagenic Reprotoxic). Some known toxicological parameters are reported in the table 3.2 [6, 20].

Table 3.2: Toxicity of C_4F_7N

Parameter	Value	Unit
LC50	12000	ppmv
NOAEC	500	ppm
TWA	65	ppmv

3.1.2 Environmental properties

This gas presents a low environmental impact for high-voltage applications, much weaker than SF_6 , as can be deduced from the parameters reported in the table 3.3.

Table 3.3: Environmental properties of C_4F_7N

Parameter	Value	Unit
GWP (ITH = 100 years)	2100	
ODP	0	
Atmospheric lifetime	30	years

GWP of C_4F_7N under an integrated time horizon of 100 years is more than 10 times lower than the one of sulphur hexafluoride (2100 vs 23500), ODP is the same (0) for both since the atmospheric lifetime of this perfluoronitrile is more than 1000 times lower than that of SF_6 (30 vs 3200) [6, 20].

3.1.3 Dielectric properties

C_4F_7N presents a very high dielectric strength (240.3 kV/cm at atmospheric pressure) and is surely one of the most promising alternatives to SF_6 between existing gases. Precisely, this gas has a dielectric strength 2.7 times higher than the one of SF_6 in uniform field under both AC and DC voltages, since in non-uniform field the difference is lower, particularly under positive impulse voltage.

In the figure 3.2 C_4F_7N and SF_6 breakdown voltage in dependence on electrodes distance under AC environment is shown; two different field uniformities are analyzed. In these tests uniform field is obtained by a sphere-to-sphere electrodes configuration since non-uniform field is achieved by a rod-to-plane electrodes configuration.

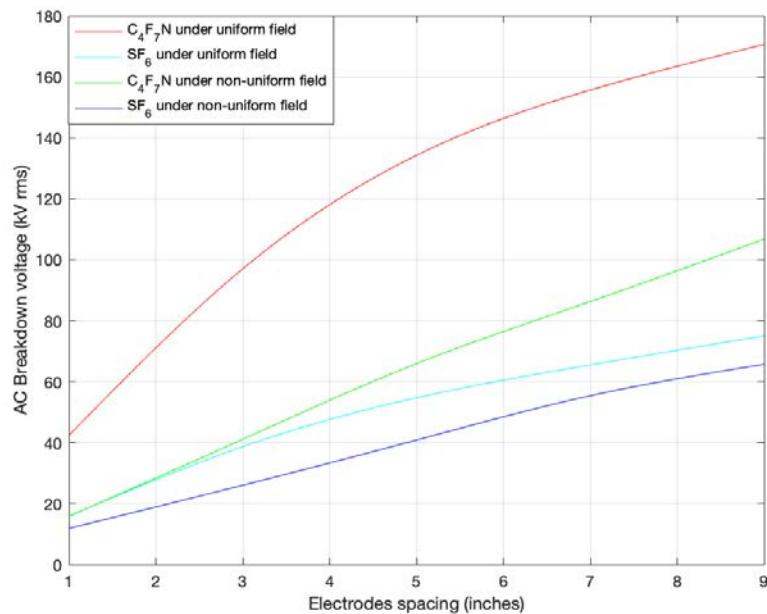


Figure 3.2: AC breakdown voltage of C_4F_7N and SF_6 with different field utilization factors

Breakdown voltage shows a direct relation with electrodes spacing: the increase of the latter leads to the increase of the other.

The difference between the uniform and non-uniform field case is considerable because in the first case C_4F_7N breakdown voltage is always much higher than that of SF_6

since in the second case this difference is much smaller.

C_4F_7N and SF_6 breakdown voltage in dependence on electrodes spacing under positive lightning impulse environment is illustrated in the figure 3.3; different field uniformities are considered.

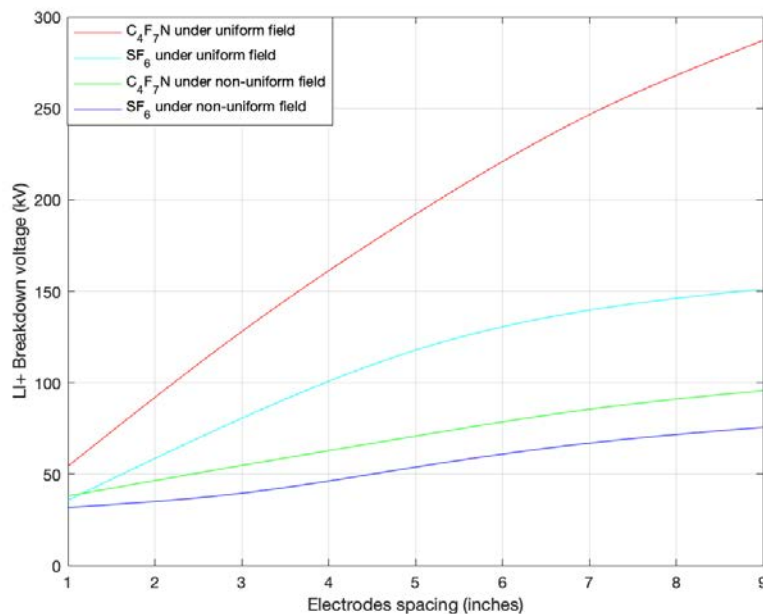


Figure 3.3: Positive lightning impulse breakdown voltage of C_4F_7N and SF_6 with different field utilization factors

A lightning impulse environment is quite different from the AC case and that results in some differences in breakdown voltage values and curves.

In case of positive impulse, the breakdown voltage of both gases results much higher than in the AC case and some relative ratios are also different: C_4F_7N breakdown voltage under non-uniform field results always lower than that of SF_6 under uniform field since in the AC case it is the opposite.

In both cases SF_6 under non-uniform field has the lowest breakdown voltage for all electrodes distance values and C_4F_7N breakdown voltage increase with electrodes spacing is much more evident in the non-uniform field case than in the uniform one, as can be seen by looking at the absolute values in the two figures [6, 20].

3.1.4 C₄F₇N mixtures

C₄F₇N has, as previously seen, a relatively high liquefaction temperature and for this reason it is difficult to replace SF₆ with this gas in pure form.

Therefore N₂, CO₂ or other buffer gases are necessary to make a suitable mixed gas for GIL applications.

The goal is to find the best compromise between minimum boiling temperature, dielectric strength and environmental impact by varying C₄F₇N content and pressure [6].

C₄F₇N / CO₂ mixture

C₄F₇N / CO₂ mixture was proposed for the first time at CIGRE 2014 by Alstom Grid (now GE Grid Solutions) and at CIRED 2015 as a SF₆ potential substitute for HV switchgears.

This mixture incorporates benefits from both its constituents gases, in particular the high dielectric strength of C₄F₇N and the low liquefaction temperature of CO₂.

C₄F₇N / CO₂ mixture is also known with the commercial name of g³ and can be considered a technically and economically viable alternative to sulphur hexafluoride for use in high-voltage GILs, with a GWP at least 98% lower than that of SF₆.

In the figure 3.4 GWP dependence on g³ mixing ratio is shown, with values of C₄F₇N content only considered up to 20% due to the fact that further increases in this parameter would only lead to a derisory dielectric strength improvement in comparison with the negative effect on GWP and liquefaction temperature.

Focusing the attention on the particular mixing ratio 4% C₄F₇N / 96 % CO₂ which is a good choice from the point of view of the synergistic effect, a GWP of about 300 is achieved, 98.4% lower than that of SF₆.

In addition, this gas mixture was shown to be thermally stable up to 800°C, which is far above the maximum temperature of an high-voltage GIL in normal conditions.

C₄F₇N / CO₂ mixture allows designers to develop environmentally friendly high-voltage GILs with the same dimensional footprint and performance as current SF₆ equivalent equipment.

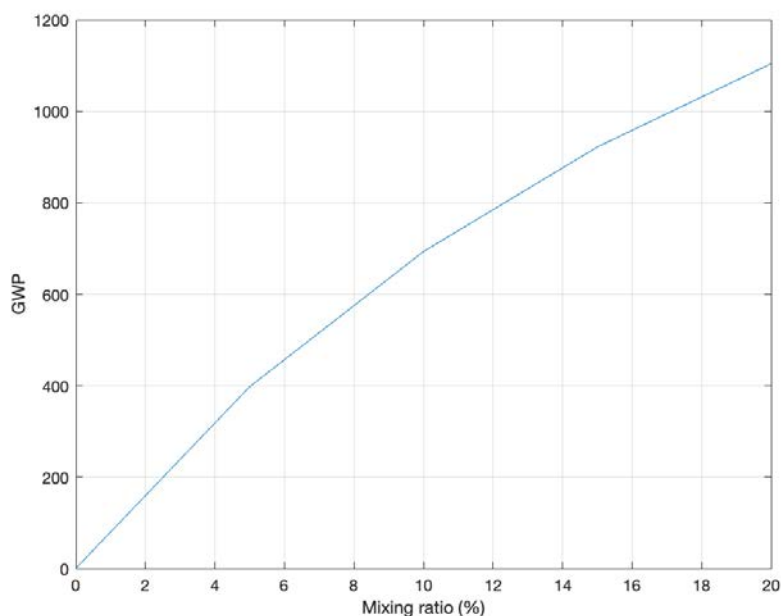


Figure 3.4: GWP (ITH = 100) of C_4F_7N / CO_2 mixture

g^3 is classified in the lowest risk category from the point of view of toxicity according to regulation (EC) No. 1272/2008 of the European Parliament and of the Council of 16 December 2008 on the classification, labeling, and packaging of substances and mixtures.

In case of discharge, byproducts could include CO (coming from the CO_2 degradation) and some fluorinated compounds coming from the degradation of C_4F_7N .

The LC_{50} determined on eventual arced g^3 gas according to OECD 403 (acute toxicity) is 64000 ppm.

This mixture is thus not classified in an hazard category according to CLP because the acute toxicity is very low.

This hazard level suggests that the arced g^3 gas would not require any different handling practices compared with those used to control arced SF_6 .

Anyway, in a GIL arcs don't occur thus these are only theoretical considerations, moreover CO detectors are widely commercially available and specific adsorbents can be also installed to further reduce any risk associated with the generation of

fluorinated byproducts during service conditions.

On the subject of the electric insulation characteristics of this mixture, several tests have been carried out considering a C₄F₇N mixing ratio ranging from 0 to 20% due to the fact that, as said before, for higher concentrations the mixture dielectric strength increases at a much slower rate (synergistic effect) not justifying the associated GWP worsening and boiling point rise.

In the figure 3.5 a 3D representation of the AC dielectric strength of C₄F₇N / CO₂ mixture in dependence on pressure and GWP is shown.

GWP is proportional to the mixing ratio thus the same diagram would have been obtained considering mixing ratio values instead of GWP ones.

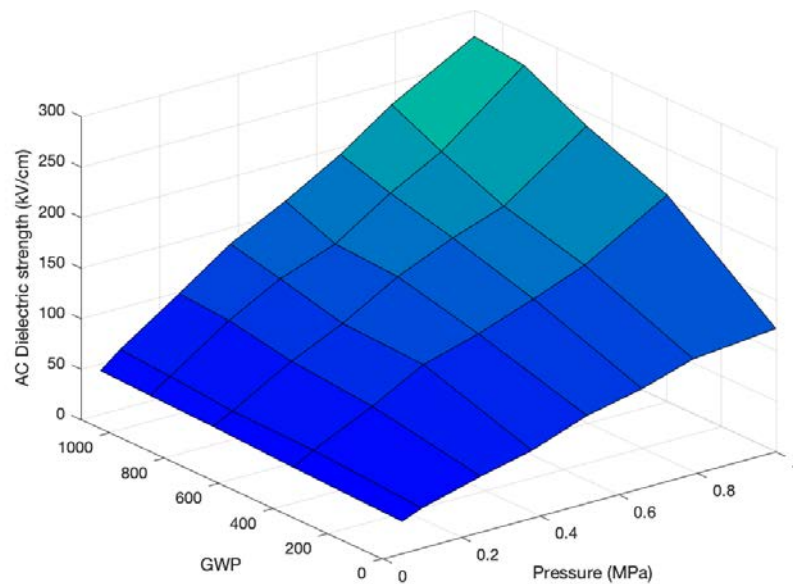


Figure 3.5: AC dielectric strength of C₄F₇N / CO₂ mixture

AC dielectric strength directly depends on pressure and GWP/mixing ratio but in the first case the dependence appears stronger than in the second one.

That means, finally, that the pressure choice affects the overall mixture insulation ability more decisively.

In the figure 3.6 the AC breakdown voltage of g³ mixtures with different mixing ratio

is compared to that of SF_6 , in dependence on the electrodes spacing and under the assumption of a uniform field at 0.1 MPa.

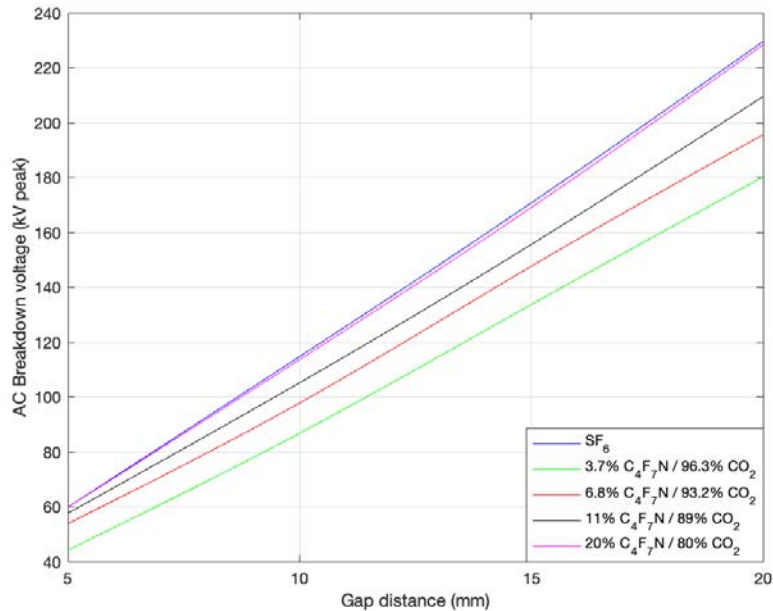


Figure 3.6: AC breakdown voltage of $\text{C}_4\text{F}_7\text{N}$ / CO_2 mixture compared to SF_6

The dielectric performance of SF_6 is reached, at 0.1 MPa, adopting a 20% $\text{C}_4\text{F}_7\text{N}$ content; however, the best compromise from the point of view of working pressure, minimum temperature and environmental impact appears to be a 3.7% $\text{C}_4\text{F}_7\text{N}$ / 96.3% CO_2 mixture.

It can be seen that the AC breakdown voltage is not directly proportional to the mixing ratio and, considering that the dielectric strength reference value to reach as minimum is not that of SF_6 but the one of the mixture 20% SF_6 / 80% N_2 , the choice of a mixing ratio near to 4% makes sense.

In the figure 3.7 a 3D representation of the dependence of mixture liquefaction temperature on pressure and mixing ratio is given and a central point is underlined: there are different possible couples of pressure-mixing ratio values which allow to obtain the same boiling point.

This means that a choice has to be done and the most logic one is the couple of values that, with the same minimum allowable working temperature, guarantees the highest mixture dielectric strength.

In order to do that, the figures 3.6 and 3.7 can be compared and it results that a 3.7% C₄F₇N /96.3% CO₂ mixture at 0.7 MPa is the best compromise with the assumption of a minimum temperature of -30 °C (standard value) even though other couples of values show only a slightly lower insulating performance.

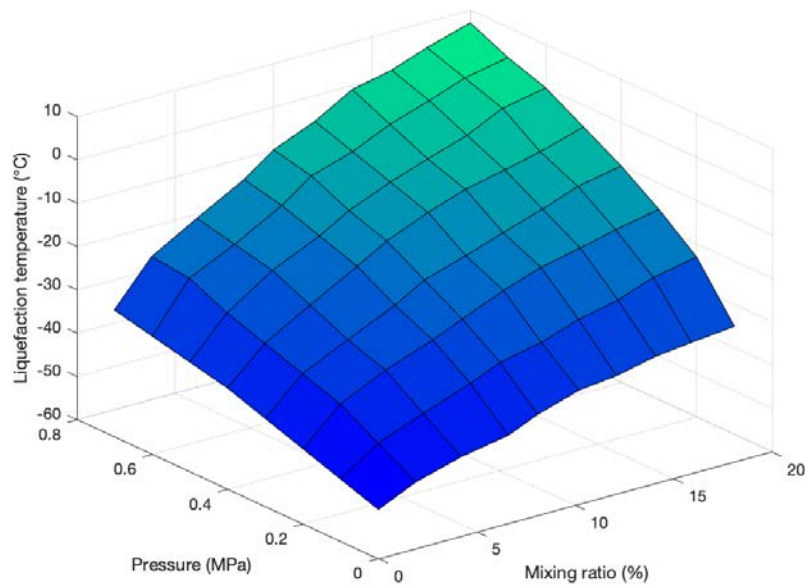


Figure 3.7: Liquefaction temperature of C₄F₇N / CO₂ mixture

It is also true that for higher mixing ratio GWP is much higher thus values over 10% should be avoided due to the environmental aspect.

This mixture reaches, at 0.55 MPa and in uniform field, 72% of SF₆ dielectric strength; in other words, there's an equivalence from the point of view of the dielectric strength, between SF₆ at 0.55 MPa and 3.7% C₄F₇N / 96.3% CO₂ mixture at 0.88 MPa or SF₆ at 0.65 MPa and 3.7% C₄F₇N / 96.3% CO₂ mixture at 1.04 MPa, leading to minimum working temperatures of -30 °C and -25 °C respectively.

In the figure 3.8 the lightning impulse breakdown voltage is analyzed as a function of

the gap distance, with both the polarities considered.

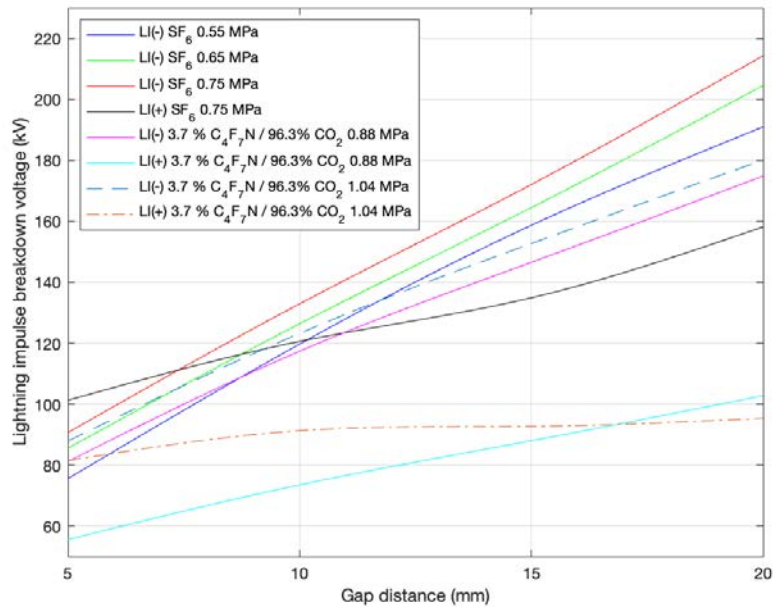


Figure 3.8: Lightning impulse breakdown voltage of 3.7% C_4F_7N / 96.3% CO_2 mixture compared to SF_6

The previously introduced equivalences, regarding pressure-dielectric strength couples of 3.7% C_4F_7N / 96.3% CO_2 mixture and SF_6 , can be identified in this diagram in the intersections between some curves related to g^3 and SF_6 respectively.

For example, under negative lightning impulse, the curve of 3.7% C_4F_7N / 96.3% CO_2 mixture at 0.88 MPa intersects the one of SF_6 at 0.55 MPa for a specific gap distance, showing in that case the same breakdown voltage.

An other observation is that positive lightning impulse breakdown voltage values are much lower than the ones of negative impulse.

Finally, the presence of protrusions in the GIL is considered and the effect of their presence on the conductor or on the enclosure on the overall insulation is analyzed.

The figure 3.9 compares PDIV of 3.7% C_4F_7N / 96.3% CO_2 mixture and SF_6 in dependence on pressure.

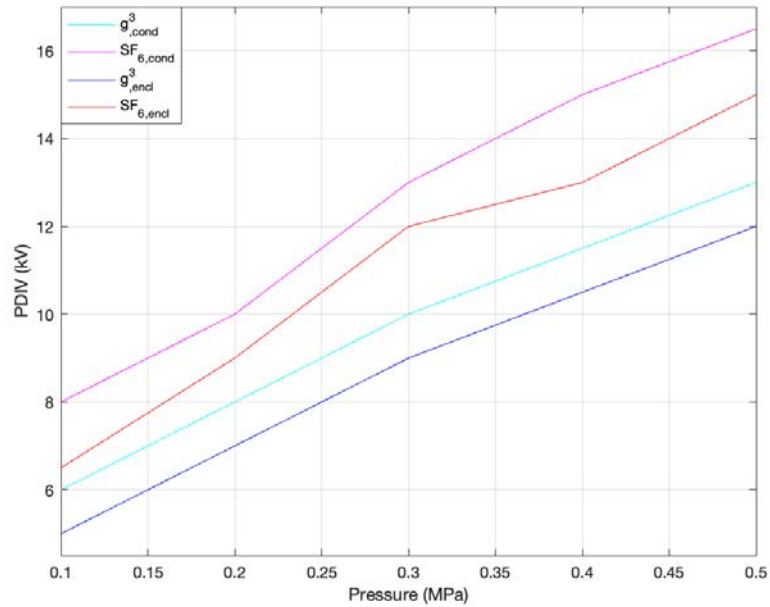


Figure 3.9: Partial discharge inception voltage of 3.7% C_4F_7N / 96.3% CO_2 mixture compared to SF_6

The hypothesis of protrusions on the enclosure results the most critical because PDIV for both g^3 and SF_6 in this case are lower than in the case with defects on the conductor.

Moreover, in both cases, g^3 performance is worse than the SF_6 one.

As it happens for breakdown voltage, partial discharge inception voltage also increases with the pressure.

Many researches demonstrated that, at the end, g^3 has the highest dielectric strength between all the C_4F_7N mixtures with other buffer gases [18].

C_4F_7N / N_2 mixture

C_4F_7N / N_2 mixture is an alternative solution to g^3 and presents some slightly different characteristics.

This mixture incorporates benefits from both its constituents gases, in particular the high dielectric strength of C_4F_7N and the low liquefaction temperature of N_2 , which

is much lower also than the one of CO_2 (- 195.8 vs - 78.5 °C).

$\text{C}_4\text{F}_7\text{N}$ / N_2 mixture has a GWP at least 97% lower than that of SF_6 , a value slightly worse than g^3 but excellent anyway.

In the figure 3.10 GWP dependence on $\text{C}_4\text{F}_7\text{N}$ / N_2 mixing ratio is shown, with values of $\text{C}_4\text{F}_7\text{N}$ content only considered up to 20% due to the fact that further increases in this parameter would only lead to a little dielectric strength improvement in comparison to the worsening effect on GWP and liquefaction temperature, the same concept introduced with g^3 description.

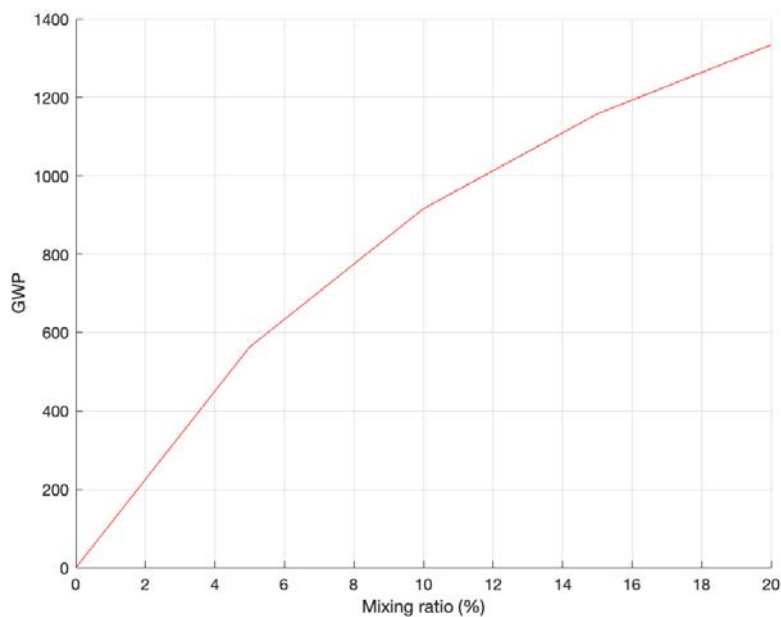


Figure 3.10: GWP (ITR =100) of $\text{C}_4\text{F}_7\text{N}$ / N_2 mixture

Making a comparison with the g^3 case, with a mixing ratio of 4% $\text{C}_4\text{F}_7\text{N}$ / 96 % N_2 , a GWP of about 500 is achieved, 97.6% lower than that of SF_6 , a slightly worse result but really good in any case.

$\text{C}_4\text{F}_7\text{N}$ / N_2 mixture would allow designers to develop environmentally friendly high-voltage GIL with the same dimensional footprint and performance as current SF_6 equivalent equipment.

In case of discharge, decomposition byproducts can be produced and they include

CF_4 , C_3F_8 , C_3F_6 , C_2F_4 , C_2F_5CN and CF_3CN , with these last two which are highly toxic gases.

Focusing on the electric insulation characteristics of this mixture, several tests have been carried out considering a C_4F_7N mixing ratio ranging from 0 to 20% due to the fact that, as said before, for higher concentrations the mixture dielectric strength increases at a much slower rate (synergistic effect) not justifying the associated GWP worsening and boiling point rise.

With regard to the electrical insulation properties, in the figure 3.11 the AC breakdown voltage of C_4F_7N / N_2 mixture with different mixing ratio is compared to that of SF_6 , in dependence on pressure.

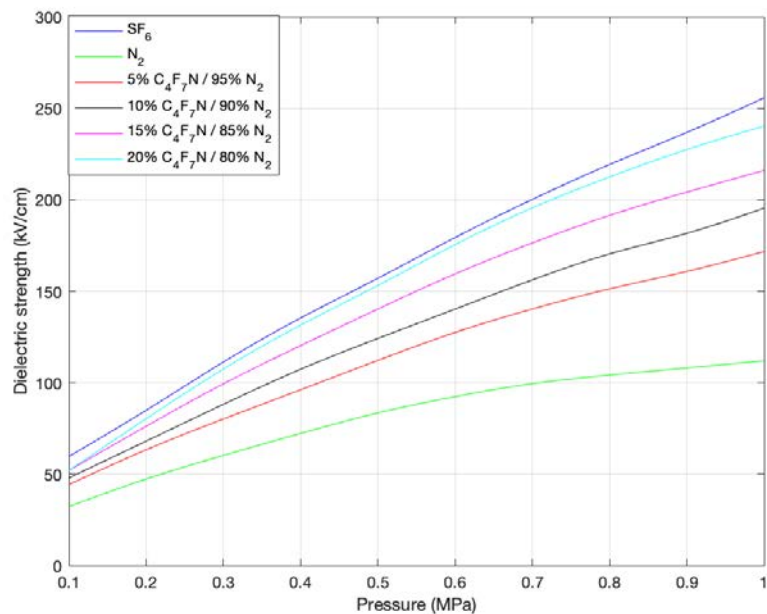


Figure 3.11: AC dielectric strength of C_4F_7N / N_2 mixture

The insulation performance of C_4F_7N / N_2 mixture increases with the mixing ratio. Relatively to SF_6 , the insulation performance of gas mixture at high pressure (0.5-0.6 MPa) shows a saturation growth trend with the mixing ratio.

The mixture breakdown voltage for a minimum operating temperature of $-30\text{ }^\circ\text{C}$ at

0.3 MPa, 0.4 MPa, 0.5 MPa, and 0.6 MPa is about 63.4%, 54.6%, 49%, and 56.4% of pure SF₆.

In the figure 3.12 a 3D representation of the dependence of mixture liquefaction temperature on pressure and mixing ratio is given and a central point, as before, is underlined: there are different possible couples of pressure-mixing ratio values which allow to obtain the same boiling point.

By comparing figures 3.11 and 3.12 it can be found that a 5% C₄F₇N / 95% N₂ mixture at 0.6 MPa is the best compromise with the assumption of a minimum temperature of -30 °C (standard value) even though other couples of values show only a slightly lower insulating performance.

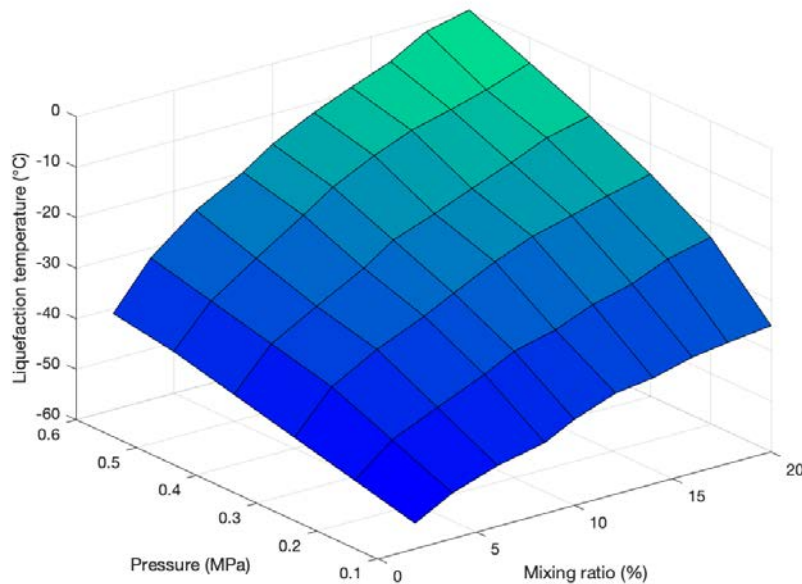


Figure 3.12: Liquefaction temperature of C₄F₇N / N₂ mixture

For higher mixing ratios GWP is much higher thus values over 12% should be avoided anyway due to the environmental impact of too high C₄F₇N contents.

The breakdown voltage of a 12% C₄F₇N / 88% N₂ mixture at 0.4 MPa is equivalent to pure SF₆ at 0.2 MPa.

In addition, relatively to SF₆, the dielectric strength of C₄F₇N / N₂ mixture reaches

its maximum value at 0.3 MPa or 0.2 MPa and decreases at higher pressure.

Always in relation to SF_6 , the breakdown voltage of this mixture at high pressure (0.5-0.6 MPa) is lower than at low pressure.

Finally, in the 3D figures 3.13 and 3.14 partial discharge inception voltages of C_4F_7N / N_2 mixture in relation to SF_6 are reported in dependence on pressure and mixing ratio.

In the first one a positive polarity is considered since in the second one a negative polarity is analyzed.

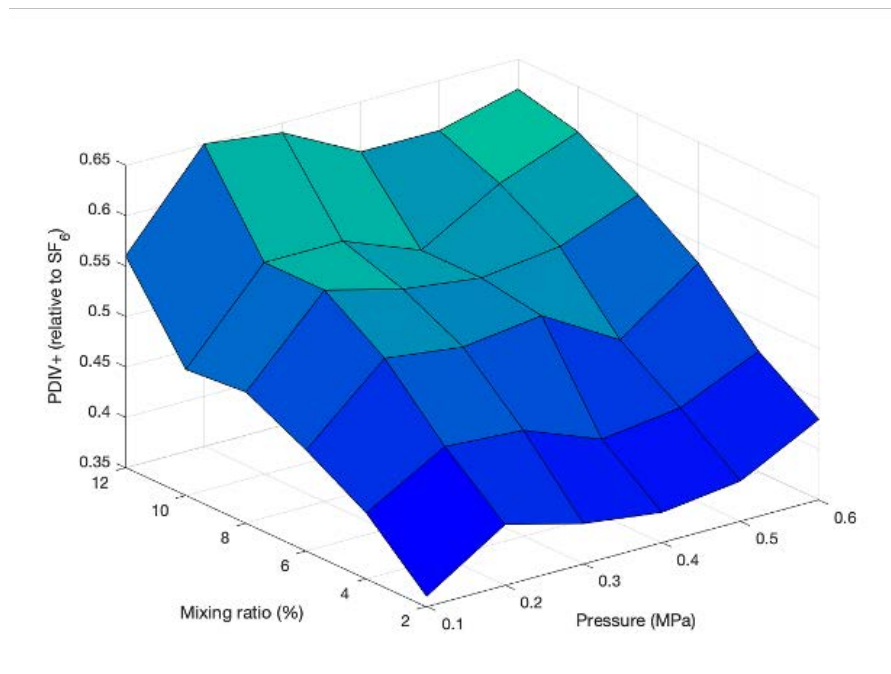


Figure 3.13: PDIV₊ of C_4F_7N / N_2 mixture in relation to SF_6

In the positive polarity case, the maximum relative PDIV value reaches 0.65, thus the insulation from partial discharges is quite worse than the one of SF_6 .

It can be noted that the highest value is localized at 0.2 MPa and with the pressure increase relative PDIV firstly decreases and at the end increases again at 0.6 MPa.

This parameter increases not only with pressure but also with the mixing ratio, in fact the maximum value is with a 12% of C_4F_7N content, the maximum one considered.

In the case of negative polarity, different elements can be underlined.

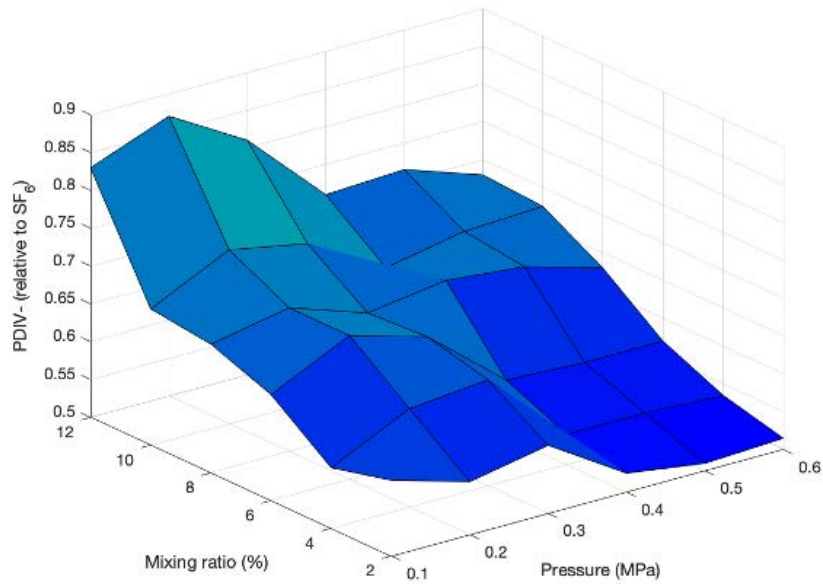


Figure 3.14: PDIV- of C₄F₇N / N₂ mixture in relation to SF₆

First of all, the maximum relative PDIV value is much higher than in the positive case and reaches 0.9, always at 0.2 MPa.

The curve is also different because relative PDIV decreases in a monotonous way reaching the lowest value at 0.6 MPa, differently from the previous case.

The lowest value is also higher than the lowest one of the positive case (0.53 vs 0.36).

At the end, C₄F₇N / N₂ mixture shows very attractive dielectric properties but, in practice, a C₄F₇N / CO₂ mixture is preferred due to the better chemical stability of CO₂ than N₂ in combination with C₄F₇N [17].

3.2 Perfluoropentanone (C₅F₁₀O)

3.2.1 Physicochemical properties

Perfluoropentanone CF₃C(=O)CF(CF₃)₂, commonly known as C₅F₁₀O, belongs to the fluoroketones (FKs) or perfluorinated ketones family, characterized by a crude formula of the form C_nF_{2n}O, where n is an integer ranging between 3 and 8.

It is also referred to as C5 PFK or C5 FK and is represented by the systematic name 1,1,1,3,4,4,4-heptafluoro-3-(trifluoromethyl)-2-butanone.

The C₅F₁₀O molecular structure is shown in the figure 3.15.

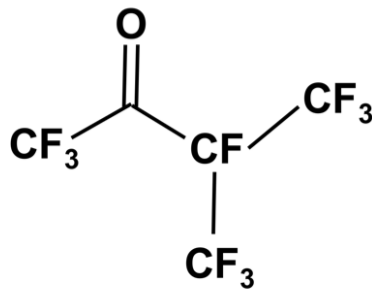


Figure 3.15: Molecular structure of the perfluoropentanone C₅F₁₀O

Some of the physicochemical parameters characterizing this gas are reported in the table 3.4.

C₅F₁₀O presents an high volatility and is stable at temperatures up to 600 °C.

Molecular weight appears to be quite high and this strictly affects the boiling point due to the connection, valid for gases in general, between an high molar mass and an high condensation point.

This fact determines the impossibility of using this gas alone at atmospheric pressure in high-voltage insulation because the liquefaction would occur at 26.9 °C, a normal operating condition for a GIL whose temperature working range can reach - 30 °C or below.

Therefore C₅F₁₀O has to be admixed with a carrier gas of high vapor pressure to reduce the liquefaction temperature and become attractive for some applications.

Table 3.4: Physicochemical properties of $C_5F_{10}O$

Parameter	Value	Unit
Molecular weight	266.04	g/mol
Density	1.55	g/cm ³
Freezing point	- 110	°C
Boiling point at 1 bar	26.9	°C
Saturated vapor pressure at - 30 °C	0.009	MPa
Saturated vapor pressure at 0 °C	0.030	MPa
Saturated vapor pressure at 20 °C	0.060	MPa
Flammability	non-flammable	
Explosiveness	non-explosive	
Chemical stability	stable	
Thermal stability	stable up to 600 °C	
Corrosivity	non-corrosive	
Appearance	colourless/odourless	

In the figure 3.16 it is presented the vapor pressure of $C_5F_{10}O$ with dependence on temperature compared to that of SF_6 .

$C_5F_{10}O$ saturated vapor pressure results much lower than the one of SF_6 for a fixed temperature and this is an other demonstration of the need to make a mixture with an other buffer gas with very low liquefaction temperature like N_2 , CO_2 or air.

The liquefaction temperature is also affected by the fluorine content: this is the reason why, between perfluoroketones, C_3F_6O has the lowest boiling point since $C_8F_{16}O$ has the highest one, as it can be seen from the figure 3.17.

C_5 PFK is substantially non-toxic in the pure state, or rather has a low inhalation toxicity, as reported in the table 3.5.

However, the breakage of the C-C bond between carbonyl carbon and α -carbon atom can easily occur in case of discharge leading to the generation of CF_3CO and C_3F_7 or C_3F_7CO and CF_3 .

They can further react producing CF_4 , C_2F_6 , C_3F_8 , C_3F_6 , C_4F_{10} , C_5F_{12} and C_6F_{14} .

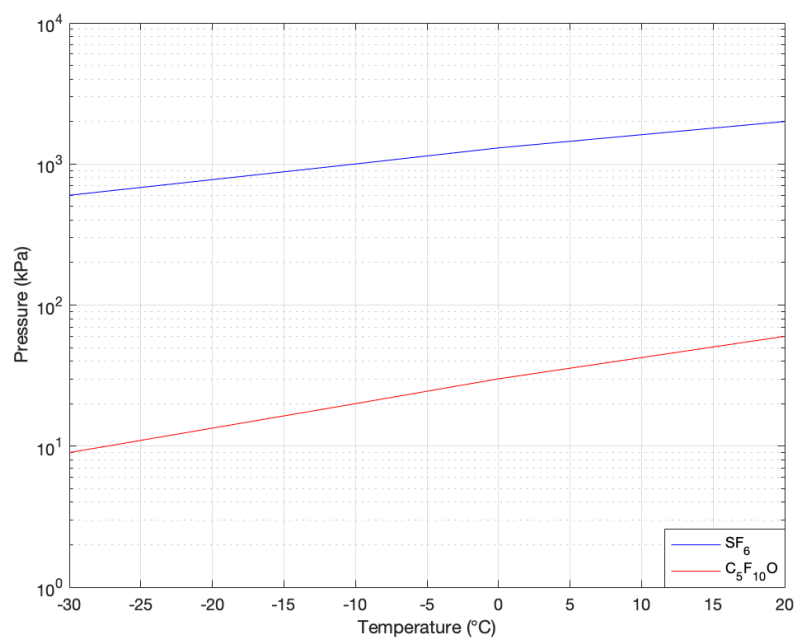
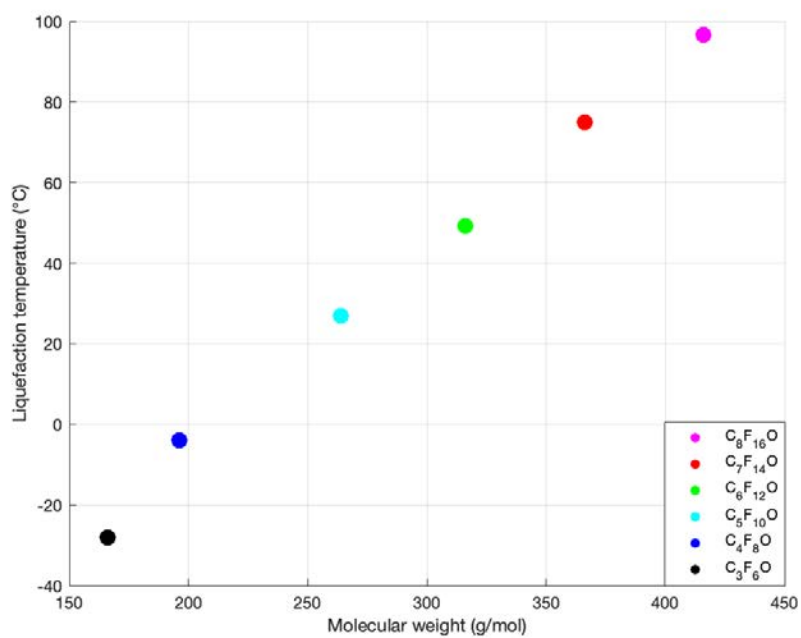
Figure 3.16: Saturated vapor pressure of $C_5F_{10}O$ and SF_6 

Figure 3.17: Liquefaction temperature at 0.1 MPa of perfluoroketones

These byproducts cannot reassemble into $C_5F_{10}O$ when the environment temperature cools down and, as a result, the breakdown voltage gradually decreases.

Among the products, C_2F_6 , C_3F_6 and C_4F_8 have choking, bronchitis, anesthetic and pneumonia effects.

Fortunately, the content of $C_5F_{10}O$ in practical application is below 20% and the concentration of products is extremely low.

It has been verified that during discharge, the product of C_3F_6 is about 50 ppm but just 6.5 ppb leak into the air, which is far less than the exposure threshold of 0.1 ppm [6].

Table 3.5: Toxicity of $C_5F_{10}O$

Parameter	Value	Unit
LC50	20000	ppm
TWA	100	ppm

3.2.2 Environmental properties

This compound was released as a commercial product by 3MTM Company under the name NOVECTM 5110 and represents one of the most promising low GWP alternatives to SF_6 .

From the point of view of the environmental impact, $C_5F_{10}O$ can be considered as an exceptional candidate due to its negligible ODP, an atmospheric lifetime of only 14 days and a GWP lower than the one of CO_2 , as shown in the table 3.6.

Table 3.6: Environmental properties of $C_5F_{10}O$

Parameter	Value	Unit
GWP (ITH = 100 years)	1	
ODP	0	
Atmospheric lifetime	14	days

GWP is very low thanks to the fact that $C_5F_{10}O$ decomposes in a few days in the atmosphere by UV photolysis to form substances not detrimental to environment [6].

3.2.3 Dielectric properties

C₅F₁₀O presents high insulation capabilities: its intrinsic dielectric strength is 180 kV/cm at atmospheric pressure, twice the one of SF₆ (89 kV/cm) at the same pressure. Studies have been made on C₆F₁₂O, which is also a gas of the perfluoroketones family and presents a dielectric strength of 235.0 kV/cm but, unfortunately, has a much higher boiling point: 49.2 °C [6].

3.2.4 C₅F₁₀O mixtures

The dew point of fluid dielectric, as introduced previously, is really important since it defines the maximum gas quantity that can be used in a given piece of equipment without the risk of condensation at the minimum operating temperature.

That is why C₅F₁₀O based mixtures are considered: mixing C5 PFK with a carrier gas characterized by a very low liquefaction temperature and a low GWP, like the natural gases O₂, N₂, CO₂ or dry air, allows to put down the boiling point of the gas to a temperature suitable for the specific application maintaining the same low GWP. Furthermore, in this way, the operating pressure range can reach much higher values due to the fact that limited practical partial pressure of C₅F₁₀O, lower than the typical working pressure of SF₆ based HV GILs, is balanced by the really higher applicable partial pressure of the buffer gas.

From the figure 3.16 it can be determined the maximum allowable C₅F₁₀O partial pressure in the mixture in dependence on the minimum operating temperature: for example, considering two minimum GIL working temperatures as - 5 °C (specific) and - 30 °C (standard), C5 PFK partial pressure results 0.028 and 0.009 MPa respectively. On the other hand, a C5 PFK mixture shows a much lower dielectric strength than pure C₅F₁₀O and this highlights the need of an accurate determination of mixture pressure and pure C5 PFK content ratio as both these parameters affect the overall dielectric insulation performance [6].

C₅F₁₀O / air mixture

C₅F₁₀O / air mixture incorporates benefits from both its components, in particular the high dielectric strength of C₅F₁₀O and the low liquefaction temperature of air.

In addition, air is easily available and this lowers mixture overall costs.

This mixture has a GWP nearly 100% lower than that of SF₆.

In the figure 3.18 GWP dependence on mixture mixing ratio is shown, with values of C₅F₁₀O content considered up to 100% due to the fact that in this case increases in this parameter don't significantly affect GWP which always remains under the unit value.

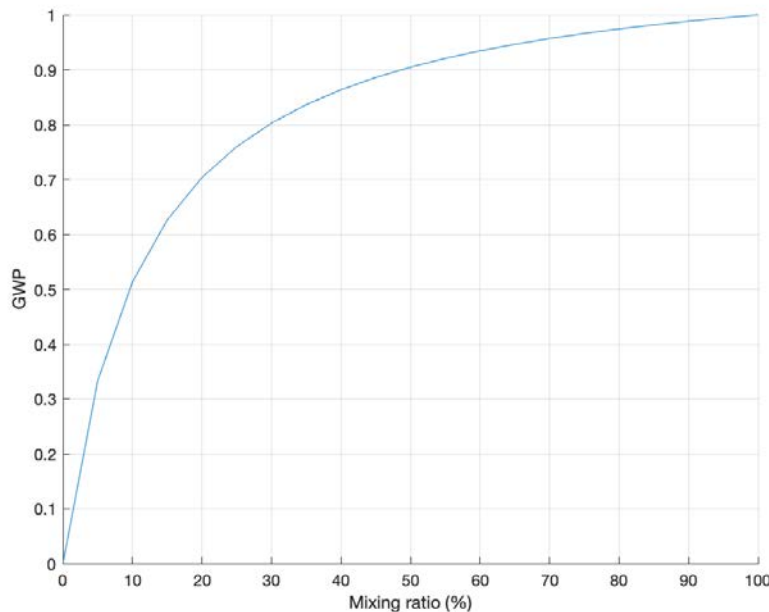


Figure 3.18: GWP (ITH =100) of C₅F₁₀O / air mixture

However, liquefaction temperature continues to be strongly and negatively influenced by the mixing ratio thus values higher than 20% cannot be adopted.

Environmental analysis show that C₅ PFK mixtures are much more eco-friendly than C₄ mixtures.

In case of discharge, byproducts could include CF₄, C₂F₆, CF₂O, C₃F₈, CO₂, C₄F₁₀

and C_3F_7H [28].

Therefore this mixture is not classified in an hazard category because the acute toxicity is very low.

Regarding dielectric properties, this mixture shows a great potential in comparison with SF_6 , as can be noted from the figure 3.19 in which $C_5F_{10}O$ / air mixture AC dielectric strength is reported in dependence on gas pressure and C_5 PFK partial pressure.

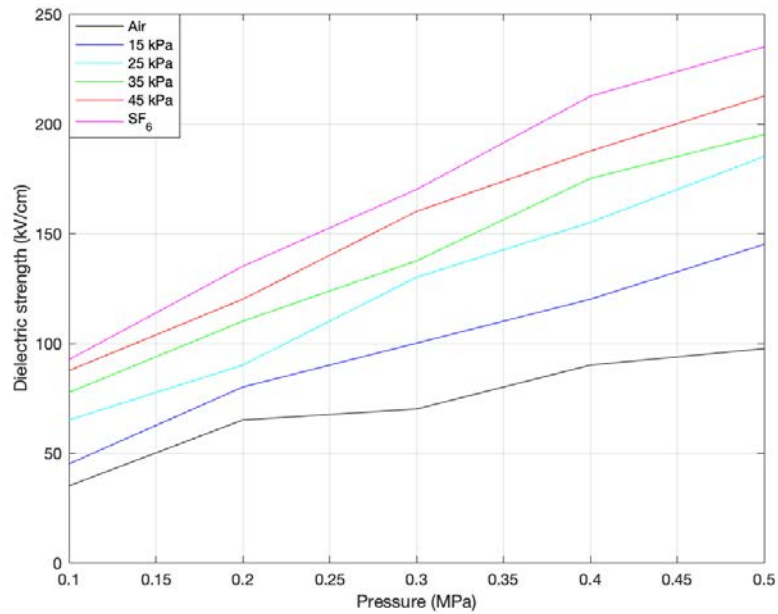


Figure 3.19: AC dielectric strength of $C_5F_{10}O$ / air mixture compared to SF_6 and pure air

For example, when the gas pressure is 0.2 MPa and the partial pressure of C_5 PFK is 25 kPa, the dielectric strength of $C_5F_{10}O$ / air mixture is 0.72 times that of SF_6 at the same pressure.

When the gas pressure is increased to 0.3 MPa, the dielectric strength of $C_5F_{10}O$ / air mixture is 0.98 times that of SF_6 at 0.2 MPa.

Finally, when the partial pressure of C_5 PFK is high enough, the relative dielectric strength of $C_5F_{10}O$ gas mixtures at each gas pressure approaches a certain value that

for the $C_5F_{10}O$ / air mixture is about 0.91.

Therefore, the insulation strength of $C_5F_{10}O$ / air gas mixtures under the same gas pressure are always lower than that of SF_6 and with the increase of partial pressure of C_5 PFK the promotion effect of the insulation strength becomes less obvious with the increase of gas pressure.

When the partial pressure of C_5 PFK reaches 45 kPa, the liquefaction temperature of the gas mixtures reach 5.56 °C, a too high value for a standard industrial GIL application.

In addition, the dielectric strength of $C_5F_{10}O$ gas mixtures at a partial pressure of 15 kPa (the liquefaction temperature is -17.78 °C) reaches only 50% of the one of SF_6 , thus an intermediate value between these two values (45 kPa and 15 kPa) has to be chosen [28].

$C_5F_{10}O$ / N_2 mixture

$C_5F_{10}O$ / N_2 mixture is very similar from the point of view of GWP and liquefaction temperature to $C_5F_{10}O$ / air mixture, since is slightly different considering dielectric properties.

N_2 , as air, is easily available and this lowers mixture overall costs.

In case of discharge, byproducts could include CF_4 , C_2F_6 , C_3F_8 , C_2F_4 , C_4F_{10} , C_3F_6 and C_3F_7H [28].

This mixture is thus not classified in an hazard category due to the fact that the acute toxicity is very low.

Looking at the dielectric properties, this mixture shows a slightly lower performance in comparison with $C_5F_{10}O$ / air mixture, as it can be seen by comparing the figure 3.20 in which $C_5F_{10}O$ / N_2 mixture AC dielectric strength is reported in dependence on gas pressure and C_5 PFK partial pressure, and the figure 3.19 relative to $C_5F_{10}O$ / air mixture.

The AC breakdown voltage of $C_5F_{10}O$ / N_2 mixture is lower than that of $C_5F_{10}O$ / air mixture under the same conditions.

The relative growth rate of breakdown voltage of $C_5F_{10}O$ / N_2 mixture is lower than

that of $C_5F_{10}O$ / air mixture, indicating that the breakdown voltage of the first one is more affected by gas pressure.

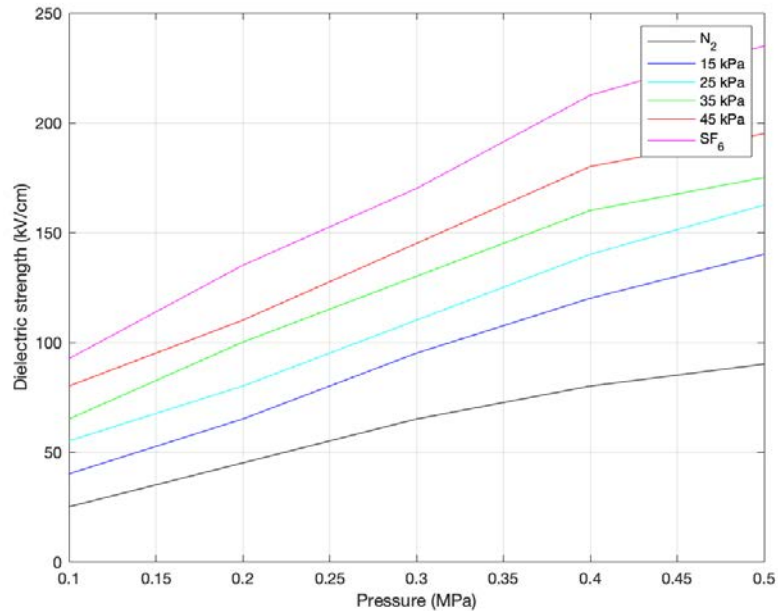


Figure 3.20: AC dielectric strength of $C_5F_{10}O$ / N_2 mixture compared to SF_6 and pure N_2

In addition, when the partial voltage of $C_5F_{10}O$ is greater than 15 kPa, the breakdown voltage of $C_5F_{10}O$ / N_2 mixture increases with the partial voltage of $C_5F_{10}O$ at a rate similar to that of $C_5F_{10}O$ / air mixture.

Looking at the figure 3.20 it can be seen that, for example, when the gas pressure is 0.2 MPa and the partial pressure of $C_5F_{10}O$ is 25 kPa, the dielectric strength of $C_5F_{10}O$ / N_2 mixture is 0.63 times that of SF_6 at the same pressure.

Increasing the gas pressure to 0.3 MPa, instead, the dielectric strength of $C_5F_{10}O$ / N_2 mixture is 0.84 times that of SF_6 at 0.2 MPa.

Finally, when the partial pressure of C_5 PFK is high enough, the relative dielectric strength of the $C_5F_{10}O$ gas mixtures at each gas pressure approaches a certain value that for the $C_5F_{10}O$ / N_2 mixture is about 0.84.

Therefore, also in this case, the insulation strength of the mixture under the same

gas pressure is always lower than that of SF_6 and with the increase of C_5 PFK partial pressure the promotion effect of the insulation strength becomes less obvious with the increase of gas pressure.

In relation to the choice of the best mixing ratio, similar consideration to the case of $\text{C}_5\text{F}_{10}\text{O}$ / air mixture can be made [28].

$\text{C}_5\text{F}_{10}\text{O}$ / CO_2 / O_2 mixture

C_5 PFK / CO_2 / O_2 mixture is an other possible alternative to SF_6 considering its GWP and its potential overall dielectric strength, as it can be noted from the figure 3.21.

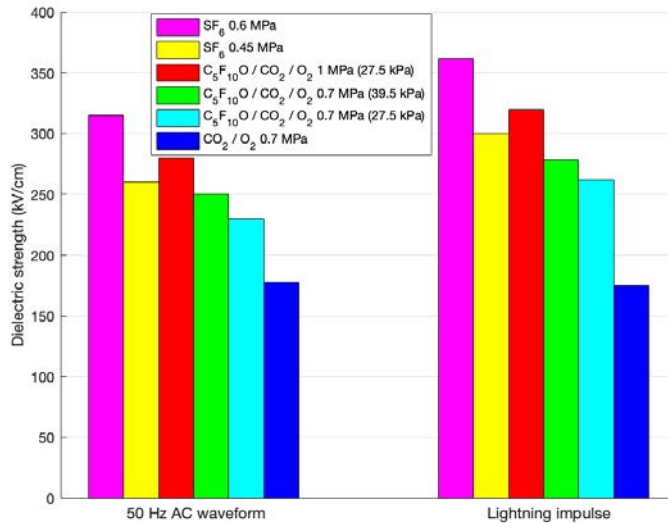


Figure 3.21: Lightning impulse and AC dielectric strength of $\text{C}_5\text{F}_{10}\text{O}$ / CO_2 / O_2 mixture and SF_6 under uniform electric field

All tests which these data are taken from are performed under the hypothesis of uniform electric field and one of the results is that adding a small quantity of pure $\text{C}_5\text{F}_{10}\text{O}$ to the CO_2 / O_2 mixture results in a significant improvement of the gas insulation performance without a GWP worsening.

More precisely it can be verified that, at 0.7 MPa, a performance rise of also 35-50 % is achieved.

In other words, the dielectric performance gap between C_5 PFK / CO_2 / O_2 mixture at 0.7 MPa and SF_6 at 0.6 MPa is less than half of the one between CO_2 / O_2 mixture at 0.7 MPa and SF_6 at 0.6 MPa.

Finally, the dielectric strength of $C_5F_{10}O$ / CO_2 / O_2 mixture at 1MPa is above the one of SF_6 at 0.45 MPa.

An interesting case of study is the one concerning the presence of small defects in the GIL, a situation more critical than the previous one since the electrical field is not uniform any more but highly non-uniform, thus affecting the dielectric insulation performance more strongly.

In these tests a 1.2 mm long needle is used and electrodes spacing is set to 10 mm.

The results are shown in the figure 3.22 where it can be pointed out that the $C_5F_{10}O$ / CO_2 / O_2 mixture at 0.7 MPa has an insulation capability slightly lower than that of SF_6 at 0.45 MPa.

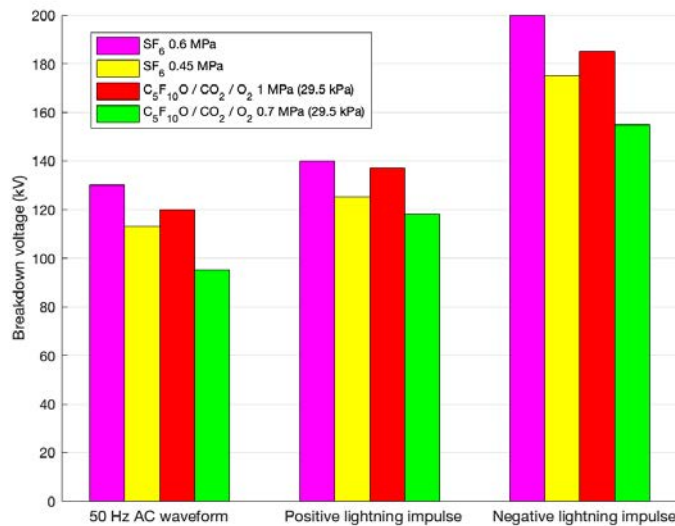


Figure 3.22: Lightning impulse and AC breakdown voltage of $C_5F_{10}O$ / CO_2 / O_2 mixture and SF_6 under particle-like field

A breakdown voltage similar to that of SF_6 at 0.6 MPa can be reached by increasing the mixture pressure up to 1 MPa [6].

C₅F₁₀O / N₂ / O₂ mixture

A last possibility is represented by a C₅F₁₀O / N₂ / O₂ mixture, also characterized by a very low GWP, a low boiling point (depending on mixing ratios) and dielectric strength slightly different from C₅F₁₀O / CO₂ / O₂ mixture.

On this last topic, the dielectric strength of C₅F₁₀O / N₂ / O₂ mixture increases with an increase in oxygen concentration under a slightly uneven electric field, as can be noted from the figure 3.23, referred to a gas pressure of 0.2 MPa and a C₅ PFK partial pressure of 15 kPa.

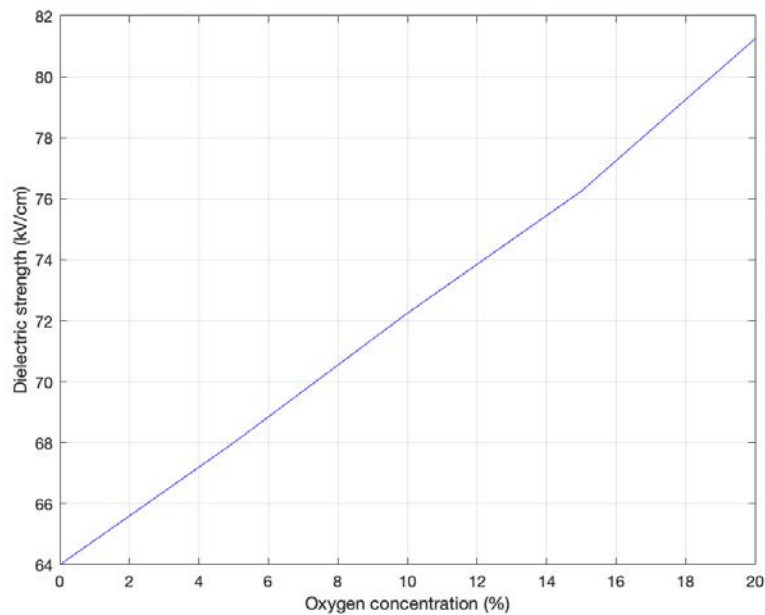


Figure 3.23: AC dielectric strength of C₅F₁₀O / N₂ / O₂ mixture in dependence on oxygen concentration

Carbon precipitates on the electrode surfaces can normally occur but they disappear after multiple discharge breakdowns when 0.5% or more of O₂ is added to the gas mixture [29].

With an increase in the oxygen concentration, the quantity of CF₄ produced, which is a typical decomposition product of this type of mixtures, decreases since the amount of C₂F₆ increases.

When the oxygen content reaches 7.5%, C₂F₄ and C₃F₆ disappear due to the reaction with oxygen to form CF₂O.

The addition of oxygen inhibits the formation of C₂F₆, C₃F₈, C₄F₁₀ and C₃F₇H to a certain extent.

CF₂O generated after the C₅F₁₀O / N₂ / O₂ mixture discharge breakdown is highly corrosive and extremely toxic, which is harmful to the equipment and personnel.

Therefore, it is not preferable to increase the dielectric strength of C₅F₁₀O / N₂ / O₂ by further increasing the oxygen concentration: the recommended C₅F₁₀O / O₂ ratio is 1:1 [29].

3.3 Trifluoroiodomethane (CF₃I)

3.3.1 Physicochemical properties

Trifluoroiodomethane CF₃I, named also iodotrifluoromethane or trifluoromethyl iodide, belongs to the halomethane family and is an experimental alternative to Halon 1301 (CBrF₃, very diffused as refrigerant liquid and the most effective fire extinguishing agent).

CF₃I molecule is formed by three fluorine atoms, one iodine atom and one central carbon atom as shown in the figure 3.24.

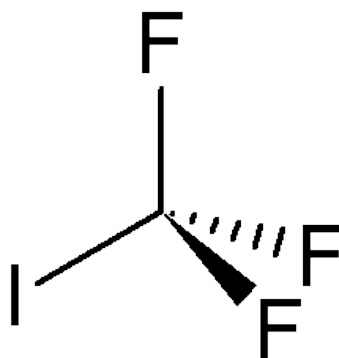


Figure 3.24: Molecular structure of trifluoroiodomethane CF₃I

Iodine and carbon atoms have a quite high electronegativity but the fluorine atom is the highest electronegative atom in nature, thus the CF_3I molecule can absorb free electrons and delay the discharge initiation.

Some of the physicochemical parameters characterizing this gas are reported in the table 3.7.

Table 3.7: Physicochemical properties of CF_3I

Parameter	Value	Unit
Molecular weight	195.91	g/mol
Density	2.55	g/cm ³
Freezing point	- 110	°C
Boiling point at 1 bar	- 22.5	°C
Saturated vapor pressure at - 30 °C	0.075	MPa
Saturated vapor pressure at 0 °C	0.25	MPa
Saturated vapor pressure at 20 °C	0.45	MPa
Flammability	non-flammable	
Explosiveness	non-explosive	
Chemical stability	stable	
Thermal stability	stable up to 700 °C	
Corrosivity	non-corrosive	
Solubility in water	slightly soluble	
Appearance	colourless/odourless	

It can be noted that CF_3I is characterized by a relatively high liquefaction temperature (- 22.5 °C) which determines the need to adopt buffer gases, typically CO_2 , in order to be used in HV applications.

In the figure 3.25 CF_3I saturated vapor pressure in dependence on temperature is reported and compared to that of SF_6 , showing that with a small pressure increment the CF_3I boiling point increases.

For example, considering a widely used pressure value for GIL of 0.5 MPa, the boiling point of pure CF_3I is around 25 °C.

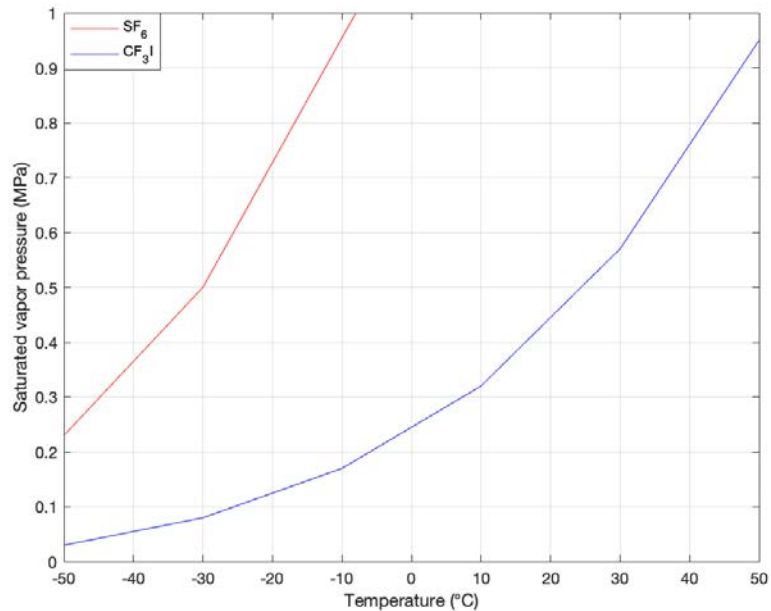


Figure 3.25: CF₃I and SF₆ saturated vapor pressure

Studies based on inhalation tests carried out on animals, show that CF₃I is a slightly toxic gas.

The US National Research Council's (NRC) committee on toxicology has recommended that CF₃I has no observed adverse level (NOAEL) on cardiac sensitization if the concentration is 0.2%, whereas the lowest observed adverse level (LOAEL) is at 0.4%.

In case of partial discharge, some decomposition products can appear including hexafluoroethane (C₂F₆), which is the predominant one, tetrafluoroethane (C₂F₄) and pentafluoroethyl iodide (C₂F₅I).

The presence of other minor byproducts like octafluoropropane (C₃F₈), trifluoromethane (CHF₃), hexafluoropropene (C₃F₆) and methyl iodide (CH₃I) could be observed. Basically, due to the three fluorine atoms composing the trifluoroiodomethane molecule, it is expected that after discharge some fluorine is formed.

This byproduct is especially important because is toxic and, moreover, is harmful for insulating material.

Finally, trifluoroiodomethane has, as said before, a weak bond between carbon and

iodine atoms thus, when a discharge occurs in CF_3I , iodine is produced.

It is important to note that the ratio between the amount of iodine produced with a 30% CF_3I / 70% CO_2 mixture and pure CF_3I is around 1/3, indicating that the volume of iodine produced is proportional to the CF_3I present in the mixture.

The production of iodine happens when a discharge occurs and the result is that I_2 molecules are deposited in a solid state on the nearby surfaces.

This represents a risk for the systems which use CF_3I firstly because the insulating capability decreases due to the fact that iodine particles are metallic and secondly because iodine can corrode materials used in the gas system.

In particular, the insulation performance is seriously affected by iodine byproduct because it creates an easier condition for sparkover.

The adoption of an activated carbon C_2X is a reliable method to adsorb iodine byproduct and greater is the quantity of the activated carbon, higher is the number of sustainable partial discharges [5, 31].

3.3.2 Environmental properties

CF_3I presents a very low GWP, thanks to the weak bond between carbon and iodine atoms, because it easily and quickly decomposes in the atmosphere due to the solar light, the iodine goes up into the troposphere and it is finally removed with the rain. Regarding the ozone depletion potential, differently from SF_6 , CF_3I has a quantified impact, although very low, caused by the fact that a small percentage of dissociated iodine reaches the stratosphere and reacts with the ozone layer.

In addition, trifluoroiodomethane atmospheric lifetime is only of few days.

Environmental parameters are summarized in the table 3.8 [5, 31].

Table 3.8: Environmental properties of CF_3I

Parameter	Value	Unit
GWP (ITH = 100 years)	1	
ODP	0.012	
Atmospheric lifetime	5	days

3.3.3 Dielectric properties

It can be highlighted that the critical reduced field strength at which $\alpha - \eta = 0$ for CF₃I is 108 kV/cm at atmospheric pressure in comparison with 89 kV/cm for SF₆ at the same pressure: in other words pure CF₃I has a dielectric strength of around 1.2 times the one of SF₆ in uniform field conditions since it is slightly lower in non-uniform field conditions [31].

3.3.4 CF₃I mixtures

CF₃I mixtures are adopted mainly to solve the high boiling point problem of the pure gas: at 0.1 MPa CF₃I has a boiling point around - 22.5 °C but if it has to be used in electrical systems the pressure needs to increase.

Therefore, the gas starts to liquefy at higher temperatures losing all the benefits that a gas insulating medium has.

In order to decrease the boiling temperature, other gases such as nitrogen and carbon dioxide are considered in mixture with CF₃I.

Regarding fluorine production as a consequence of eventual partial discharges, it is worth noting that with CF₃I / natural gas mixture there is almost no fluorine detected after the discharge [31, 34].

CF₃I / CO₂ mixtures

CF₃I / CO₂ mixture incorporates benefits from both its constituents gases, in particular the high dielectric strength of C₅F₁₀O and the low liquefaction temperature of CO₂.

In addition, CO₂ is easily available and this lowers mixture overall costs; moreover, CF₃I mixture with CO₂ is the most chemically stable between all its mixtures with natural gases.

This mixture has a GWP nearly 100% lower than that of SF₆, being an unit value in comparison with 23500 of SF₆.

However, liquefaction temperature continues to be strongly and negatively influenced by the mixing ratio thus too high values cannot be adopted.

The figure 3.26 shows that the boiling point of CF_3I at 0.7 MPa, a pressure typically adopted in SF_6 GIL systems, is 38 °C demonstrating the need of the addition of a buffer gas to reduce the liquefaction temperature.

In the figure 3.27 pressure-reduced ionization coefficients are reported as a function of E/p for different pure gases and CF_3I mixtures.

It can be noted that a 30% CF_3I / 70% CO_2 mixture has a higher reduced field strength in relation to mixtures with low CF_3I contents.

With only a 30% CF_3I content the insulation performance of the mixture reaches approximately 0.75 to 0.80 times the one of pure SF_6 .

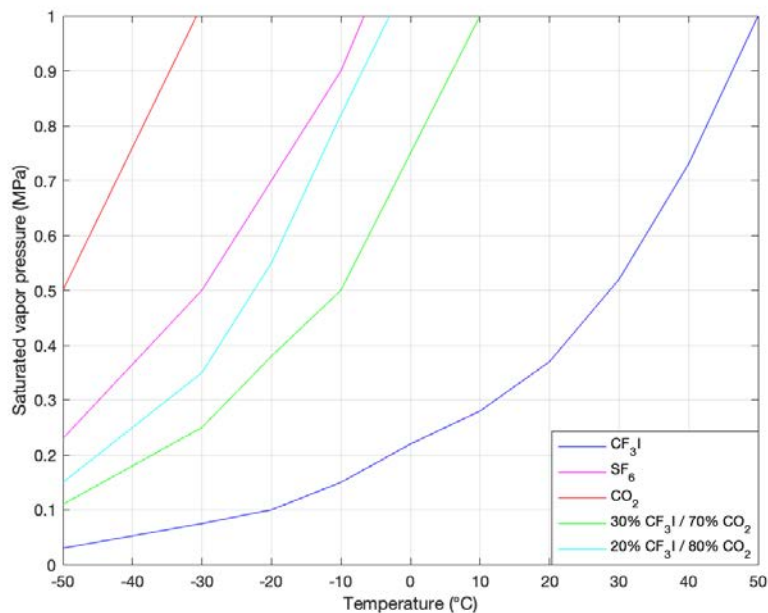


Figure 3.26: Saturated vapor pressure of CF_3I and SF_6

This specific mixing ratio therefore offers a reasonably high dielectric strength while being able to maintain the gaseous form at typical working pressures (for example 0.7 MPa) with a boiling temperature of around - 4°C.

In addition, possible byproducts such as iodine can be substantially reduced adopting a 30% CF_3I / 70% CO_2 mixture, a really important aspect considering that iodine deposition can compromise the insulation performance and must be therefore mini-

mized.

Regarding dielectric properties, this mixture shows a good potential, as can be noted from the figure 3.28 in which 30% CF₃I / 70% CO₂ mixture AC dielectric strength is reported in dependence on gas pressure and in comparison with 20% SF₆ / 80% N₂ mixture (reference), under two different field conditions.

It can be seen that 30% CF₃I / 70% CO₂ mixture dielectric strength is always lower than that of 20% SF₆ / 80% N₂ mixture, in both the field conditions even if under non-uniform field the difference is much lower.

Moreover, dielectric strength under uniform field is always much higher than under non-uniform field.

A deeper characterization of the 30% CF₃I / 70% CO₂ mixture as insulation medium is conducted considering lightning impulse experiments with both polarities on two electrode configurations.

The 50% breakdown voltage is determined adopting the up-and-down method, thus through some simulations in COMSOL the equivalent maximum electric field at the breakdown voltage is obtained.

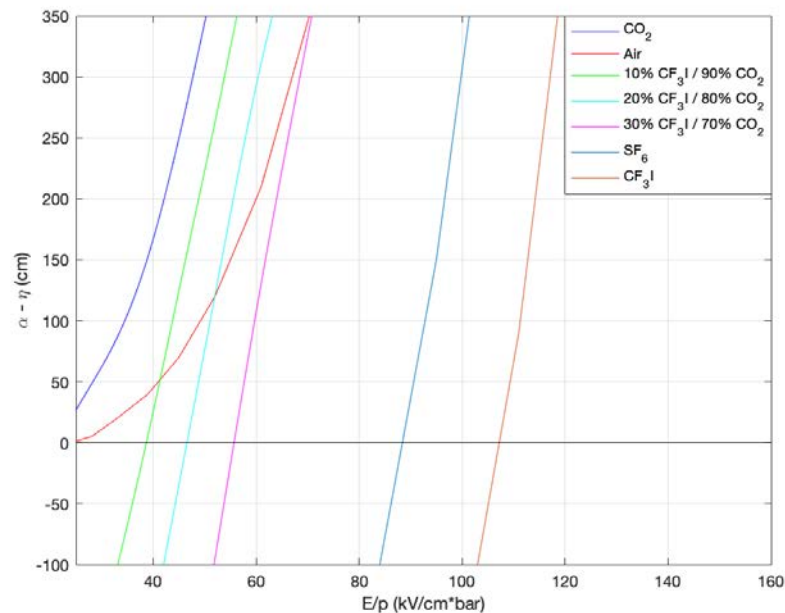


Figure 3.27: Effective ionization coefficients of CF₃I mixtures compared to pure gases

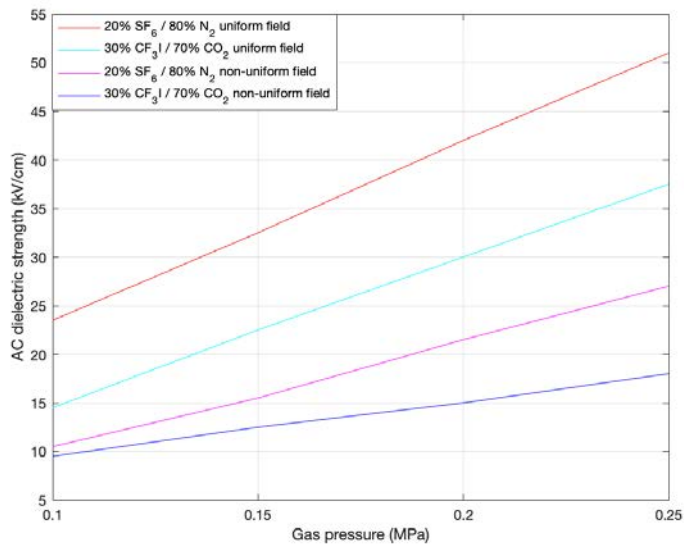


Figure 3.28: AC dielectric strength of 30% CF₃I / 70% CO₂ mixture in comparison with 20% SF₆ / 80% N₂ mixture

In the figure 3.29 the dependence of the lightning impulse breakdown voltage on the gap distance is shown.

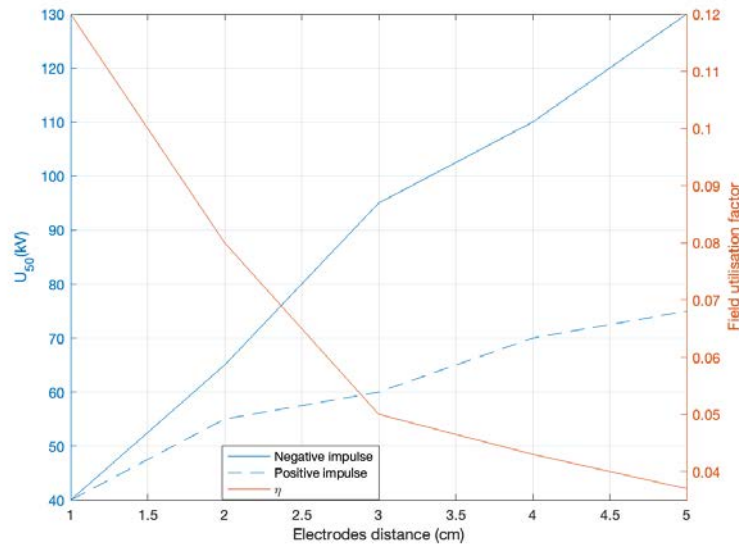


Figure 3.29: U₅₀ of a 30% CF₃I / 70% CO₂ mixture in a rod-plane electrode configuration under lightning impulses and field utilization factor

In the previous figure the field utilization factor is also reported: this is an approximate index of field uniformity of the electrode geometry, where an higher field utilization factor represents a more uniform electric field configuration.

$$\eta = \frac{E_{mean}}{E_{max}}$$

where $E_{mean} = \frac{U_{50}}{g}$ and g represents the electrodes distance.

A rod-plane electrode configuration is chosen to deal with very non-uniform electric field behavior and is reported in the figure 3.30.

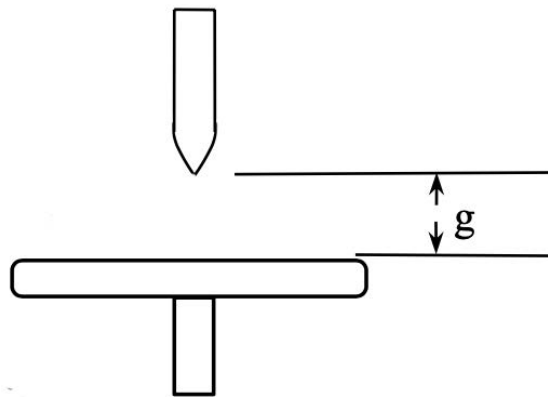


Figure 3.30: A rod-plane electrode configuration

Although the breakdown voltage is the same for both lightning impulse polarities for a 1 cm gap, this is not true when the gap distance becomes bigger.

When the gap length is increased, U_{50} for both impulse polarities increases but the increment under negative impulse is more significant in comparison with that under positive impulse: in the first case for a 5 cm gap the breakdown voltage is almost 3 times the one for 1 cm gap since in the second case the increment is about 1.8 times. In addition, the field utilization factor decreases as the gap length is increased indicating higher non-uniformity.

Generally, it can be said that for the rod-plane electrode configuration breakdown is due to streamers: in negative streamers, the space charge build-up impedes the negative avalanche, while the space charge in positive streamers propagates toward the cathode; due to this process negative streamers require higher electric fields and then

higher breakdown voltages than positive streamers to obtain the full gap breakdown. In the figure 3.31 the equivalent maximum electric field at the breakdown voltage is considered.

On the other hand, also a plane-plane electrode configuration is considered and represented in the figure 3.32.

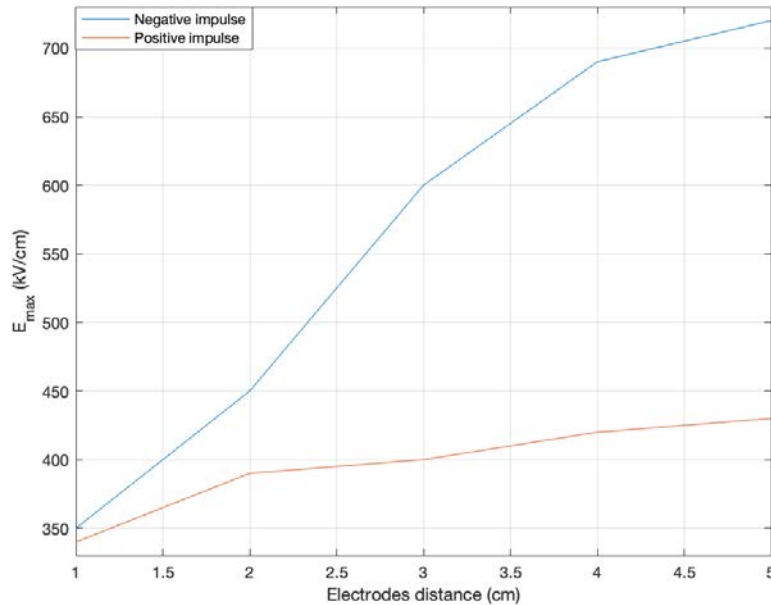


Figure 3.31: E_{max} of a 30% CF_3I / 70% CO_2 mixture in a rod-plane electrode configuration under lightning impulses

Compared with similar gap distances in a rod-plane electrodes configuration, it can be seen that in a plane-plane configuration higher voltages are required in order to achieve breakdown.

In the figures 3.33 and 3.34 U_{50} and E_{max} under positive and negative impulse are plotted in relation to gap length.

Results show a behavior that is opposite from what is observed in the rod-plane configuration.

In the plane-plane configuration the breakdown voltage under positive impulse is higher than under negative impulse.

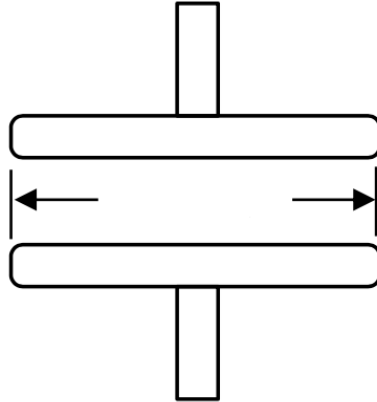
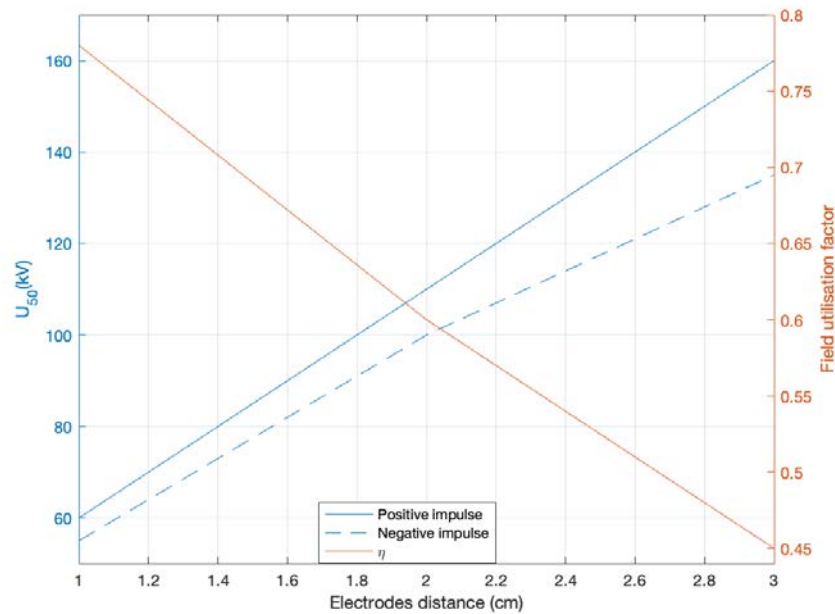


Figure 3.32: A plane-plane electrode configuration

Figure 3.33: U_{50} of a 30% CF₃I / 70% CO₂ mixture in a plane-plane electrode configuration under lightning impulses and field utilization factor

Considering a 1 cm gap the difference between both polarities is of only 3% and the observed voltage difference increases with gap length, reaching 12.7% and 29% for 2 cm and 3 cm gaps respectively.

It can be also noted that U_{50} increases quite linearly with gap length in a plane-plane

configuration, up to 3 cm.

Under positive impulse there is an increase of 2.8 times from a 1 cm gap to a 3 cm gap since under negative impulse the increment is approximately of 2.4 times.

These trends can be found both in U_{50} and E_{max} curves in fact E_{max} seems to increase linearly with gap length although the increment is not as much as for U_{50} being, from a 1 cm to 3 cm gap, 1.56 times under a positive impulse and just 1.3 times under a negative impulse.

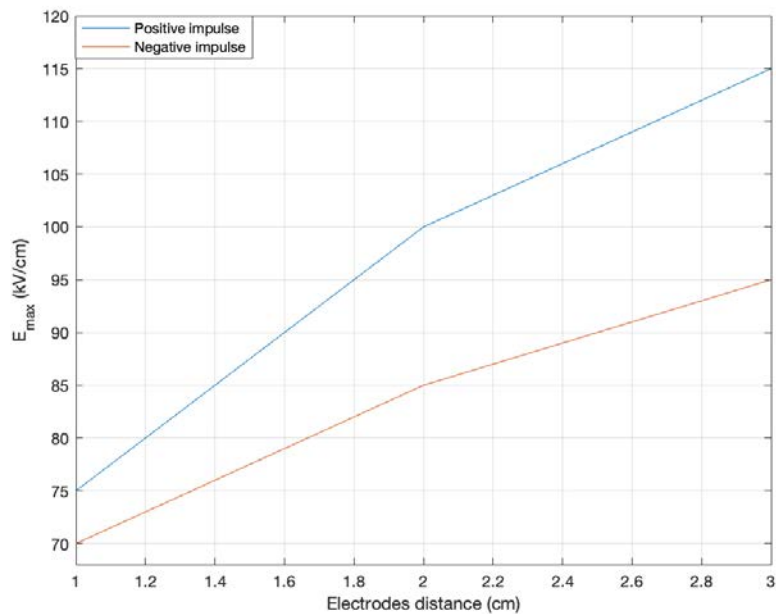


Figure 3.34: E_{max} of a 30% CF_3I / 70% CO_2 mixture in a plane-plane electrode configuration under lightning impulses

Finally, in order to characterize the dependence of mixture dielectric strength also on the pressure, a coaxial configuration is considered and results are reported in the figure 3.35.

As expected, it can be seen that breakdown voltage increases with pressure.

At 0.2 MPa the measured U_{50} is around 84 kV since, taking in consideration air insulation at the same pressure, this parameter is 38 kV which makes 30% CF_3I / 70% CO_2 mixture dielectric strength 2.2 times higher than that of air under similar

conditions.

CF₃I / CO₂ mixture dielectric properties reach a saturation value for the 30% CF₃I / 70% CO₂ mixing ratio: this is the reason why these proportions are adopted in industrial applications and this solution results an attractive alternative to 20% SF₆ / 80% N₂ mixture [31, 34].

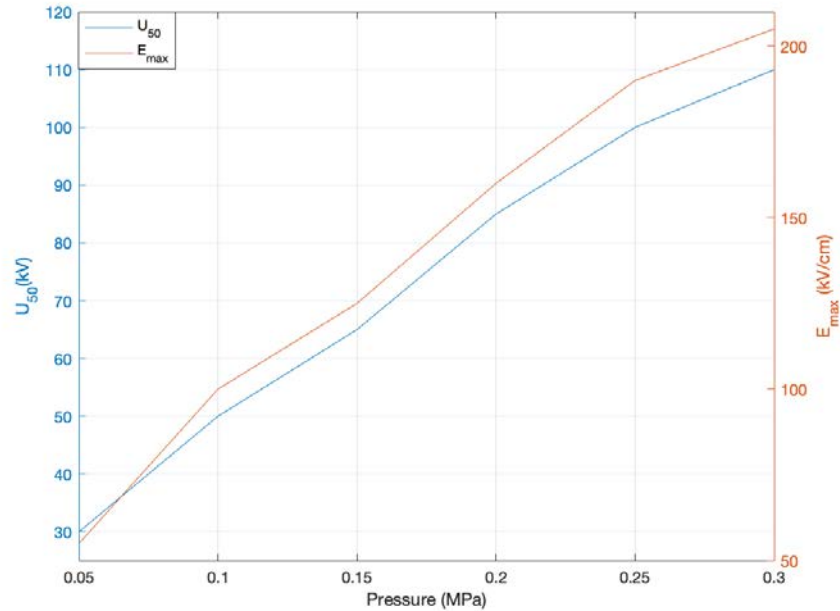


Figure 3.35: U_{50} and E_{max} of a 30% CF₃I / 70% CO₂ mixture in a coaxial cylindrical electrodes configuration under positive lightning impulses

CF₃I / N₂ mixtures

CF₃I / N₂ mixture can be an other alternative solution: replacing CO₂ with N₂ leads to a further decrease of the boiling point and a very low GWP.

In the figure 3.36 GWP dependence on mixture mixing ratio is shown, with values of CF₃I content considered up to 100% due to the fact that in this case increases in this parameter don't significantly affect GWP which always remains under 1.

In addition N₂, as CO₂, is easily available and this lowers mixture overall costs.

As regards the electrical properties, N₂ has an intrinsic strength slightly higher than

the one of CO_2 and this affect the overall theoretic mixture dielectric properties, as can be noted from the figure 3.37 in which pressure-reduced net ionization coefficients are reported as a function of pressure for different pure gases and CF_3I mixtures.

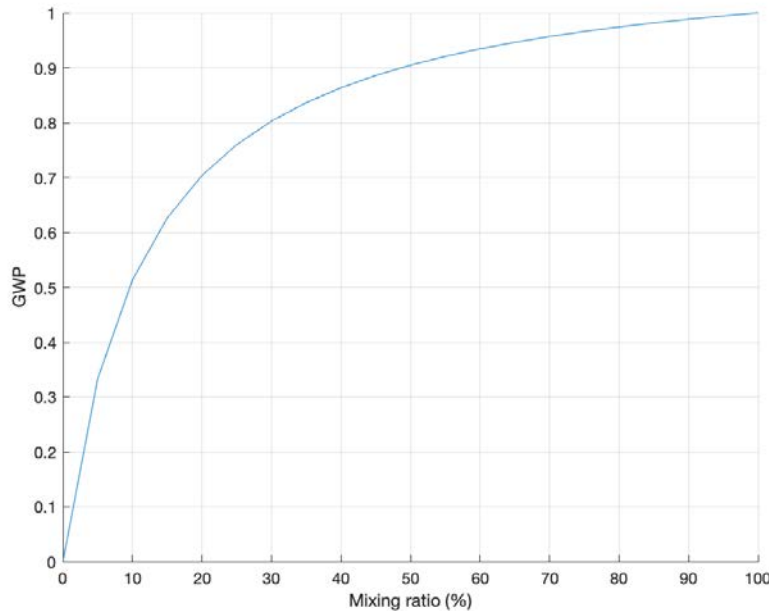


Figure 3.36: GWP (ITH =100) of CF_3I / N_2 mixture

It can be underlined that a 30% CF_3I / 70% N_2 mixture has a higher reduced field strength in relation to mixtures with lower CF_3I contents.

Moreover, by comparing this figure with the analogous figure of the previous section, it can be highlighted that CF_3I / N_2 mixture ionization curves are slightly more at the right in the diagram than CF_3I / CO_2 mixture ones, showing better theoretical insulation properties.

Figure 3.38 presents the breakdown voltage of 30% CF_3I / 70% N_2 mixture in comparison with a 20% SF_6 / 80% N_2 mixture under a quasi-uniform field (sphere-sphere geometry with a field utilization factor equal to 0.93) and a non-uniform field (needle-plane geometry with a field utilization factor equal to 0.23).

In relation to the comparison between CF_3I / N_2 mixture and SF_6 / N_2 mixture, it is worth noting that, also in this case, the sulphur hexafluoride mixture has higher

breakdown voltage than trifluoroiodomethane mixture.

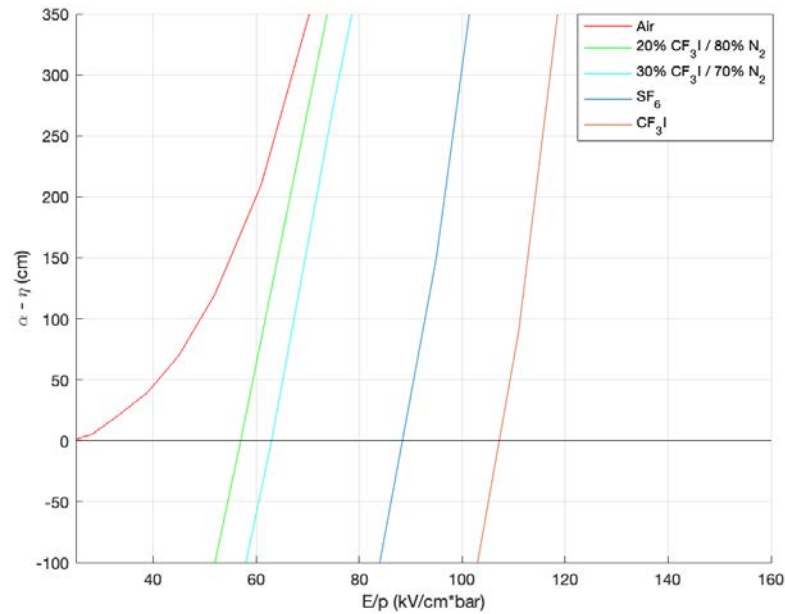


Figure 3.37: Net ionization coefficients of CF₃I / N₂ mixtures in comparison with SF₆, pure CF₃I and air

Moreover, CF₃I / N₂ mixture shows a slightly worse insulation capability respect to CF₃I / CO₂ and this could appear as a contradiction with the previous ionization coefficients results, but actually this is a consequence of the better stability of CO₂ rather than N₂ with CF₃I.

In the figure 3.39 the LI breakdown voltage of two CF₃I / N₂ mixtures is reported. The breakdown voltage under positive polarity results higher than its equivalent under negative polarity, and the difference between positive and negative breakdown voltage is smaller for CF₃I / N₂ gas mixtures in comparison with CF₃I / CO₂ gas mixtures, as can be seen comparing this figure to the analogue of the previous section.

Furthermore, a polarity effect can be seen in the impulse breakdown voltage results for the coaxial system: the breakdown voltages obtained under negative polarity are much lower than those under positive polarity, particularly at high pressures.

Moreover, the breakdown voltages are shown to be increasing but at decreasing rate

as a function of gas pressure up to 0.4 MPa.

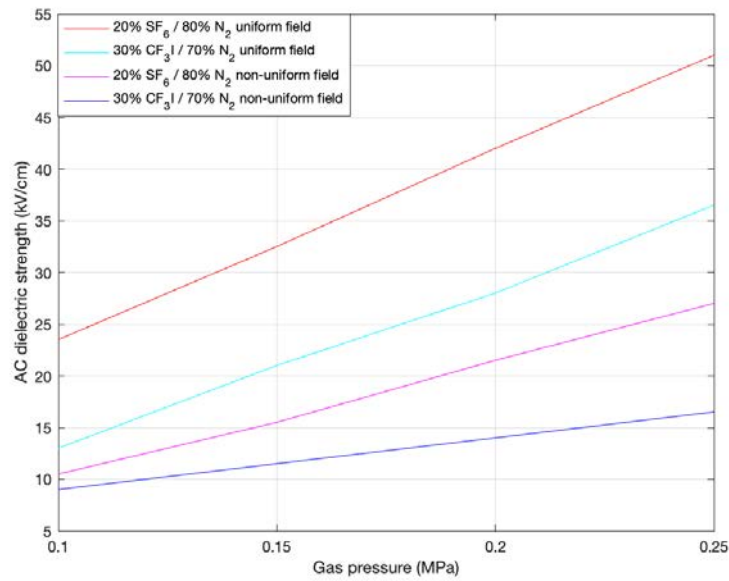


Figure 3.38: AC dielectric strength of 30% CF₃I / 70% N₂ mixture in comparison with 20% SF₆ / 80% N₂ mixture

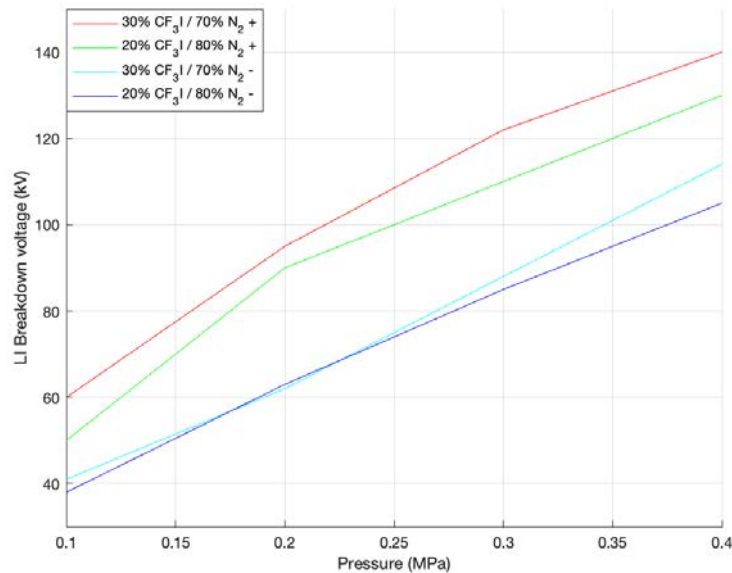


Figure 3.39: Lightning impulse breakdown voltage of CF₃I / N₂ mixtures

In the figure 3.40 the pressure-normalized maximum dielectric strength for CF₃I mixtures is reported.

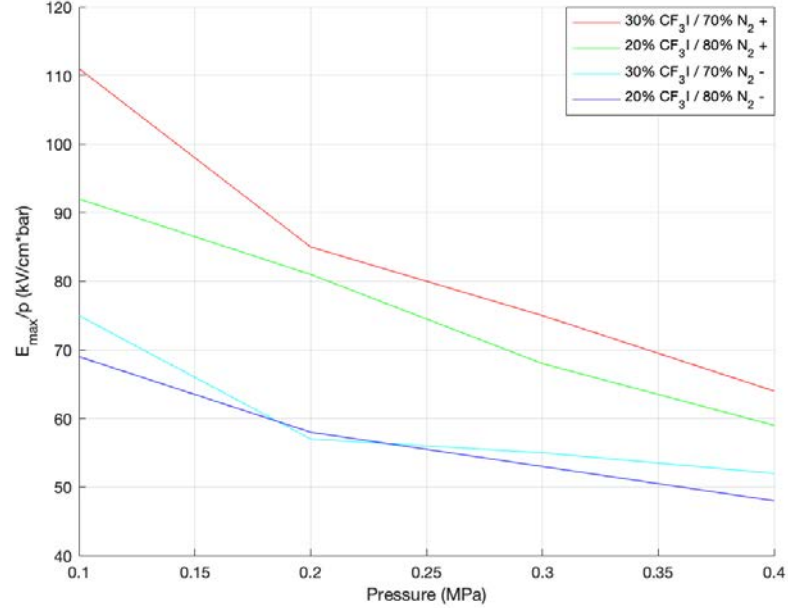


Figure 3.40: Maximum normalized dielectric strength of CF₃I / N₂ mixtures

As can be observed on this figure, the $(E_{max}/p)_B$ decreases with a steep slope in the low pressure range and, thereafter, with a gradual decreasing slope.

From BOLSIG+ computations, an estimation of the critical value of $(E/p)_{crit}$ is obtained for different CF₃I gas mixtures.

It is expected that, below the $(E/p)_{crit}$, there should be no occurrence of breakdown.

However, $(E_{max}/p)_B$ values at higher pressures under negative polarity can be smaller than the critical value of $(E/p)_{crit}$ for CF₃I gas mixtures.

This may be attributed to the existence of an electron avalanche with the support of electron emission from the microscopically irregular surface on the cathode.

It can be observed that, for positive polarity at low pressures, CF₃I / N₂ mixture has an higher $(E_{max}/p)_B$ than SF₆ and, thereafter, this decreases much more quickly than with SF₆.

At 0.4 MPa, the $(E_{max}/p)_B$ of 30 CF₃I / 70% N₂ mixture is 80% that of SF₆ [34].

3.4 R12 (CCl_2F_2)

3.4.1 Physicochemical properties

Dichlorodifluoromethane CCl_2F_2 , commonly known as R12, freon 12 or FC 12, is a synthetic gas very diffused as refrigerant but characterized by some features which make it an attractive candidate also as an insulation medium.

This gas belongs to the class of organic compounds named chlorofluorocarbons, which are alkyhalide compounds that are made of chlorine, fluorine and carbon atoms.

R12 is also much cheaper than SF_6 and has a cost for kilogram of 5.3 US \$.

R12 molecular structure is shown in figure 3.41.

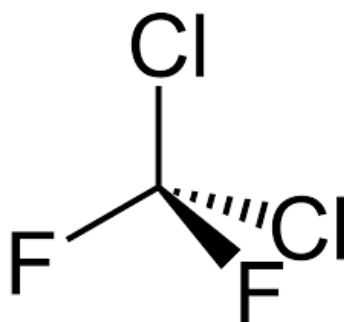


Figure 3.41: Molecular structure of dichlorodifluoromethane CCl_2F_2

R12 molecule is composed of one carbon atom, two chlorine atoms and two fluorine atoms, with the last ones which give electronegative properties to this gas, characteristic that facilitates the attachment process.

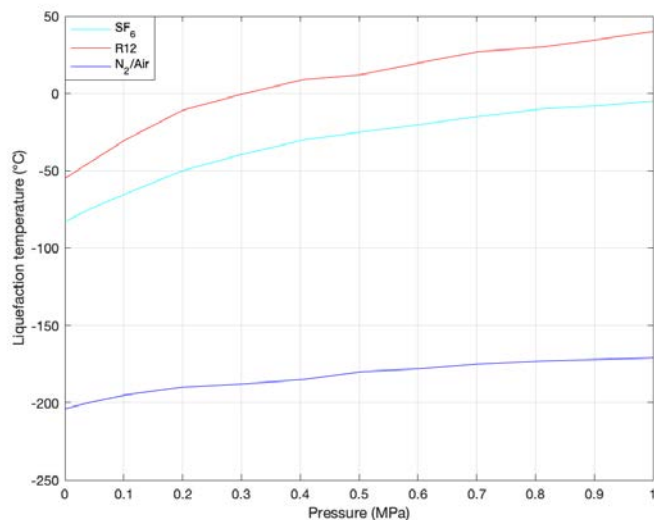
Some of the physicochemical parameters characterizing this gas are reported in the table 3.9.

Dichlorodifluoromethane appears as a colourless gas having a faint ethereal odor.

The boiling point at 1 bar of R12 is relatively high (- 29.8 °C) and its dependence on pressure, compared with the one of SF_6 and N_2 / air is reported in the figure 3.42 [40].

Table 3.9: Physicochemical properties of R12

Parameter	Value	Unit
Molecular weight	120.914	g/mol
Density	1.49	g/cm ³
Freezing point	- 157.7	°C
Boiling point at 1 bar	- 29.8	°C
Saturated vapor pressure at - 30 °C	0.10	MPa
Saturated vapor pressure at 0 °C	0.30	MPa
Saturated vapor pressure at 20 °C	0.63	mbar
Flammability	non-flammable	
Explosiveness	non-explosive	
Chemical stability	stable	
Thermal stability	stable up to 600 °C	
Corrosivity	non-corrosive	
Solubility in water	0.286	g/l
Appearance	colourless/ethereal	

Figure 3.42: Liquefaction temperatures of SF₆, R12 and N₂ / air in dependence on pressure

3.4.2 Environmental properties

Taking into account the environmental impact, R12 presents much better characteristics compared with SF₆, resulting in a much lower GWP and atmospheric lifetime, as shown in the table 3.10.

Table 3.10: Environmental properties of R12

Parameter	Value	Unit
GWP (ITH = 100 years)	2400	
ODP	1	
Atmospheric lifetime	12	years

This table shows that GWP of R12 is ten times less than that of SF₆ and the atmospheric lifetime is 300 times lower.

However R12 has the drawback of an higher ODP than the one of SF₆ due to the fact that contains chlorine, characterized by ozone depletion properties.

Fortunately, this problem can be partially solved by employing R12 with mixtures of N₂ and air or adopting some technics to eliminate harmful emissions as, for example, R12 decomposition into hydrogen chloride that is collected as an harmless compound through a neutralizing process [40].

3.4.3 Dielectric properties

R12 presents good insulation capabilities considering that its intrinsic dielectric strength is 80.1 kV/cm at atmospheric pressure compared with 89.0 kV/cm of SF₆ in the same conditions.

Therefore, this gas has a dielectric strength, in pure form, which reaches 0.9 times the one of SF₆ showing a great potentiality in industrial applications.

The comparison is reported in the figure 3.43 which shows also that the dielectric strength depends on gas pressure in a monotonous way.

The difference between R12 and SF₆ dielectric strength remains quite constant for all the pressure range considered [40].

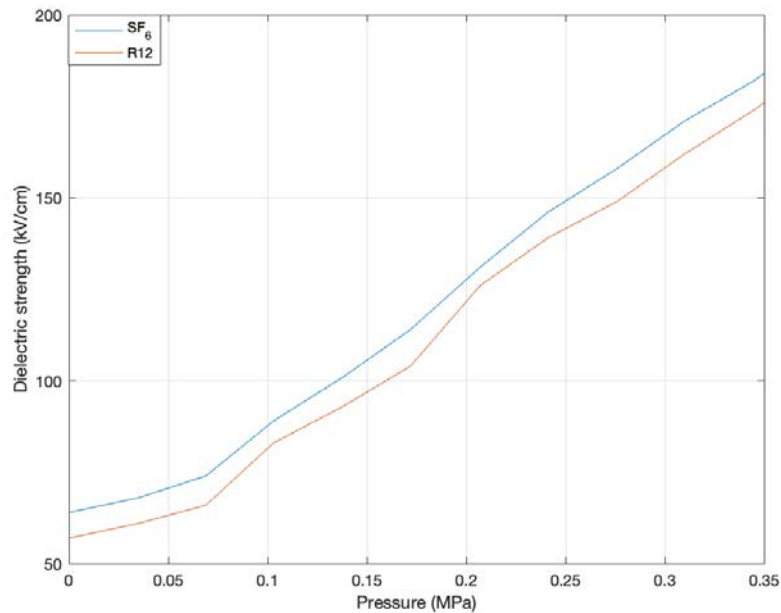


Figure 3.43: Dielectric strength of R12 compared with that of SF_6

3.4.4 R12 mixtures

Liquefaction factor is an important point for choosing an alternative gas due to the fact that the insulation strength degrades when temperature decreases because its pressure gets low.

As seen before, R12 has a boiling point of $-29.8\text{ }^\circ\text{C}$ at atmospheric pressure which is higher than the one of SF_6 ($-63\text{ }^\circ\text{C}$).

Such a high temperature is a disadvantage of R12 gas and this is the reason why nitrogen or air, both characterized by a boiling point of $-196\text{ }^\circ\text{C}$ at atmospheric pressure, are chosen to be admixed with R12.

If N_2 /air and R12 are mixed disadvantages of high liquefaction point can be eliminated. Mixed gas liquefaction temperature is shown in the figure 3.44, which suggests that if the ratio of base gas is increased also liquefaction temperature increases.

An other important aspect regards the synergistic effect: when two gases are mixed and they show non-linear behavior thus this non-linearity is used to describe their synergistic effect.

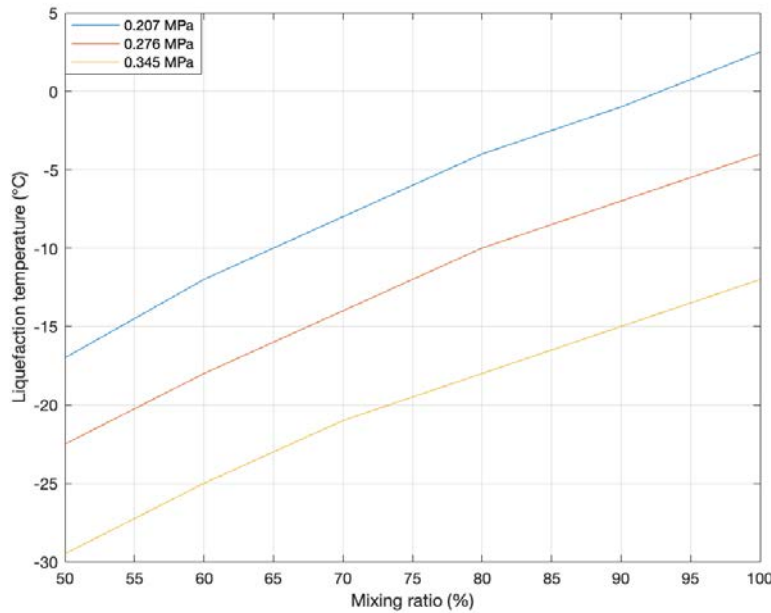


Figure 3.44: Liquefaction temperatures of R12 / N₂ or air mixture in dependence on mixing ratio

There are four types of synergistic effects which are: positive synergistic effect, negative synergistic effect, linear relation effect and synergistic effect.

The connection between synergistic effect index C , mixing ratio and breakdown voltage is shown in the following equation:

$$V_m = V_2 + \frac{k(V_1 - V_2)}{k + (1 - k)C}, V_1 > V_2$$

where V_1 and V_2 represent the breakdown voltages of the pure gases, V_m is the breakdown voltage of mixed gas, k is the mixing ratio and C is the synergistic effect index.

Using the previous equation the synergistic effect of R12 / air and R12 / N₂ mixtures is calculated and given in tables 3.10 and 3.11, reported in the respective sections.

These tables specify that C value of both mixtures declines when the increase in pressure is at the same ratio as that of the mixing gas.

When gas pressure increases beyond 0.069 MPa at 0.70-0.80 mixing ratios, C value becomes negative and synergistic effect changes to positive synergistic effect; thus, as

pressure increases, C value becomes less.

The more evident the synergistic effect is, the better benefits of using mixed gases as insulating gas are.

The advantage of additive gases is to deenergize high energy electron and return them to lower energy level because at high energy level attachment of electrons is very difficult [40].

- $C > 1$ shows negative synergistic effect.
- $C = 1$ shows linear relation effect.
- $0 < C < 1$ shows synergistic effect.
- $C < 0$ shows positive synergistic effect.

R12 / air mixture

R12 / air mixture shows good dielectric properties and is a very attractive solution thanks to the unlimited availability of air as buffer gas.

Figure 3.45 illustrates AC dielectric strength of R12 gas and its mixtures with air.

In this study, pure R12, 50% R12 / 50% air, 60% R12 / 40% air, 70% R12 / 30% air, 80% R12 / 20% air and 90% R12 / 10% air are presented.

It can be seen that by adding 50% of R12 to air rapidly increases breakdown strength of air; however, by increasing the percentage of R12 the breakdown strength doesn't follow a linear trend.

This is a consequence of the fact that R12 has an high attachment cross-section at low energies (0-0.5 eV) thus when a small amount of R12 is added almost all the low energy electrons attached cause a rapid increase in the breakdown voltage.

The gap distance also affects dielectric strength which increases with this parameter: when the distance between electrodes is increased it needs high potential for balancing the electric field between the electrodes as shown by the relation

$$E = f \cdot \frac{V}{D}$$

where f is the non-uniformity constant, D is the distance between the electrodes and V is the applied voltage.

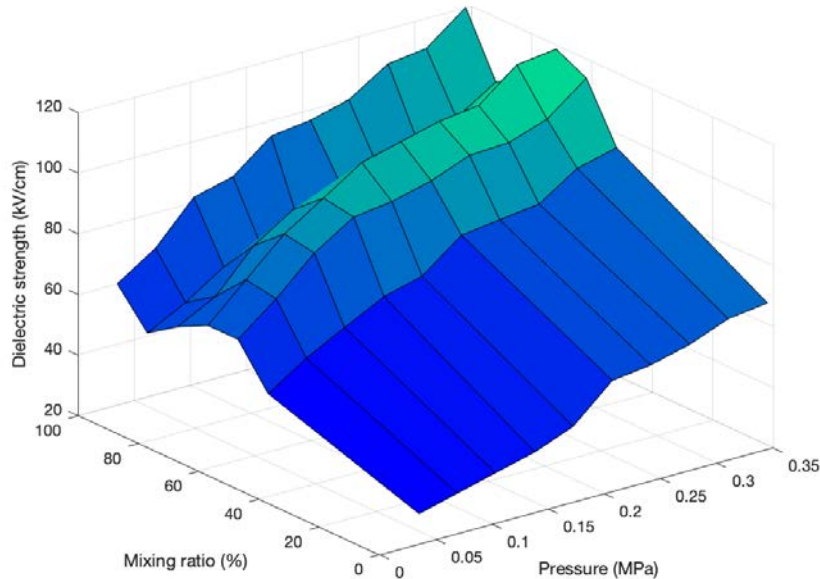


Figure 3.45: AC dielectric strength of R12 / air mixture in dependence on pressure and mixing ratio

Figure 3.46 contains the Paschen's curve for different ratios of R12 / air in the PD product range of 0.2-2.5 MPa·mm where the distance from one electrode to the other is D and P is the pressure.

It can be noted that with the increase in pressure, breakdown voltage also increases even if there is a steady decrease in the slope of the curve when it's considered a sphere-sphere electrodes configuration, effect that results in a deviation from Paschen's law considering that the dielectric strength on an ideal gas has to be linear in theory. As regards the breakdown characteristic of R12 / air mixture in DC environment, figure 3.47 represents this situation highlighting that the best dielectric strength of R12 / air mixture (70% / 30% mixing ratio) is achieved in DC.

In addition, breakdown characteristic of R12 / air in impulse environment is considered and reported in the figure 3.48.

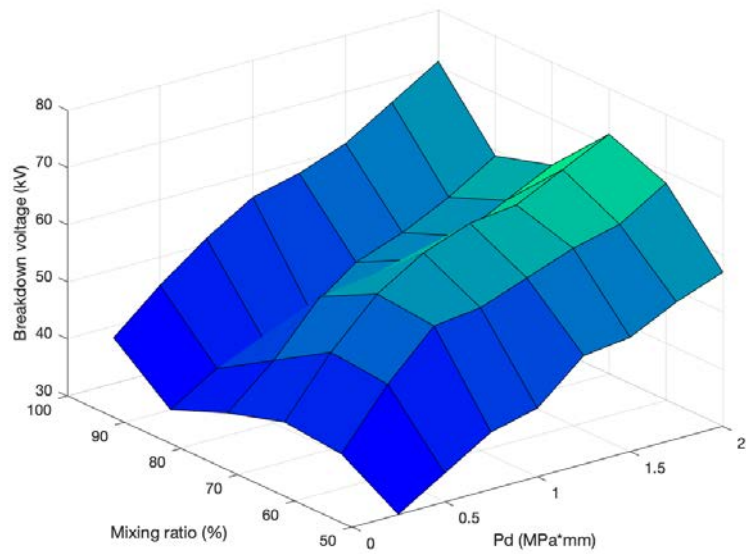


Figure 3.46: Paschen's curve of R12 / air mixture

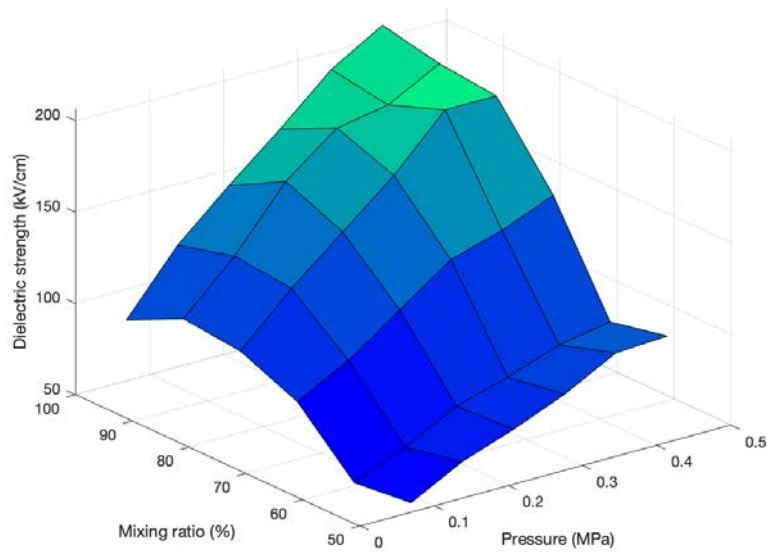


Figure 3.47: DC dielectric strength of R12 / air mixture in dependence on pressure and mixing ratio

Positive impulse is analyzed and the result is that breakdown voltage increases with pressure and mixing ratio.

The dielectric strength of R12 / air mixture under positive impulse is higher than in AC and DC case.

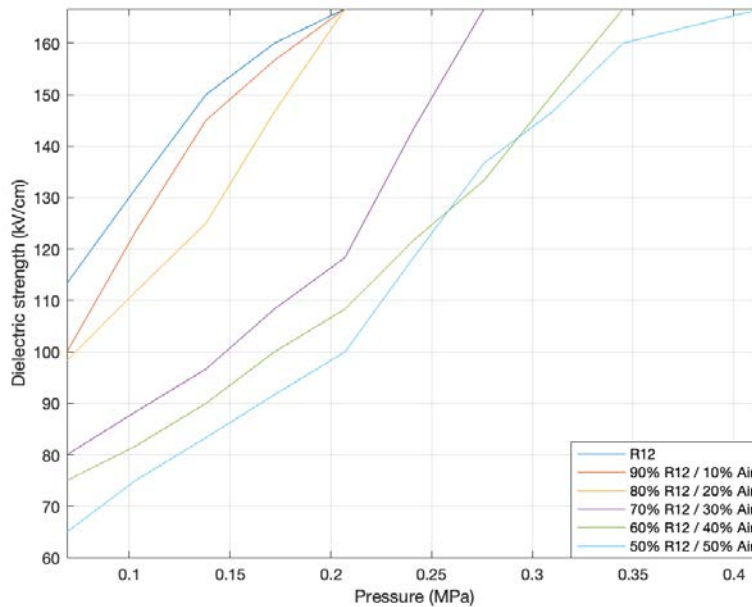


Figure 3.48: Positive impulse dielectric strength of R12 / air mixture in dependence on pressure and mixing ratio

By adding air, the dielectric strength of the mixture is greater than that of pure R12 due to the so called positive synergistic effect.

The advantage of adding air to pure gas is that it decreases its boiling temperature and also GWP.

For what concerns the synergistic effect, results for R12 / air mixture are reported in the table 3.11.

The mixing ratio 70% R12 / 30% air at 0.31 MPa gives the best optimum value of the synergistic index C.

Moreover, the synergistic effect is positive for all the pressures considered (excepted 0.28 MPa) if a 70% R12 content is adopted [40].

Table 3.11: Synergistic effect of R12 / air mixture

Pressure (MPa)	K (%)			
	50	60	70	80
	C			
0.03	0.70	0.009	- 0.03	0.79
0.07	0.61	- 0.06	- 0.20	0.96
0.10	0.74	0.008	- 0.13	0.81
0.14	0.56	- 0.14	- 0.28	0.13
0.17	0.94	0.104	- 0.26	0.96
0.21	0.60	0.045	- 0.33	1.43
0.24	0.64	- 0.04	- 0.34	1.54
0.28	0.99	0.258	0.048	1.67
0.31	0.71	0.198	- 0.39	1.28
0.34	0.86	0.140	- 0.03	1.71

R12 / N₂ mixture

Nitrogen is the most stable available gas, moreover it is inert and has a negligible GWP and a very low boiling temperature.

By adding N₂ to R12 its boiling point and its GWP decrease.

Experimental evidences show that adding a small amount of R12 significantly increases nitrogen dielectric strength and further addition doesn't bring a rapid increase in breakdown voltage due to the attachment of low energy electron because attachment of high energy electron is very difficult.

In the figure 3.49 dielectric strength of R12 with a different mixing ratio of nitrogen is represented in dependence on pressure.

The best dielectric strength can be achieved with a 80% R12 / 20% N₂ mixture reaching 0.95 times the one of SF₆.

Figure 3.50 gives the Paschen's curve of R12 / N₂ mixture at different mixing ratios and pressures.

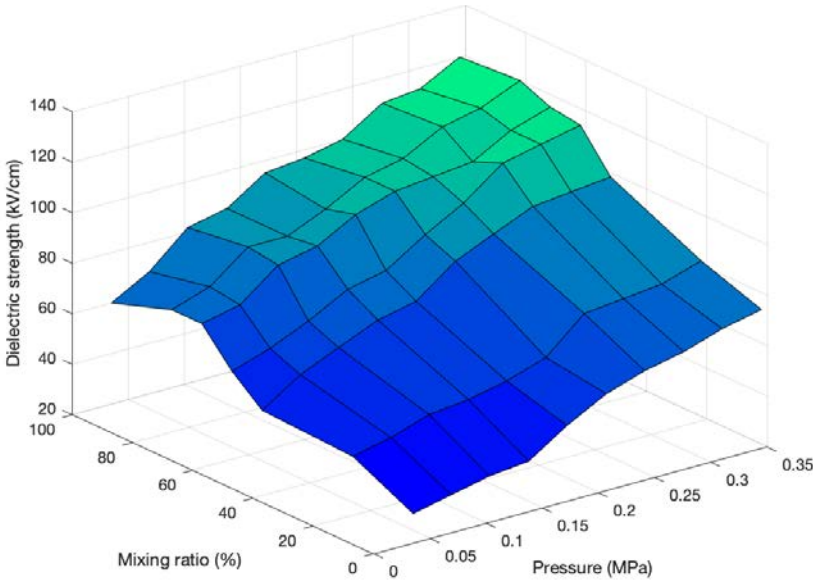


Figure 3.49: AC dielectric strength of R12 / N₂ mixture in dependence on pressure and mixing ratio

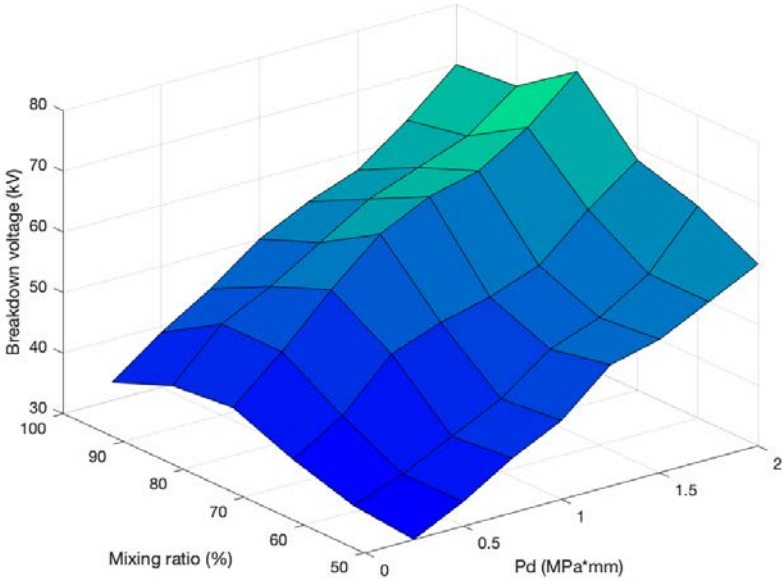


Figure 3.50: Paschen's curve of R12 / N₂ mixture

Relating to the synergistic effect, results for R12 / N₂ mixture are reported in the table 3.12.

Table 3.12: Synergistic effect of R12 / N₂ mixture

Pressure (MPa)	K (%)			
	50	60	70	80
	C			
0.03	1.33	0.57	0.61	0.07
0.07	1.11	1.09	0.99	0.01
0.10	0.38	0.71	0.86	- 0.50
0.14	0.44	0.37	0.04	- 1.07
0.17	0.55	0.71	- 0.20	- 1.11
0.21	0.98	0.96	- 0.48	- 1.28
0.24	0.91	0.79	- 0.43	- 1.03
0.28	1.29	0.89	- 0.41	- 1.05
0.31	1.42	1.04	- 0.41	- 1.28
0.34	0.99	1.19	- 0.26	- 0.97

The mixing ratio 80% R12 / 20% N₂ shows the lowest value of C and gives a better result than pure R12 [40].

3.5 R134a (C₂H₂F₄)

3.5.1 Physicochemical properties

Tetrafluoroethane CF₃CH₂F, commonly known as R134a, is a very diffused synthetic gas, like also R12, as refrigerant gas but potentially a good candidate as a dielectric medium.

This gas is a hydrofluorocarbon (HFC) and haloalkane refrigerant with thermodynamic properties similar to R12.

Tetrafluoroethane is cheap, more than R12 and much more than SF₆: its cost for

kilogram is of 4 US \$.

R134a molecular structure is reported in the figure 3.51.

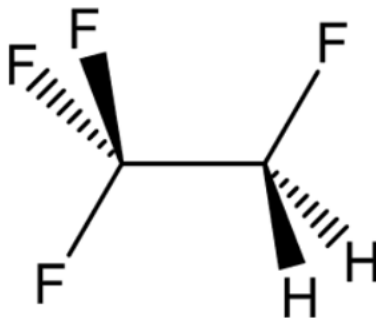


Figure 3.51: Molecular structure of tetrafluoroethane C₂H₂F₄

Some of the parameters characterizing this gas are highlighted in the table 3.13.

Table 3.13: Physicochemical properties of R134a

Parameter	Value	Unit
Molecular weight	102.03	g/mol
Density	4.25	g/cm ³
Freezing point	- 103.3	°C
Boiling point at 1 bar	- 26.3	°C
Saturated vapor pressure at - 30 °C	0.12	MPa
Saturated vapor pressure at 0 °C	0.30	MPa
Saturated vapor pressure at 20 °C	0.60	MPa
Flammability	non-flammable	
Explosiveness	non-explosive	
Chemical stability	stable	
Solubility in water	0.150	g/l
Corrosivity	non-corrosive	
Appearance	colourless/odourless	

The boiling point at 0.1 MPa of R134a is relatively high (- 26.3 °C) and its dependence on pressure, compared with SF₆ and N₂ / air is reported in the figure 3.52 [41].

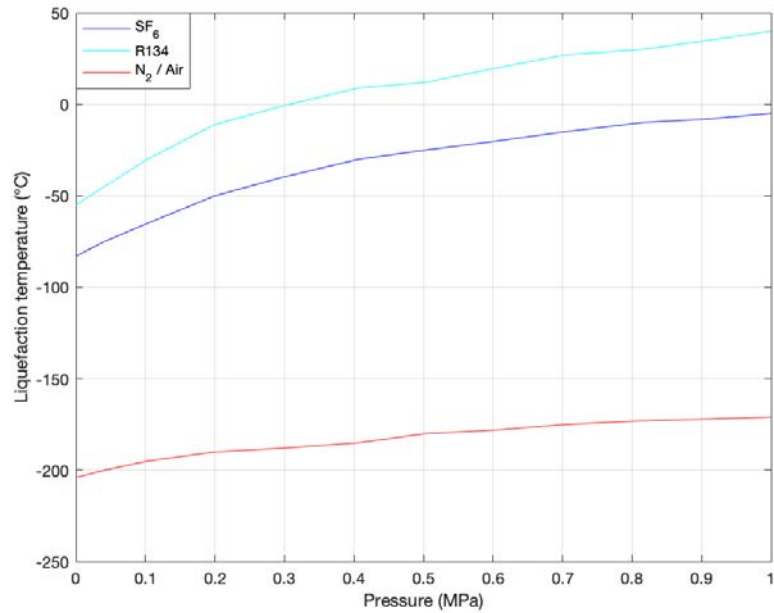


Figure 3.52: Liquefaction temperature of SF₆, R134a and N₂ / air in dependence on pressure

3.5.2 Environmental properties

In terms of environmental impact, R134a has much better characteristics in comparison with SF₆, precisely a much lower GWP and atmospheric lifetime, as shown in the table 3.14.

Table 3.14: Environmental properties of R134a

Parameter	Value	Unit
GWP (ITH = 100 years)	1300	
ODP	0	
Atmospheric lifetime	14	years

This table shows that GWP of R134a is almost 20 times less than that of SF₆ and the atmospheric lifetime is 230 times lower.

Differently from R12, R134a has a negligible ODP and thus seems to be a better

alternative gas than the previous one [41].

3.5.3 Dielectric properties

R134a presents good dielectric properties thanks to its intrinsic dielectric strength of 75.7 kV/cm at atmospheric pressure compared to 89.0 kV/cm of SF₆ in the same conditions.

Therefore this gas has a dielectric strength, in pure form, which reaches 0.85 times the one of SF₆ resulting in a very attractive insulating gas for industrial applications. This parameter is illustrated in the figure 3.53 which also demonstrates that the dielectric strength depends on gas pressure [41].

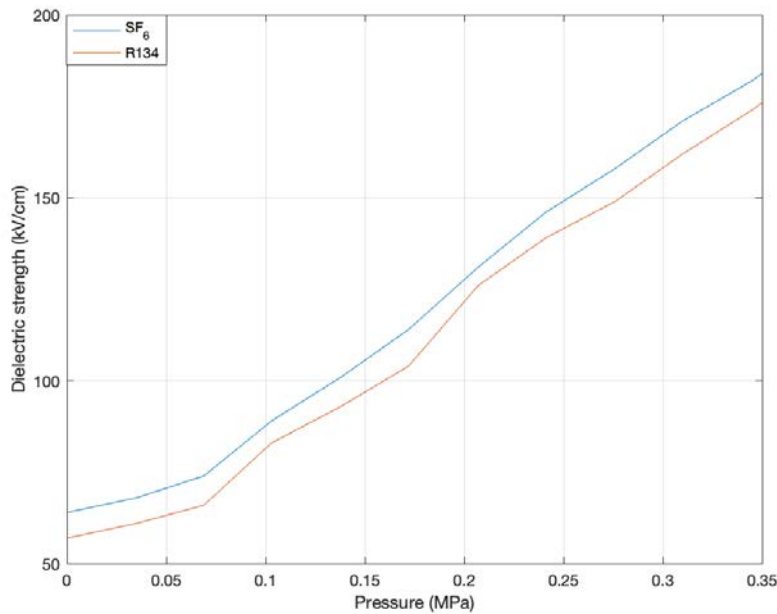


Figure 3.53: Dielectric strength of R134a compared to that of SF₆

3.5.4 R134a mixtures

Liquefaction factor, as said previously, plays a pivotal role in choosing the appropriate alternative gas due to the fact that the insulation strength degrades when temperature, and then pressure, decreases.

The relatively high R134a boiling temperature can be a problem in some working situations and this is why also in this case nitrogen or air, both characterized by a boiling point of - 196 °C at atmospheric pressure, are generally added to R134a to form a mixture with a lower liquefaction temperature.

Liquefaction temperature of the mixture is illustrated in the figure 3.54, where it can be noted that the boiling point increases when the mixing ratio is increased.

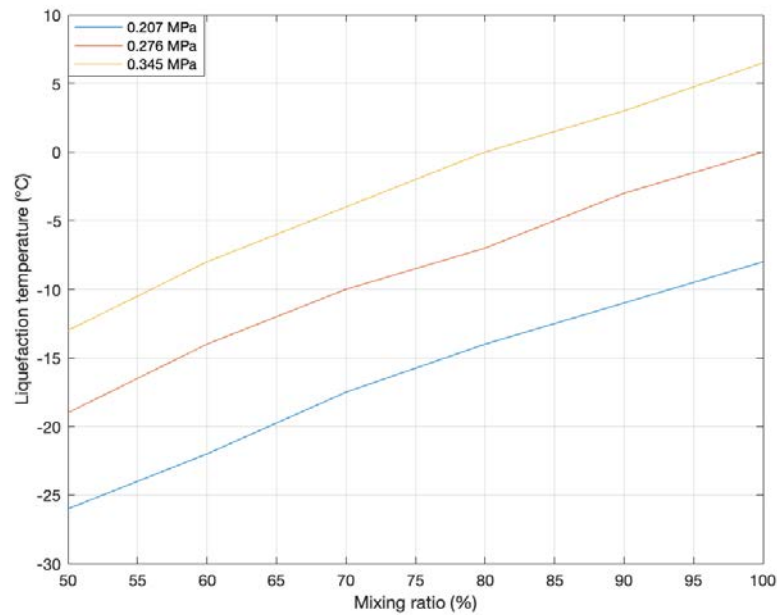


Figure 3.54: Liquefaction temperature of R134a / N₂ or air mixture in dependence on mixing ratio

The synergistic effect also has to be taken into account analyzing the non-linear behavior of the mixture composed of the pure gas and the buffer gas.

Considering the connection between synergistic effect index C , mixing ratio and breakdown voltage represented by the known equation

$$V_m = V_2 + \frac{k(V_1 - V_2)}{k + (1 - k)C}, V_1 > V_2$$

the synergistic effect of R134a / air and R134a / N₂ mixtures is calculated and given in tables 3.14 and 3.15, reported in the respective sections.

These tables specify that C value of both mixtures declines when the pressure maximizes at the same mixing gas ratio.

When the gas pressure increases beyond 0.069 MPa at 0.70 - 0.80 mixing ratios, C value becomes negative and synergistic effect changes to positive synergistic effects; therefore, as pressure increases, C value becomes less [41].

R134a / air mixture

R134a / air mixture has good dielectric properties and the use of air as buffer gas appears to be advantageous due to its unlimited availability.

Figure 3.55 shows the AC dielectric strength of R134a / air mixture.

In this case, pure R134a, 50% R134a / 50% air, 60% R134a / 40% air, 70% R134a / 30% air, 80% R134a / 20% air and 90% R134a / 10% air are presented.

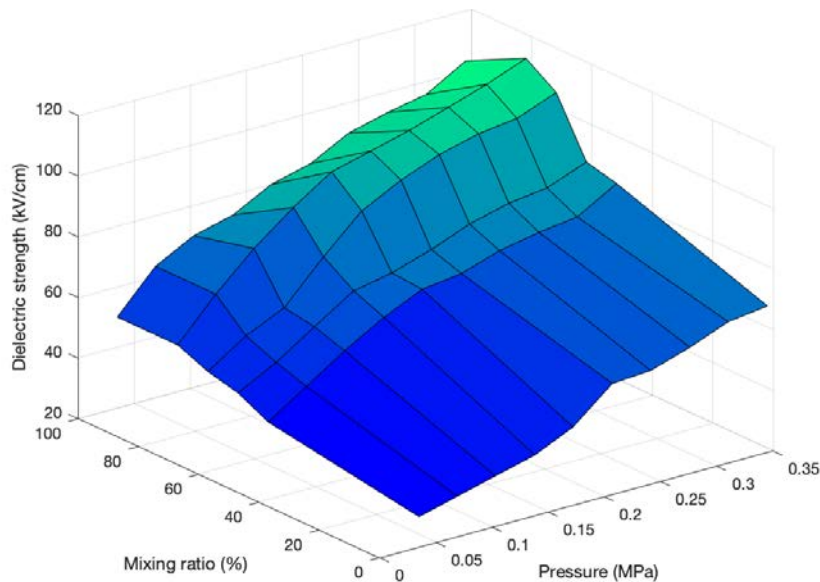


Figure 3.55: AC dielectric strength of R134a / air mixture in dependence on pressure and mixing ratio

It can be seen that adding 50% of R134 to air rapidly increases breakdown strength

of air; however, by increasing the percentage of R134a the breakdown strength lacks similar inclination.

This is a consequence of the fact that R134a has a high attachment cross-section at low energies (0-0.5 eV) so, when a small amount of R134a is added almost all the low energy electrons attached cause a rapid increase in the breakdown voltage.

The gap distance also affects the dielectric strength which increases with this parameter: increasing electrodes gap distance there exist need of maximum potential for balancing the electric field between electrodes as shown by the relation

$$E = \frac{V}{D}$$

where D is the distance between the electrodes and V is the applied voltage.

Figure 3.56 provides the Paschen's curve for different ratios of R134a / air in the PD product range of 0.2-2.5 MPa·mm where the distance from one electrode to the other is D and P is the pressure.

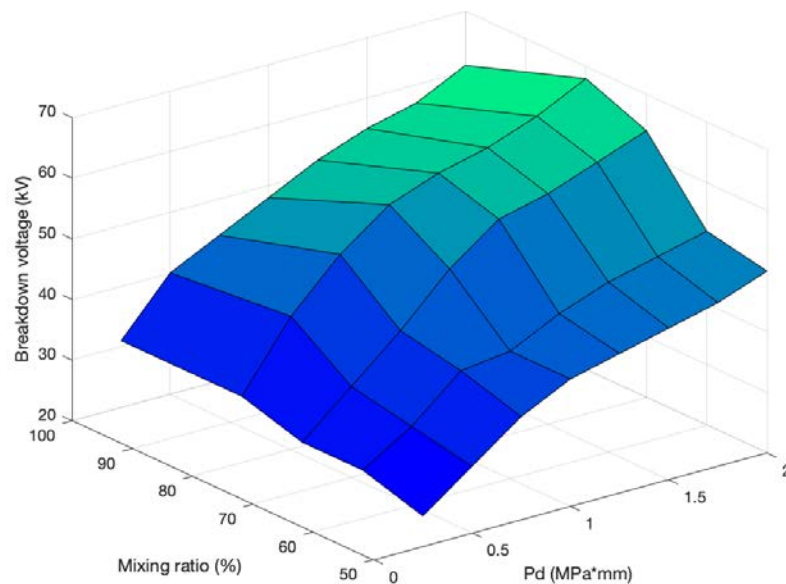


Figure 3.56: Paschen's curve of R134a / air mixture

It can be noted that with the increase in pressure, breakdown voltage also increases even if there is a steady decrease in the slope of the curve when we consider a

sphere-sphere electrodes configuration, effect that results in a deviation from Paschen's law considering that dielectric strength on an ideal gas has to be linear in theory.

By adding air, the dielectric strength of the mixture is greater than that of pure R134a due to the so called positive synergistic effect.

Results for R134a / air mixture are reported in the table 3.15.

Table 3.15: Synergistic effect of R134a / air mixture

Pressure (MPa)	K (%)			
	50	60	70	80
	C			
0.03	1.01	0.26	- 1.12	- 0.98
0.07	0.68	0.49	- 0.91	- 0.47
0.10	0.87	0.80	- 0.54	- 0.35
0.14	0.52	0.38	- 0.45	- 0.09
0.17	0.98	0.76	- 0.20	0.23
0.21	0.57	0.28	- 0.20	- 0.30
0.24	0.34	0.10	- 0.13	- 0.39
0.28	0.41	0.08	0.35	- 0.22
0.31	0.49	- 0.03	0.02	0.02
0.34	0.77	0.143	0.14	0.14

The mixing ratio 70% R134a / 30% air at 0.31 MPa gives the optimum value of the synergistic index C [41].

R134a / N₂ mixture

Nitrogen is the most stable available gas, moreover it is inert and has a negligible GWP and a very low boiling temperature.

By admixing N₂ to R134a the overall boiling point and GWP decrease.

Experimental evidences show that adding a small amount of R134a significantly increases nitrogen dielectric strength and further addition doesn't bring a rapid increase in breakdown voltage due to the attachment of low energy electron because attachment

of high energy electron is very difficult.

In the figure 3.57 the dielectric strength of R134a with a different mixing ratio of nitrogen is represented in dependence on pressure.

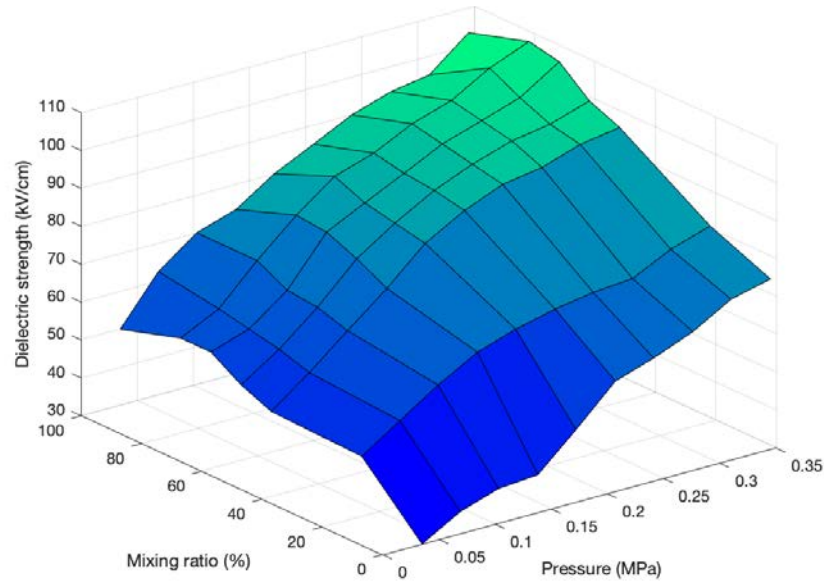


Figure 3.57: AC dielectric strength of R134a / N_2 mixture in dependence on pressure and mixing ratio

The best dielectric strength can be achieved with a 80% R134a / 20% N_2 mixture reaching 0.85 times the one of SF_6 .

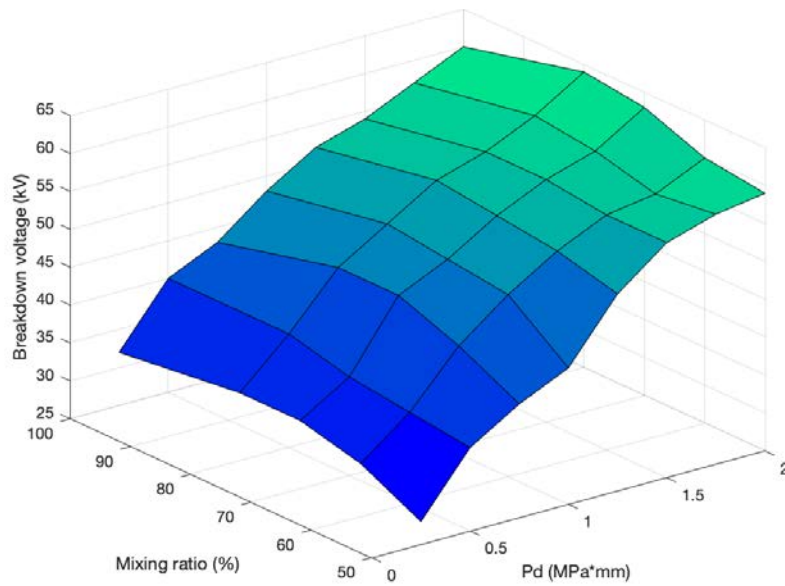
Moreover, the dielectric strength increase is higher in dependence on pressure increase than R134a content increase.

Figure 3.58 provides the Paschen's curve of R134a / N_2 mixture at different mixing ratios and pressures.

The pressure-gap distance product strongly affects the mixture breakdown voltage.

In terms of synergistic effect, results for R134a / N_2 mixture are reported in the table 3.16.

The mixing ratio 80% R134a / 20% N_2 at 0.31 MPa shows the lowest value of C and it gives a better result than pure R134a [41].

Figure 3.58: Paschen's curve of R134a / N₂ mixtureTable 3.16: Synergistic effect of R134a / N₂ mixture

Pressure (MPa)	K (%)			
	50	60	70	80
	C			
0.03	0.15	- 0.12	- 0.43	- 0.97
0.07	0.42	0.39	0.29	0.43
0.10	0.28	0.24	0.30	0.06
0.14	0.06	- 0.06	- 0.30	- 0.59
0.17	0.02	- 0.11	- 0.05	- 0.58
0.21	- 0.04	0.34	- 0.03	- 0.73
0.24	0.006	- 0.12	- 0.30	- 0.70
0.28	0.05	- 0.05	- 0.26	- 0.64
0.31	0.06	- 0.07	- 0.37	- 1.00
0.34	0.30	0.09	- 0.25	- 0.60

3.6 R410A (50% CH₂F₂ / 50% C₂HF₅)

3.6.1 Physicochemical properties

The mixture of 50% pentafluoroethane CHF₂CF₃ and 50% difluoromethane CH₂F₂, commonly known as R410A, is a synthetic gaseous mixture recently identified as a potential alternative to SF₆.

This is the cheapest insulating gas considered in this document, with a cost for kilogram of only 3 US \$.

The molecular structure of the two gases constituting the R410A mixture is reported in figure 3.59.

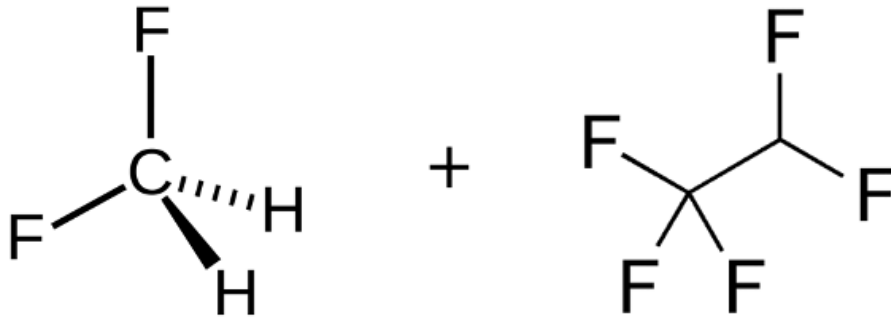


Figure 3.59: Molecular structure of difluoromethane CH₂F₂ and pentafluoroethane C₂HF₅

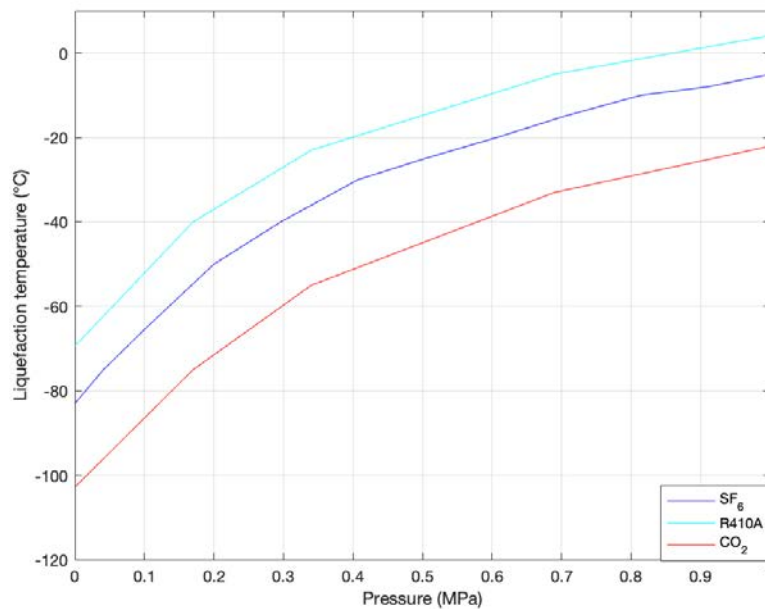
Some of the physicochemical parameters characterizing this mixture are reported in the table 3.17.

The boiling point at 0.1 MPa of R410A (- 52.7 °C) is slightly higher than the one of SF₆ but anyway lower than the one of R12 and R134.

Its dependence on pressure, compared to SF₆ and CO₂ is reported in the figure 3.60. Looking at the saturated vapor pressures, it can be seen that these values are much higher than the ones of R12 and R134a: as a consequence, this gas mixture can be adopted in many more industrial applications, in particular those with very low working temperatures [42].

Table 3.17: Physicochemical properties of R410

Parameter	Value	Unit
Molecular weight	72.6	g/mol
Density	0.0037	g/cm ³
Freezing point	- 155	°C
Boiling point at 1 bar	- 52.7	°C
Saturated vapor pressure at - 30 °C	0.28	MPa
Saturated vapor pressure at 0 °C	0.86	MPa
Saturated vapor pressure at 20 °C	» 1	MPa
Flammability	non-flammable	
Explosiveness	non-explosive	
Chemical stability	stable	
Corrosivity	non-corrosive	
Appearance	colourless/odourless	

Figure 3.60: Liquefaction temperatures of SF₆, R410A and CO₂ in dependence on pressure

3.6.2 Environmental properties

From the point of view of the environmental impact, R410A has great properties in comparison to SF₆, most of all a much lower GWP and atmospheric lifetime, as reported in the table 3.18.

Table 3.18: Environmental properties of R410A

Parameter	Value	Unit
GWP (ITH = 100 years)	1700	
ODP	0	
Atmospheric lifetime	17	years

This table shows that GWP of R410A is almost 15 times less than the one of SF₆ and the atmospheric lifetime is 200 times lower.

R410A has a negligible ODP, like R134a [42].

3.6.3 Dielectric properties

R410A shows good dielectric properties thanks to its intrinsic dielectric strength of 75.8 kV/cm at atmospheric pressure compared with 89.0 kV/cm of SF₆ in the same conditions.

Therefore, this gas has a dielectric strength, in pure form, which reaches 0.85 times the one of SF₆ resulting in an attractive potential candidate for industrial applications, especially those which have to work in very cold regions.

A comparison between the dielectric strength of R410A and SF₆ is provided by the figure 3.61 which also shows that this parameter depends on gas pressure in a monotonous way.

The dielectric strength difference between R410A mixture and SF₆ remains quite constant for all the pressure range considered.

Making a comparison between some alternative gases, it can be said that, as regards the dielectric strength under uniform field: SF₆>R12>R410A>R134a>CO₂>N₂>air [42].

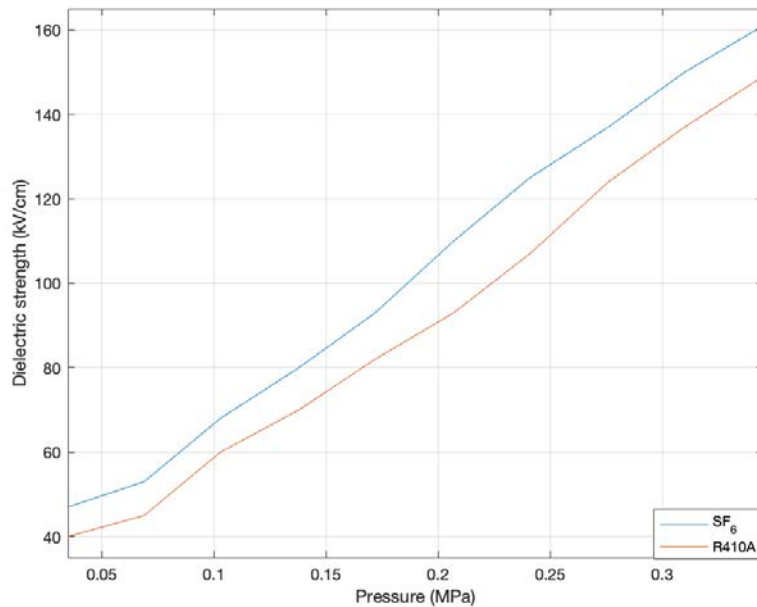


Figure 3.61: Dielectric strength of R410A compared to that of SF₆

3.6.4 R410A mixtures

Considering the liquefaction factor, fundamental in choosing the appropriate alternative gas due to the fact that insulation strength degrades when temperature, and thus pressure, decreases, it can be seen that R410A boiling temperature is higher than the one of SF₆ and this can be a problem in some working situations, reason for which a buffer gas, in this case air or carbon dioxide (- 78 °C of boiling point) instead of nitrogen, is generally added to the mixture to form a gas with a lower liquefaction temperature.

Liquefaction temperature of the mixture is illustrated in the figure 3.62, where as predictable the boiling point increases when the mixing ratio is increased.

Synergistic effect also has to be taken into account by analyzing the non-linear behavior of the mixture composed of the pure gas and the buffer gas.

Considering the connection between synergistic effect index C , mixing ratio and

breakdown voltage represented by the known equation

$$V_m = V_2 + \frac{k(V_1 - V_2)}{k + (1 - k)C}, V_1 > V_2$$

synergistic effect of R410A / air and R410A / CO₂ mixtures is calculated and given in tables 3.18 and 3.19, reported in the respective sections.

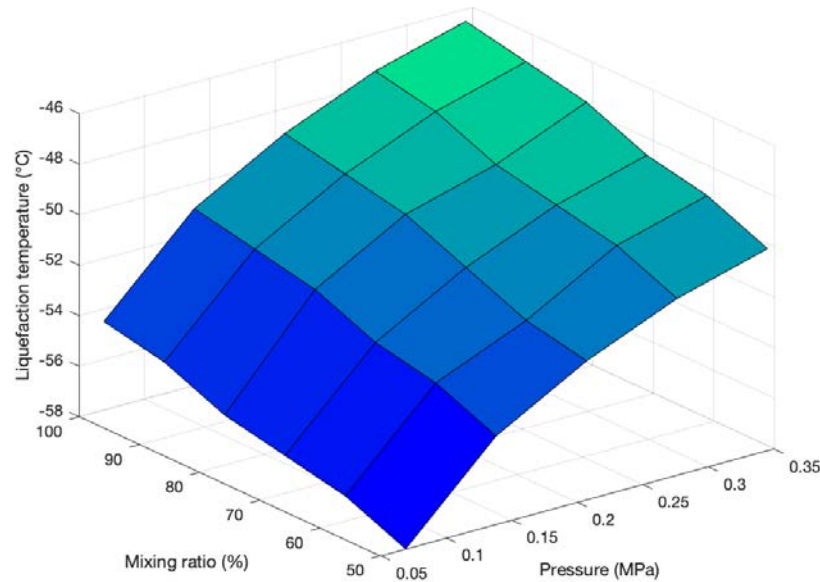


Figure 3.62: Liquefaction temperatures of R410A / CO₂ mixture in dependence on mixing ratio

These tables specify that C value of both mixtures declines when the pressure maximizes at the same mixing gas ratio.

When the gas pressure increases beyond 0.035 MPa at 0.80-0.90 mixing ratios, C value becomes negative and synergistic effect changes to positive synergistic effects; therefore, as pressure increases, C value becomes less [42].

R410A / air mixture

R410A / air mixture presents good dielectric properties and the use of air as buffer gas appears to be advantageous due to its unlimited availability.

In this case, pure R410A, 50% R410A / 50% air, 60% R410A / 40% air, 70% R410A / 30% air, 80% R410A / 20% air and 90% R410A / 10% air are presented.

Figure 3.63 shows AC dielectric strength of R410A / air mixture.

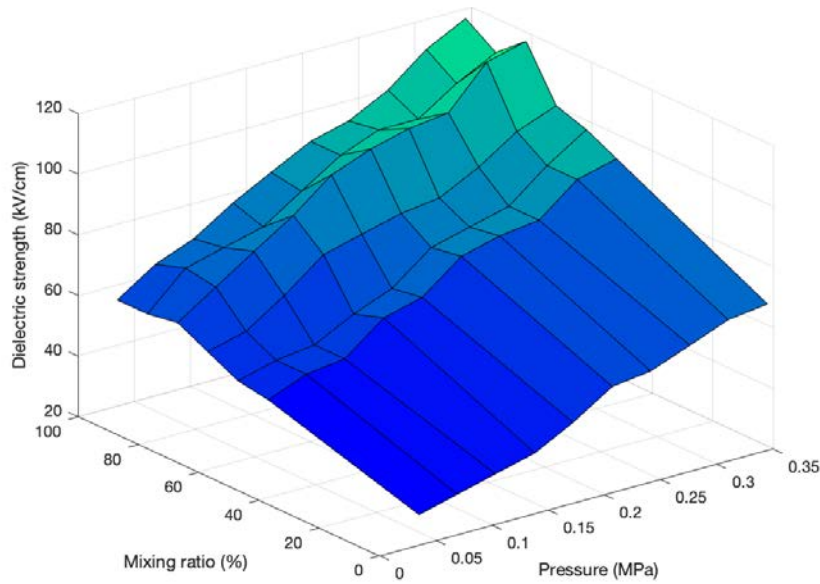


Figure 3.63: AC dielectric strength of R410A / air mixture in dependence on pressure and mixing ratio

It can be seen that by adding 50% of R410A to air rapidly increases breakdown strength of air; however, by increasing the percentage of R410A the breakdown strength lacks similar inclination.

This is a consequence of the fact that R410A has an high attachment cross-section at low energies so, when a small amount of R410A is added almost all the low energy electrons attached cause a rapid increase in the breakdown voltage.

The gap distance also affects the dielectric strength which increases with this parameter: increasing electrodes gap distance there exist need of maximum potential for balancing the electric field between electrodes as shown by the relation

$$E = \frac{V}{D}$$

where D is the distance between the electrodes and V is the applied voltage.

Figure 3.64 instead shows the dielectric strength of R410A / air mixture in a DC environment.

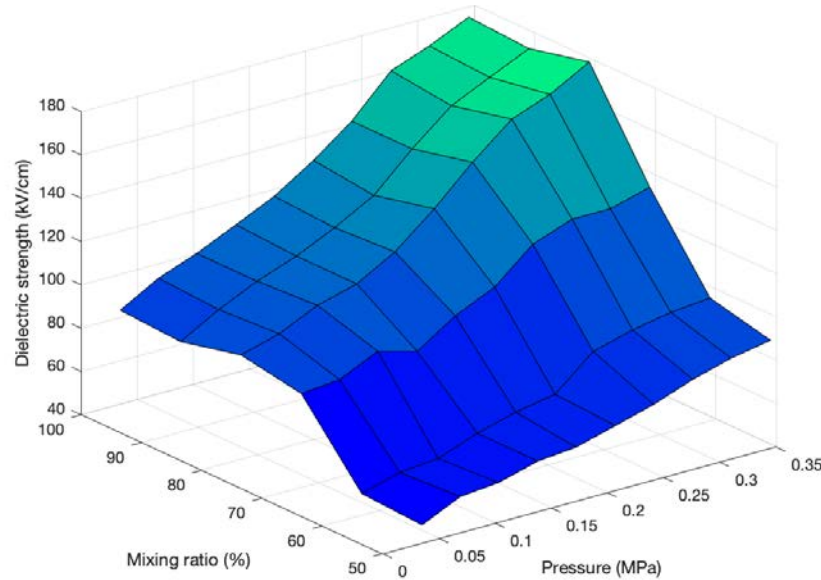


Figure 3.64: DC dielectric strength of R410A / air mixture in dependence on pressure and mixing ratio

Figure 3.65 provides Paschen's curve for different ratios of R410A / air in the PD product range of 0.2-2.5 MPa·mm where D is the distance from one electrode to the other and P is the pressure.

It can be noted that with the increase in pressure, breakdown voltage also increases even if there is a steady decrease in the slope of the curve when we consider a sphere-sphere electrodes configuration, effect that results in a deviation from Paschen's law considering that dielectric strength on an ideal gas has to be linear in theory.

By adding air, dielectric strength of the mixture is greater than that of pure R410A due to the so called positive synergistic effect.

Results for R410A / air mixture are reported in the table 3.19.

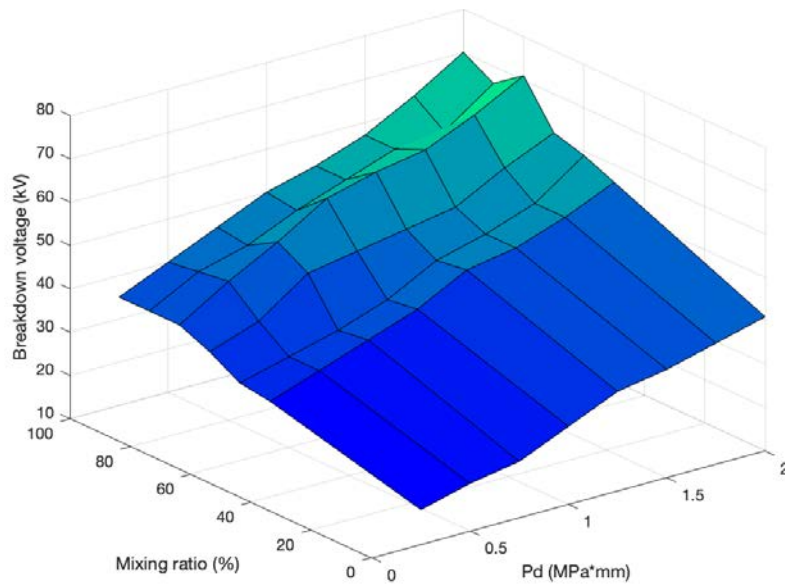


Figure 3.65: Paschen's curve of R410A / air mixture

Table 3.19: Synergistic effect of R410A / air mixture

Pressure (MPa)	K (%)				
	50	60	70	80	90
	C				
0.03	1.02	0.89	1.02	- 0.13	1.42
0.07	0.85	1.22	0.85	- 0.53	1.63
0.10	1.05	1.69	1.09	- 0.006	1.71
0.14	0.72	1.29	1.14	- 0.56	- 0.01
0.17	0.68	1.28	0.9	- 0.76	- 0.11
0.21	0.98	1.74	0.6	- 0.68	0.35
0.24	0.72	1.51	0.15	- 0.59	0.39
0.28	1.17	1.68	0.44	- 0.46	- 0.41
0.31	0.81	1.26	0.74	- 1.13	- 0.44
0.34	0.57	0.65	0.31	- 1.19	- 0.09

The mixing ratio 80% R410A / 20% air at 0.34 MPa gives the optimum value of synergistic index C [42].

R410A / CO₂ mixture

Carbon dioxide is the most stable, inert, and easily available gas in the market, incorporates a low GWP and a very low boiling point of - 78 °C.

The mixing of CO₂ with R410A reduces liquefaction temperature as well as global warming potential in comparison to pure R410A gas.

Carbon dioxide has excellent arc quenching capability and its mixture with R410A can provide better dielectric strength than the pure R410A.

Experimental results show that the mixture for specific ratios increases insulation strength but a further increase in the mixing ratio doesn't increase dielectric strength because of the fact that the attachment of electrons at lower energy levels is easy but at higher energy levels it is more difficult and thus dielectric strength doesn't increase further.

Dielectric properties of R410A and its mixture with carbon dioxide under AC environment, at various pressure and different mixing ratio are shown in figure 3.66.

The dependence of mixture dielectric strength on gas pressure appears stronger than on mixing ratio.

Similarly, in the figure 3.67 DC dielectric strength of R410A with a different mixing ratio of carbon dioxide is represented in dependence on pressure.

It can be noted that dielectric strength values reached in the DC case are much higher than the one reached in the AC case.

From these experimental results, it can be seen that for the mixing ratio 80% R410A / 20% CO₂ at 0.310-0.345 MPa, 0.95 times the dielectric strength of SF₆ can be achieved.

Figure 3.68 provides the Paschen's curve of R410A / CO₂ mixture at different mixing ratios.

It can be observed the strong connection between the pressure-gap distance product and the mixture breakdown voltage.

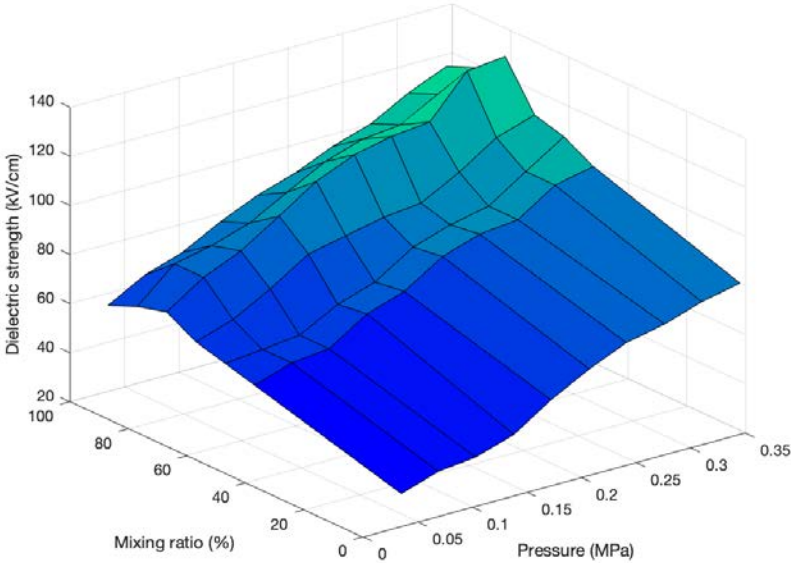


Figure 3.66: AC dielectric strength of R410A / CO₂ mixture in dependence on pressure and mixing ratio

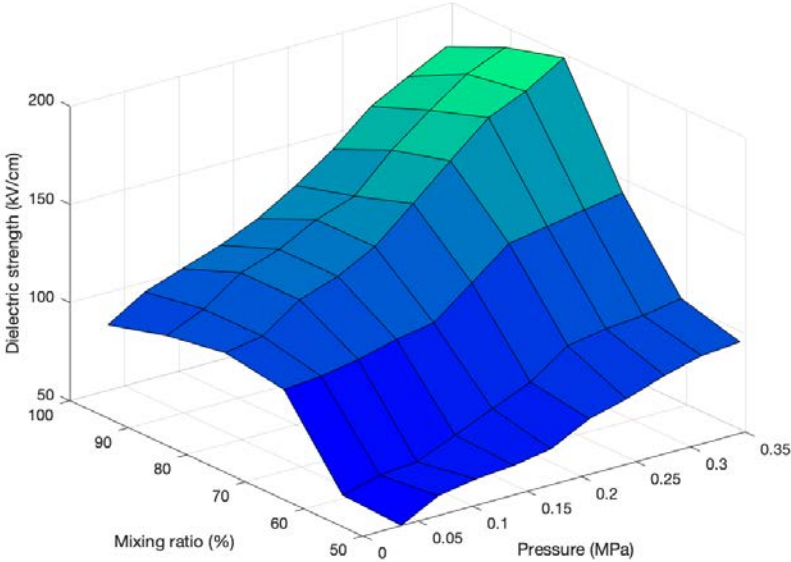
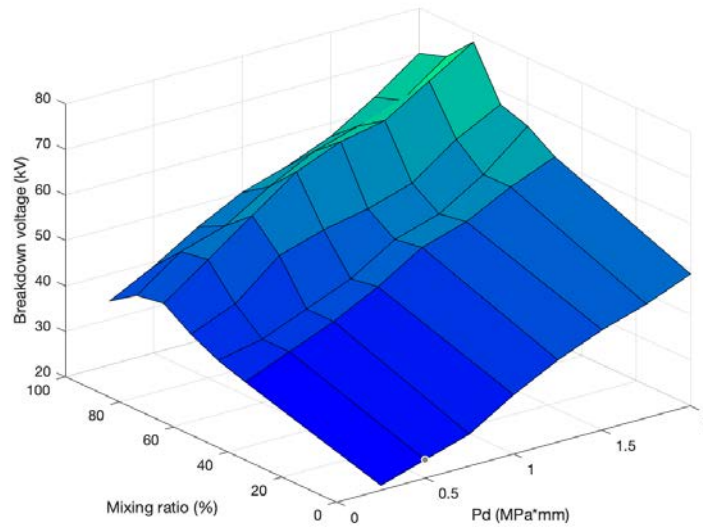


Figure 3.67: DC dielectric strength of R410A / CO₂ mixture in dependence on pressure and mixing ratio

Figure 3.68: Paschen's curve of R410A / CO₂ mixture

Results for R410A / CO₂ mixture synergistic effect are reported in the table 3.20.

The mixing ratio 80% R410A / 20% CO₂ at 0.34 MPa shows the lowest C value [42].

Table 3.20: Synergistic effect of R410A / CO₂ mixture

Pressure (MPa)	K (%)				
	50	60	70	80	90
	C				
0.03	0.80	0.46	0.34	- 1.16	0.72
0.07	0.48	0.68	0.11	- 1.44	0.92
0.10	0.78	1.30	0.35	- 1.07	0.94
0.14	0.47	0.98	0.47	- 1.59	- 1.51
0.17	0.34	0.75	0.14	- 1.66	- 1.49
0.21	0.70	1.34	0.005	- 1.47	- 1.73
0.24	0.38	0.75	- 0.32	- 1.25	- 1.47
0.28	0.72	1.04	- 0.09	- 1.16	- 1.30
0.31	0.46	0.78	0.16	- 1.80	- 1.33
0.34	0.29	0.22	- 0.18	- 1.90	- 1.60

Chapter 4

Gas-Insulated Line design

In this chapter, comparative considerations regarding the most important parameters of the gas mixtures previously analyzed are provided.

In addition, a GIL rough sizing for each optimized mixture is proposed.

4.1 Insulating mixture choice

4.1.1 Environmental impact

The goal of this project is to find an eco-friendly alternative which could replace SF₆ in HV GILs, for this reason all the target gases that have been considered in this document are characterized by a much lower GWP and this clearly appears looking at the figure 4.1.

SF₆ mixtures GWP curves show values much higher than the ones of the considered alternative mixtures, reaching 23500 for a 100% mixing ratio, at least 100 times the maximum GWP value reached by the worst alternative mixture analyzed from the point of view of the environmental impact.

Taking into account only the alternative solutions (figure 4.2), it can be observed that, between all the mixtures, R12 / N₂ shows the worst GWP at high mixing ratios since C₄F₇N / N₂ has the worst GWP at low mixing ratios.

A particular note has to be made about C₅F₁₀O and CF₃I mixtures: they show very

low GWP for all the possible mixing ratios, thanks to the fact that both the pure gases are characterized by a GWP of 1.

GWP curves of these two types of mixtures are reported in the figure 4.3.

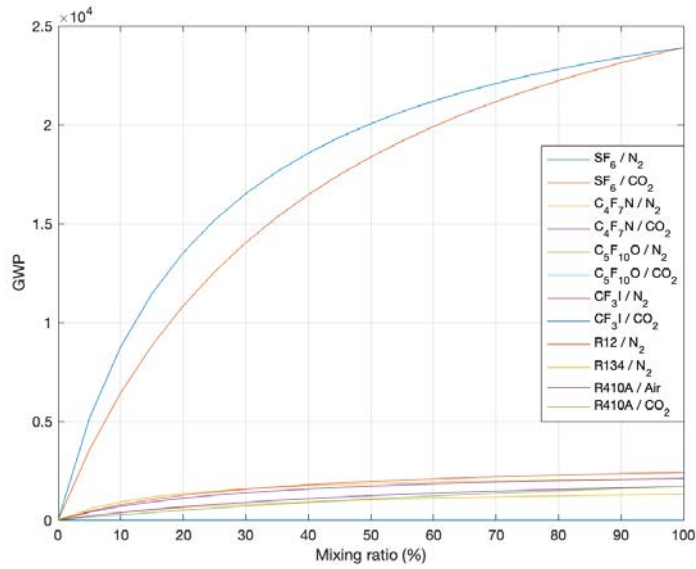


Figure 4.1: SF₆ mixtures GWP compared to that of alternative mixtures

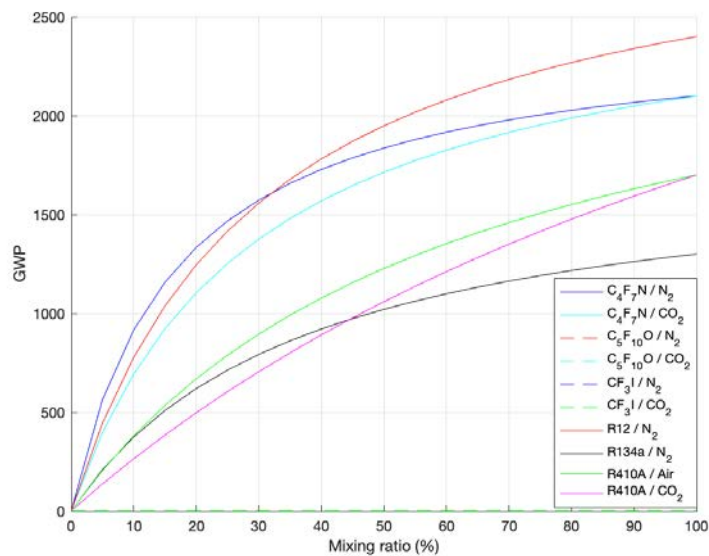


Figure 4.2: Alternative mixtures GWP in dependence on mixing ratio

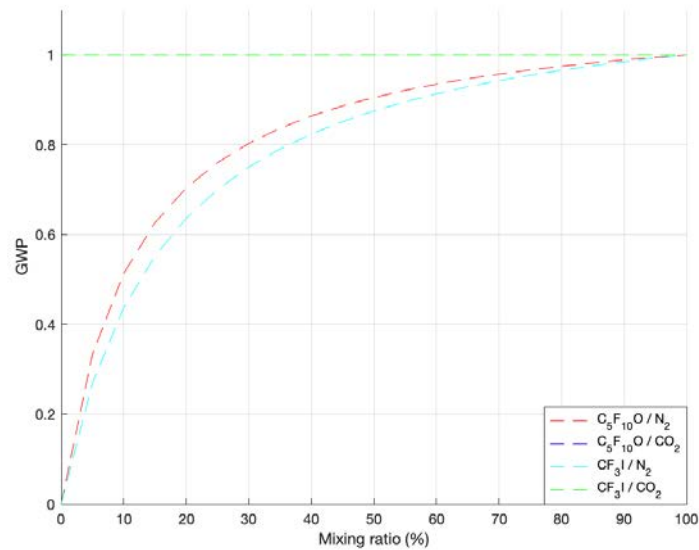


Figure 4.3: A detail of the figure 4.2

These diagrams are obtained by applying the formula which allows the calculation of GWP for a gas mixture, reported in the section 1.4.

An other important parameter to compare is the ODP: the SF₆ reference value is 0 therefore this parameter should be 0 also for a good alternative mixture.

A comparison of ODP for all the pure gases analyzed is reported in the table 4.1; this parameter, anyway, becomes lower when considering mixtures and some technical solutions are available to reduce it.

Table 4.1: ODP of some pure alternative gases

SF ₆	C ₄ F ₇ N	C ₅ F ₁₀ O	CF ₃ I	R12	R134a	R410A
0	0	0	0.012	1	0	0

All the studied gases result non-ozone-depletive with the exception of CF₃I (low depletion potential) and R12 which instead shows an high ODP value making it necessary to find adequate countermeasures for its adoption.

The last parameter is the atmospheric lifetime, summarized for all the considered pure gases in the figure 4.4 in which SF₆ is not reported due to graphic matters (it has a lifetime of 3200 years, more than 100 times higher than all the other values).

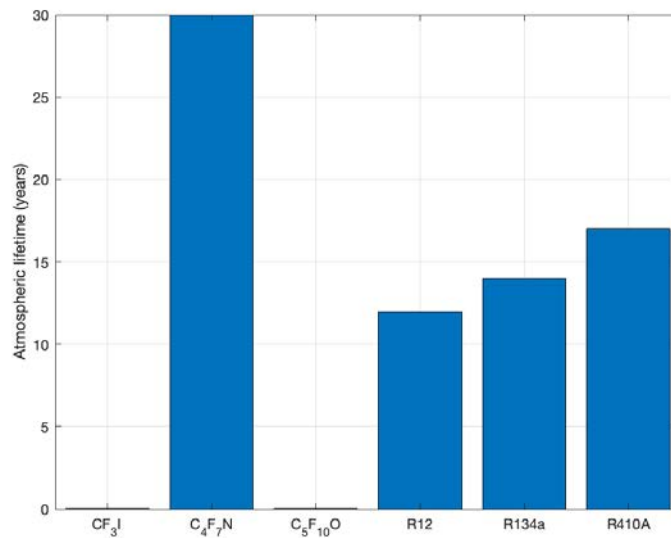


Figure 4.4: Atmospheric lifetime of some pure alternative gases

C₅F₁₀O and CF₃I show the lowest values, being their atmospheric lifetime of only few days.

4.1.2 Liquefaction temperature

A fundamental property of an insulating gas is its boiling point: in order to guarantee a good insulation the dielectric medium must remain in the gaseous state and this is possible only if the gas liquefaction temperature is compatible, and thus low enough, with the GIL working temperatures range.

The figure 4.5 illustrates the liquefaction temperatures of different pure alternative gases in dependence on pressure.

It can be seen that, as regards this specific parameter, the best alternative gas is the mixture R410A (liquefaction temperature only slightly higher than that of SF₆) since the worst is C₅F₁₀O (values very high considering that just at 0.1 MPa, a too low pressure for industrial applications, the boiling point is 50 °C).

Fortunately, these liquefaction temperatures can be lowered by admixing pure gases with other buffer gases like CO₂, dry air or N₂ with the last one which has the lowest

boiling point and then leads to the maximum decrease of this parameter.

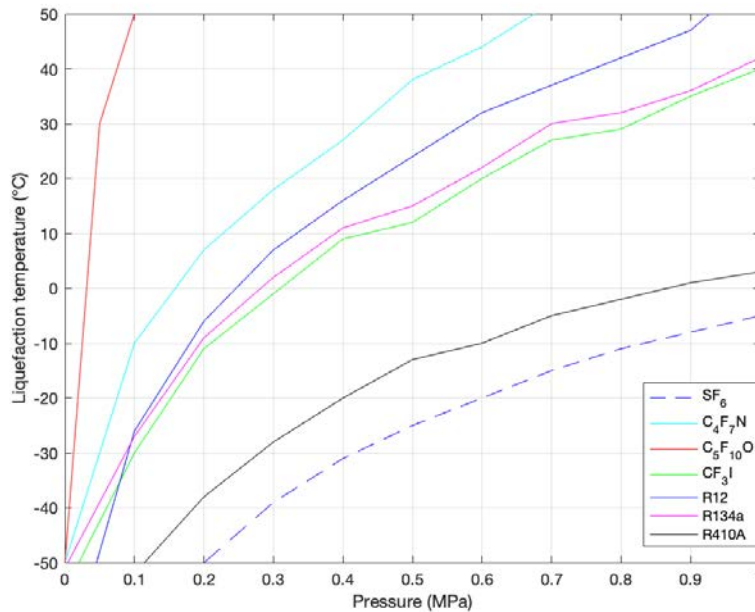


Figure 4.5: Liquefaction temperature of some pure alternative gases in dependence on pressure

In the figure 4.6 the influence of the buffer gas on the mixture boiling point is strongly underlined: in this case the example of some C_4F_7N / CO_2 mixtures is reported and what emerges is that the greater the natural gas content is, the lower the liquefaction temperature is at a certain pressure.

Looking at the figure in much more detail, it can be noted that in order to achieve a mixture boiling point which could allow the use at a GIL standard working temperature of $-30\text{ }^\circ\text{C}$ it is necessary to adopt a mixing ratio, in the case of g^3 mixture, not higher than 5%.

Analysis identical to this one have been done for all the alternative gases considered in this document and therefore, for each of them, the best couple of mixing ratio and gas pressure has been chosen also in dependence on this parameter.

At the end, the combination of liquefaction temperature with GWP and dielectric strength determines the final choice.

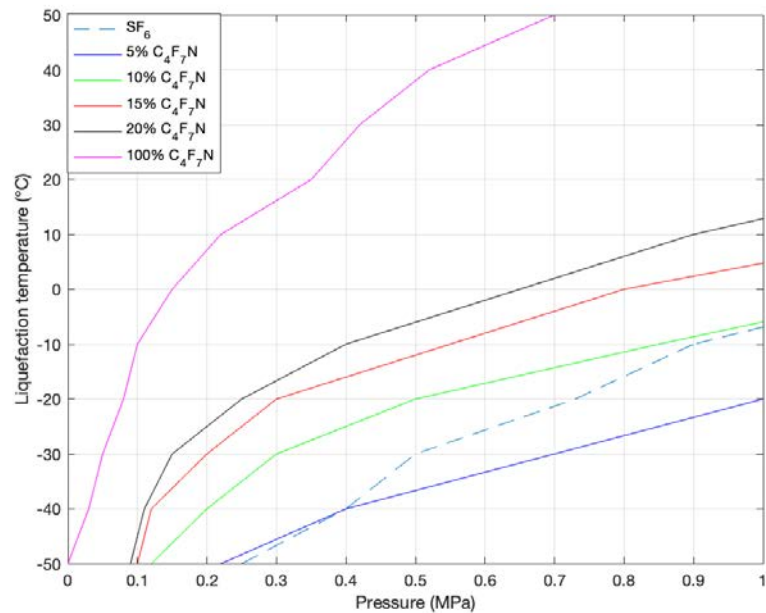


Figure 4.6: Liquefaction temperature of C_4F_7N / CO_2 mixtures in dependence on pressure

4.1.3 Insulation properties

Alternative gases are considered in order to solve the environmental problem linked to the use of a such strong greenhouse gas as SF_6 .

However, the insulation excellent properties of SF_6 must not be too weakened so that the GIL exceptional functionality can be preserved and so alternative mixtures dielectric strength represents a third fundamental parameter to be taken into account. All the pure alternative gases considered in this work present a great intrinsic dielectric strength, the lowest of which is 0.8 times the one of SF_6 , as reported in the figure 4.7. C_4F_7N has the highest dielectric strength, reaching 2.7 times that of SF_6 , and also for this reason its mixtures are the most studied in the recent period as a potential eco-friendly alternative.

$C_5F_{10}O$ also presents an high intrinsic dielectric strength, being it about twice the one of SF_6 , but unfortunately the very high liquefaction temperature affects its attractiveness.

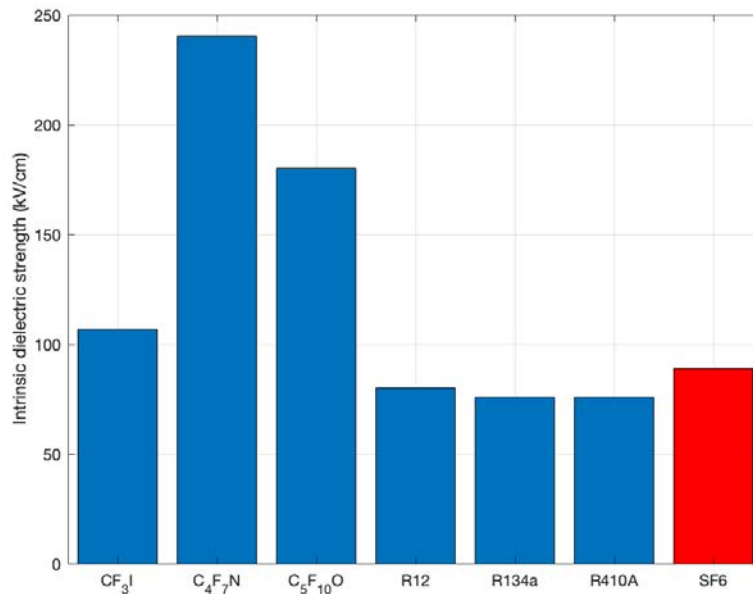


Figure 4.7: Intrinsic dielectric strength of some pure gases

The rest of the mixtures instead show values around the one of SF₆ (higher than that of CF₃I, lower than the other ones) but the synergistic effect plays a pivotal role when considering mixtures with other buffer gases.

Alternative gases insulation properties have been analyzed also through the use of BOLSIG+ software which simulates gas electron collisions and allows to obtain, thanks to calculations on compound cross sections, net ionization and rate coefficients. In the figure 4.8, some pure gases at low pressure (10 kPa) are compared as regards the reduced Townsend coefficient and it can be noted that, in relation to SF₆ and some PFCs, CF₃I and C₅F₁₀O show the highest critical reduced field (value for which the net ionization coefficient goes to 0), confirming what known from the literature. Some target gases like NOVEC 4710 are not reported because its data related to this parameter are not available in the LXCat database.

This analysis, anyway, becomes fundamental when considering gas mixtures: it demonstrates the great influence which the choice of the mixing ratio has on the mixture overall dielectric strength.

In the figure 4.9 the case of C₄F₇N / CO₂ mixture at very low pressure (100 Pa) is

studied, this time considering the rate coefficient which is obtained by multiplying the net ionization coefficient and the drift velocity, and what emerges is that the reduced critical field directly increases with the increase of the mixture mixing ratio.

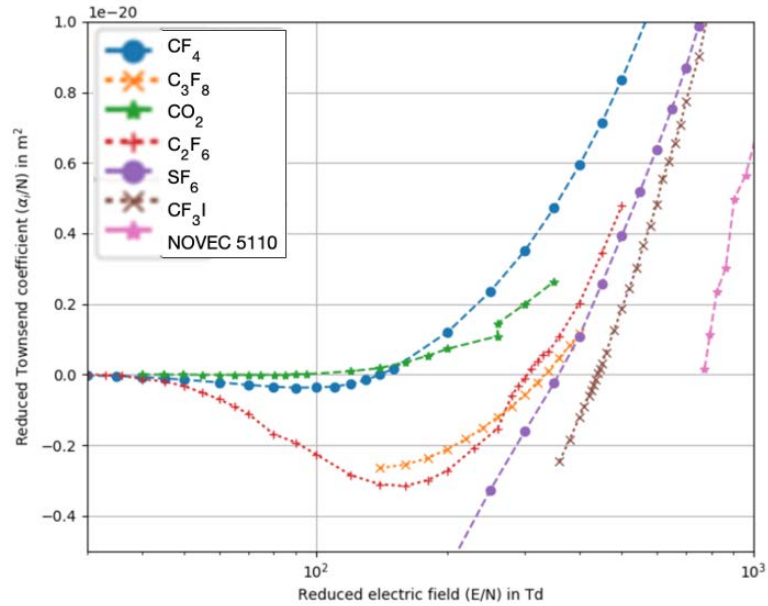


Figure 4.8: Reduced Townsend coefficient of some pure gases

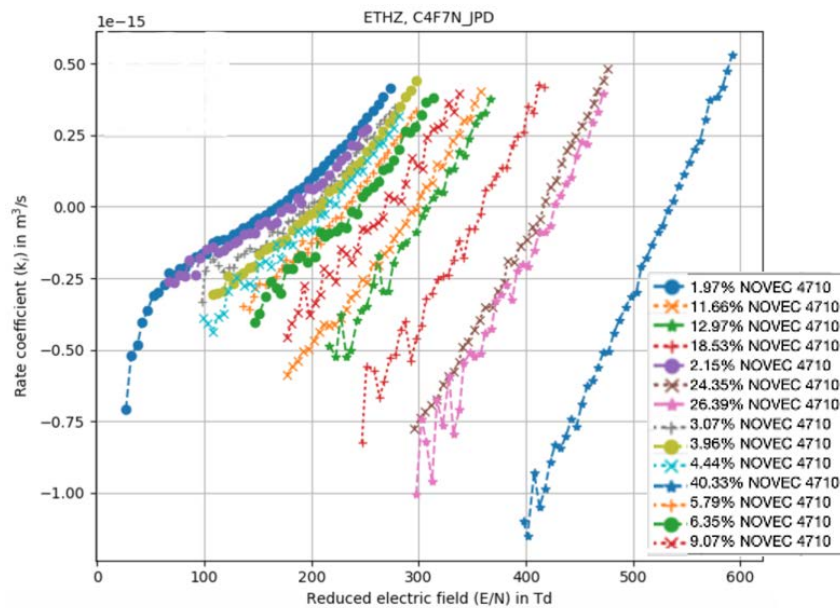


Figure 4.9: Rate coefficient of some C_4F_7N / CO_2 mixtures

In the figure 4.10 the analogue case of C_4F_7N / N_2 mixtures is reported: comparing the two figures, it results that a mixture with N_2 leads to an higher critical reduced field and this would mean that C_4F_7N / N_2 mixtures have better insulation properties than C_4F_7N / CO_2 mixtures with the same mixing ratio and at the same pressure. This is theoretically true, but practically the C_4F_7N / CO_2 mixture is preferred thanks to the better chemical stability of CO_2 than N_2 .

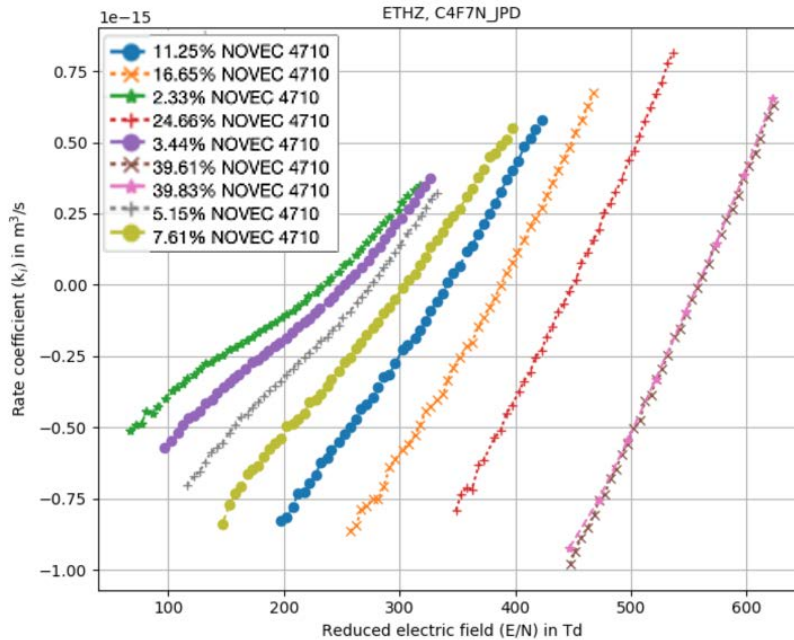
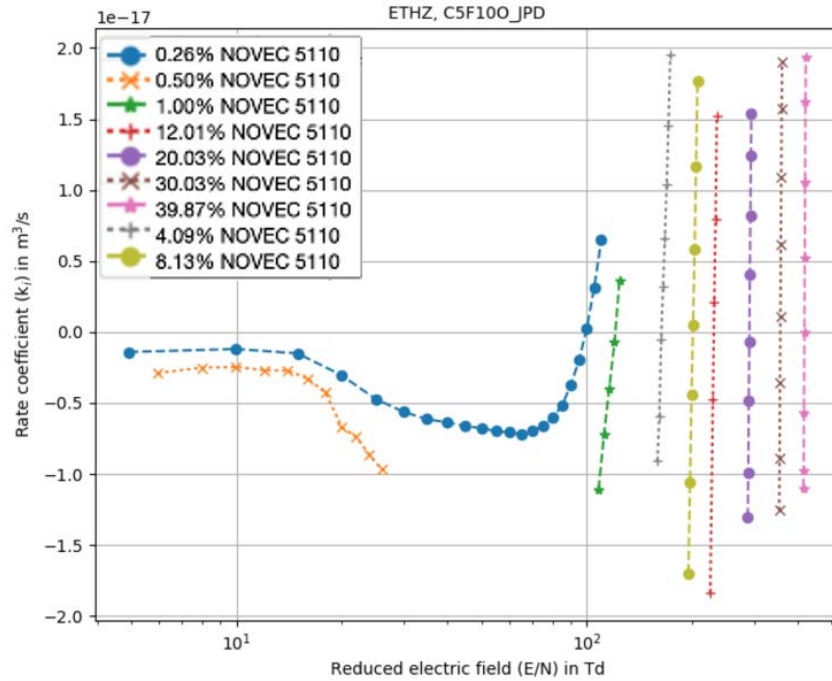
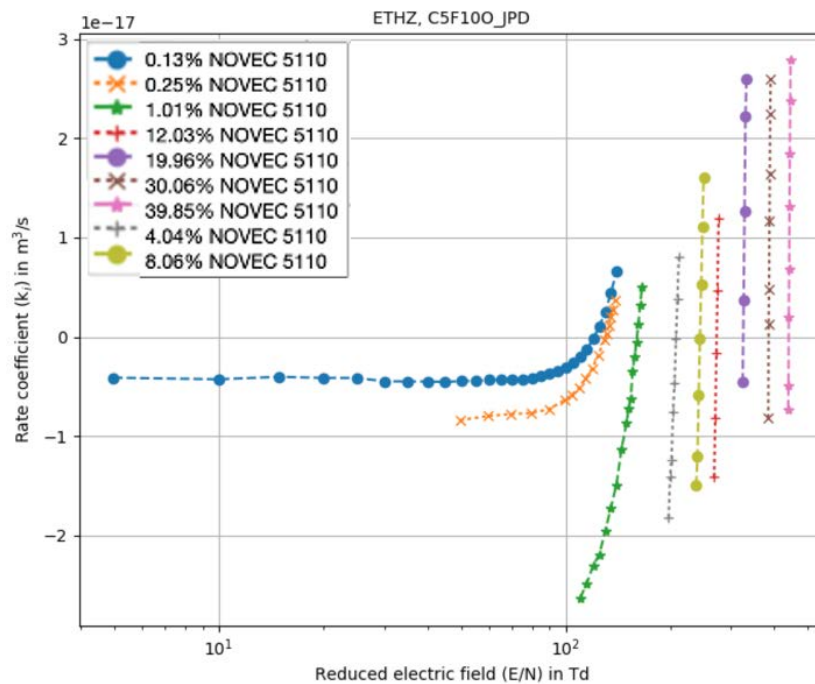


Figure 4.10: Rate coefficient of some C_4F_7N / N_2 mixtures

In the figures 4.11 and 4.12 the focus is on $C_5F_{10}O$ mixtures (the considered gas pressure is of 10 kPa) and considerations similar to those made for NOVEC 4710 lead to the conclusion that NOVEC 5110 mixtures have worse dielectric properties than the other ones under the same conditions.

Also in this case, mixtures with CO_2 have a lower dielectric strength but an higher chemical stability than with N_2 , therefore the first ones are preferred in practice.

A direct comparison between some examples of NOVEC 4710 and 5110 mixtures with very low mixing ratio and low gas pressure (10 kPa) is reported in the figure 4.13, in which an other demonstration of the better insulation properties of N_2 mixtures than CO_2 ones and of C_4 mixtures than C_5 ones is given.

Figure 4.11: Rate coefficient of some $\text{C}_5\text{F}_{10}\text{O}$ / CO_2 mixturesFigure 4.12: Rate coefficient of some $\text{C}_5\text{F}_{10}\text{O}$ / N_2 mixtures

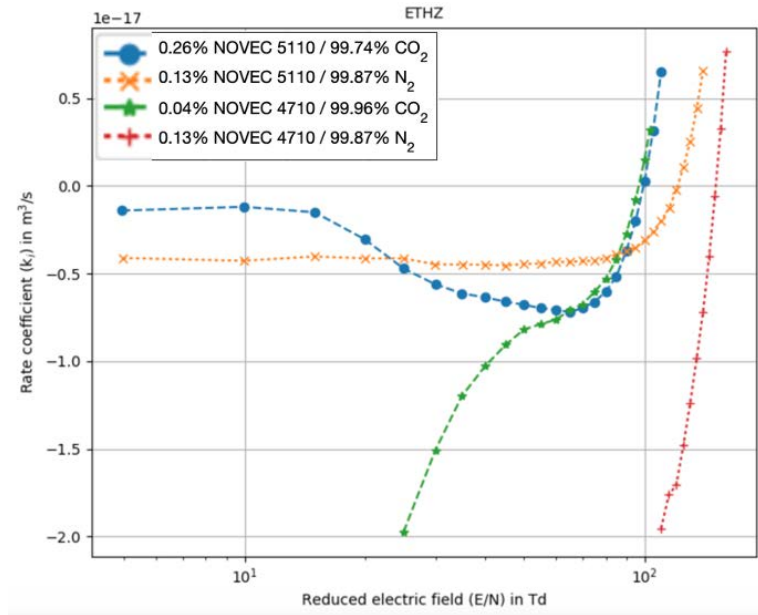


Figure 4.13: Comparison between the rate coefficients of some NOVEC 4710 and 5110 mixtures

In the figure 4.14 a more detailed parallel between some C_4F_7N and $C_5F_{10}O$ mixtures at 926 Pa including also O_2 as buffer gas is proposed.

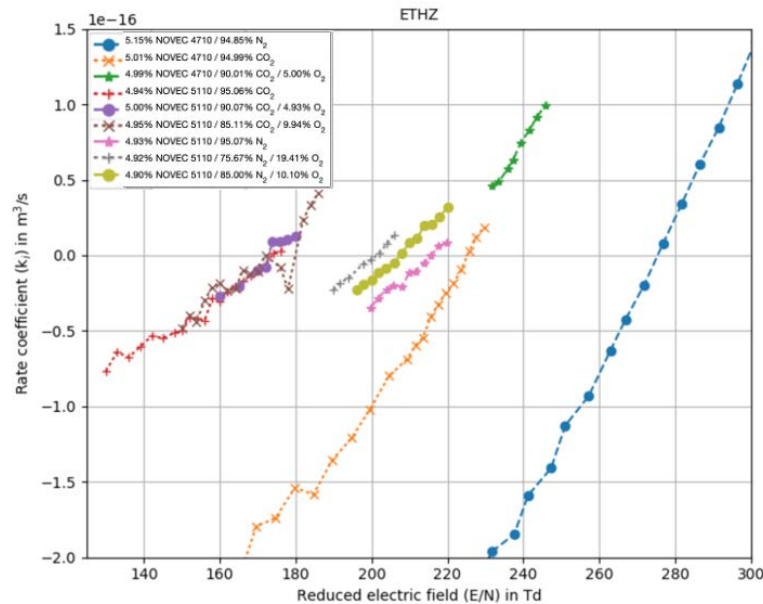


Figure 4.14: Rate coefficient of some C_4 and C_5 mixtures also including O_2

It can be noted that the O_2 presence worsens the mixtures insulation properties, mainly due to the fact that it replaces a certain amount of N_2 (more evident effect) or CO_2 both of which have an higher intrinsic dielectric strength than oxygen.

Finally, an example of the evaluation of a certain mixture suitability to replace the 20% SF_6 / 80% N_2 mixture from the point of view of the dielectric properties is illustrated in the figure 4.15.

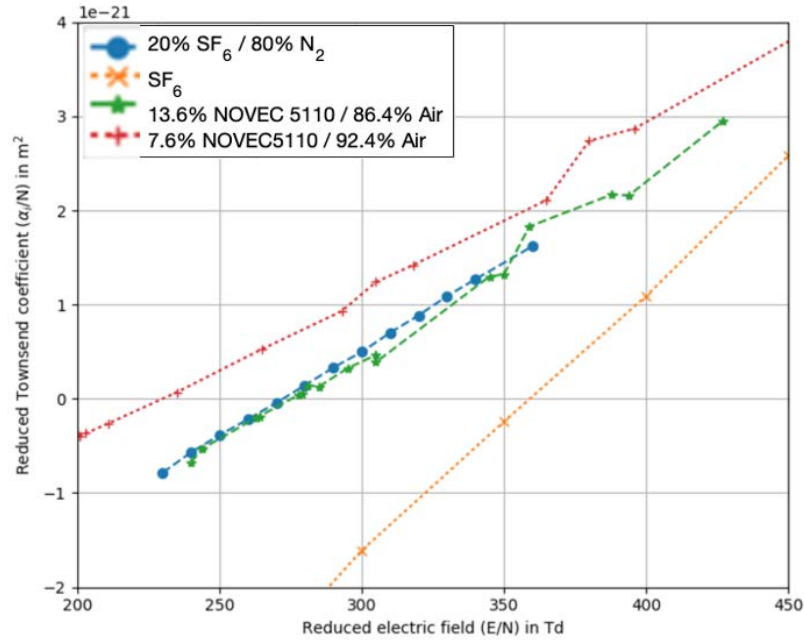


Figure 4.15: Reduced Townsend coefficient of C_5 / air mixtures compared to 20% SF_6 / 80% N_2 mixture

In this case two NOVEC 5110 / air mixtures at 10 kPa are analyzed and it can be observed that with only a 13.6% of $C_5F_{10}O$ content the dielectric strength of the SF_6 reference mixture is exceeded.

At the end, considering BOLSIG+ calculations, some reported laboratory experimental results and giving attention to the values for which the mixture synergistic effect results the best one, specific combinations of buffer gas type, mixing ratio and gas pressure can be chosen for each pure gas analyzed.

In order to make the best choice, the results reported in the previous two sections must also be taken into account and this is the topic of the following section.

4.1.4 The best compromise

The goal of this section is to collect all the informations given in the last ones and to transform them into six combinations, one for each studied gas, of buffer gas type, mixing ratio, pressure, GWP and minimum working temperature of the mixture.

The targets are:

- A GWP lower than 2500 (if possible, lower than 1000 which is a standard value that defines a gas as eco-friendly);
- A relatively low minimum working temperature, basically at least lower than $-5\text{ }^{\circ}\text{C}$ in order to find some practical applications;
- A dielectric strength higher or at least similar to that of 20% SF_6 / 80% N_2 mixture.

In order to achieve them, GWP and liquefaction temperature curves, ionization coefficients and synergistic effect have been analyzed and compared, concluding that good choices could be:

- 4% $\text{C}_4\text{F}_7\text{N}$ / 96% CO_2 (GWP = 300) at 0.6 MPa which presents a minimum working temperature of $-30\text{ }^{\circ}\text{C}$;
- 5% $\text{C}_5\text{F}_{10}\text{O}$ / 95% CO_2 (GWP < 1) at 0.6 MPa which presents a minimum working temperature of $-5\text{ }^{\circ}\text{C}$;
- 30% CF_3I / 70% CO_2 (GWP < 1) at 0.6 MPa which presents a minimum working temperature of $-7\text{ }^{\circ}\text{C}$;
- 70% R12 / 30% air (GWP = 2200) at 0.4 MPa which presents a minimum working temperature of $-45\text{ }^{\circ}\text{C}$;
- 80% R134a / 20% N_2 (GWP = 1200) at 0.4 MPa which presents a minimum working temperature of $-40\text{ }^{\circ}\text{C}$;
- 80% R410A / 20% CO_2 (GWP = 1500) at 0.4 MPa which presents a minimum working temperature of $-60\text{ }^{\circ}\text{C}$;

4.2 GIL dimensioning

The basic design criteria for a GIL deal with [1]:

- electric field strength at rated voltages;
- maximum temperature of conductor and enclosure pipe;
- mechanical strength of enclosures for gas pressure and external load;
- current forces including short-circuit currents.

In order to prove the correct design of the GIL, some tests are carried out [1]:

- high-voltage test;
- rated current test;
- short-circuit current test;
- internal arc test;
- mechanical tests;
- vibration tests;
- thermal tests;
- partial discharge test;
- gas-tightness test;
- resistance of conductor test.

These planning issues are investigated also to check the interferences of the GIL with other network equipment like cables and overhead lines when operated in parallel or in series.

The reliability of the GIL itself and in conjunction with the network, grounding, touch voltages, safety, environmental impact and limitations, electric phase angle

compensation, loadability including overloading restrictions and insulation coordination are the main issues to be covered when the functionality of the GIL at specific network conditions has to be checked.

The design of the GIL in the network mainly depends on the requirements of the power transmission rating which leads to the voltage and current ratings and must fit into the power transmission network.

The GIL is applied at all voltage levels of high voltage from 110 kV up to 800 kV thanks to its suitability for high power supply.

The test voltages are related to the insulation coordination for power frequency, lightning and switching impulse voltage reported in the table 4.2 [1].

The maximum magnetic field strength depends on the rated current and the distance from the measuring point to the GIL.

The GIL design follows the IEC 62271-204 “Rigid high-voltage, gas-insulated transmission lines for rated voltages of 72.5 kV and above” standard.

Table 4.2: GIL voltage levels (kV)

Nominal voltage levels	110	220	345	380	500	735
Highest voltage of the equipment	123	245	362	420	550	800
Power frequency withstand voltage	230	460	520	630	710	960
Lightning impulse withstand voltage	550	1050	1175	1425	1550	2100
Switching impulse withstand voltage	NA	NA	950	1050	1175	1425

The absolute dimensions of a gas-insulated line are determined by considering the dielectric, thermal and mechanical factors.

Conductor and enclosure diameters and their thicknesses are defined according to voltage level, gas pressure, rated current and gas mixture mixing ratio.

The dielectric strength is the main parameter in determining the GIL dimensions and the required current rating.

Thermal considerations become predominant for more highly rated systems and larger dimensions are necessary to maintain temperatures within acceptable limits.

Standard values of some other important technical parameters for 420 kV and 550

kV GILs, which are the voltage levels that this work focuses on, are reported in the table 4.3 [1].

Table 4.3: Technical parameters of 420 kV and 550kV gas insulated lines

Parameter	Value (1)	Value (2)	Unit
Rated voltage	420	550	kV
Rated power	3000	4500	MVA
Rated current	4000	4500	A
Short circuit current	63	100	kA
Gas pressure	0.7	0.7	MPa
Weight per metre	25	30	kg
Mixing ratio	20% SF ₆ / 80% N ₂	60% SF ₆ / 40% N ₂	%

These parameters are taken as a reference, a starting point from which this study develops considering a different design for each alternative mixture adopted.

This research deals with the definition of the best GIL absolute dimensions in dependence on the insulating gas mixture considered and therefore on its pressure and mixing ratio.

For a GIL system, it is important to minimize the occurrence of gas discharge, thus the GIL maximum electric field value needs to be designed lower than the critical reduced field strength of whichever mixture to be used as the insulation medium.

The focus is on the electrostatic aspect, analysed through COMSOL simulations regarding a 3D model of the elbow's area of a gas-insulated line.

This choice is made because the elbow's area is the most stressed part of the structure and also presents the highest, therefore the most critical, electric field values.

A representation of the GIL 3D model is shown in the figure 4.16.

The model contains some components, typical of a gas-insulated line, which could be critical points from the point of view of the electric field distributions.

The main elements are:

- outer enclosure;

- inner conductor;
- support insulators;
- conical insulator.



Figure 4.16: GIL 3D model representation

When it comes to the materials adopted, the outer enclosure and the inner conductor are made of aluminum since all the insulators are made of cast resin.

The meshing step of the 3D model is illustrated in the figure 4.17.

In line with the required level of accuracy of the simulations, a normal size mesh is chosen.

It can be noted that the support insulators are horizontally disposed, differently from what happens in practice with the insulators which are inclined by 30° with respect to the horizontal.

This choice is made only so that it is possible to consider a single electric field plot layer in the following representation.

In order to reach the target of optimizing the absolute dimensions of the GIL, some considerations have to be made.

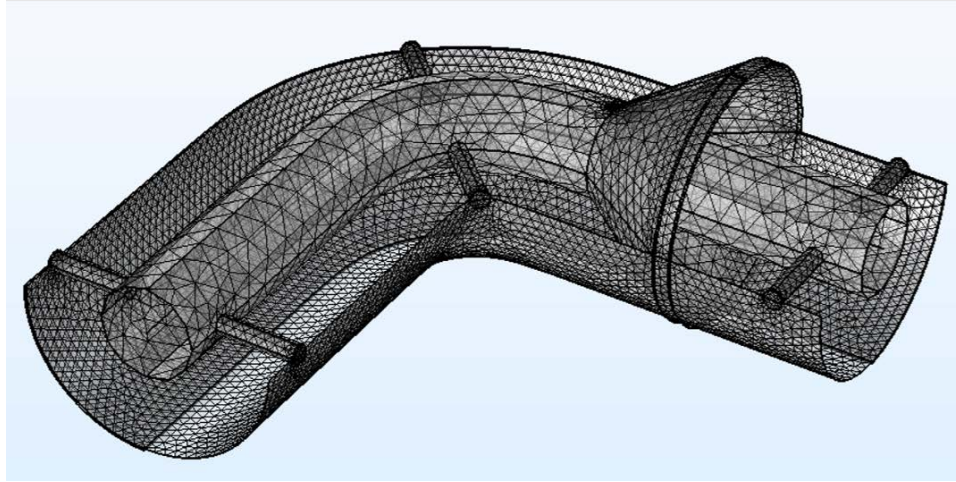


Figure 4.17: GIL 3D model mesh

From the literature, it is known that there is an optimal ratio between the radius of external enclosure and internal conductor that minimizes the GIL maximum electric field value and this can be easily obtained studying the following equation [1, 5]:

$$E_{max} = \frac{V}{R_{in} \cdot \ln\left(\frac{R_{ext}}{R_{in}}\right)}$$

where E_{max} is the maximum electric field value, V is the applied voltage, R_{ext} is the external enclosure radius and R_{in} is the inner conductor radius.

It can be found that the minimum of this equation is reached with the ratio

$$\frac{R_{ext}}{R_{in}} = e \approx 2.72$$

and this condition is a fixed point of all the simulations performed.

In addition to this also the absolute dimensions are a fundamental parameter which has to be considered in the design because of their strong influence on the electric field distributions and values.

Most of the attention is paid to the case of a 420 kV rated voltage GIL and the reference value of the maximum electric field achieved in a standard GIL is

$$E_{max} = 3.5 \text{ kV/mm}$$

referred to the adoption, very diffused at this voltage level, of an insulating gas mixture of 20% SF₆ / 80% N₂ at 0.7 MPa.

For a such scenario, the standard dimensions are

- $R_{ext} = 250$ mm;
- $R_{in} = 92$ mm;
- Enclosure thickness = 7 mm.

Starting from these elements, a study on the best combination of gas pressure, mixing ratio and GIL absolute dimensions is performed by varying the geometrical dimensions as long as the E_{max} threshold value of 3.5 kV is reached, process repeated for each insulating mixture reported in this document.

Every mixture is in fact characterized by a different dielectric strength, therefore a different combination of the three parameters previously mentioned results for each solution.

An example of the electric field distribution for a certain combination of pressure, mixing ratio and GIL geometrical dimensions, for a given mixture is illustrated in the figure 4.18.

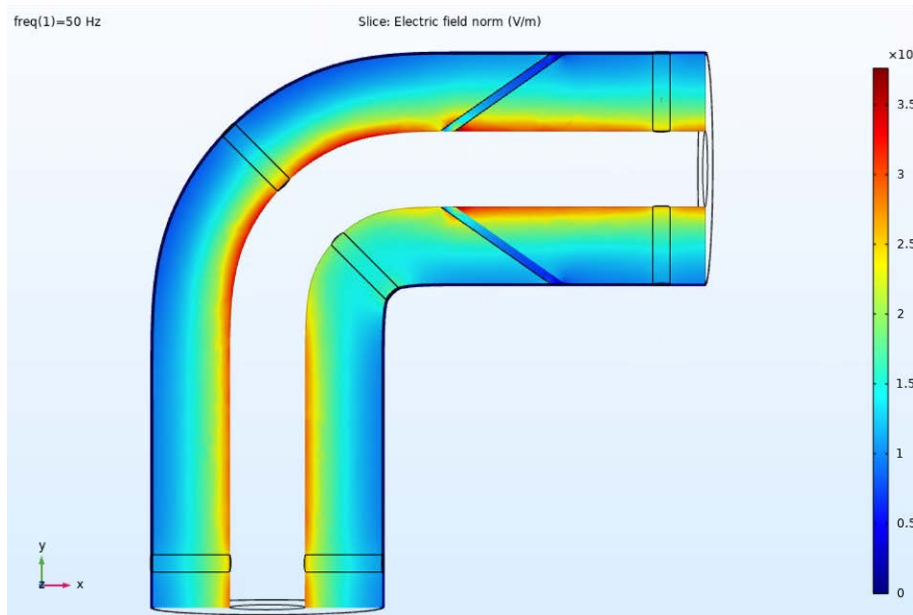


Figure 4.18: Elbow's area electric field distribution

A first important thing that can be deduced from this plot is that the maximum electric field values are localized in the curved stretch, justifying the choice of modeling an elbow's area for the simulations, being it the most stressed part of the structure.

The insulators also play an important role in the electric field distribution: the support insulators have only a little influence on the electric field which appears slightly weakened across them, the conical insulator instead affects the electric field distribution in a stronger way as it can be seen by taking a look at the connection to the inner conductor, where the electric field seems much distorted, besides the fact that it also results much less intense along the conical insulator.

Repeating the procedure previously described, optimum GIL dimensions are defined for each alternative insulating mixture proposed in the previous section:

- 4% C₄F₇N / 96% CO₂ mixture at 0.6 MPa, GIL external radius of 250 mm;
- 5% C₅F₁₀O / 95% CO₂ mixture at 0.6 MPa, GIL external radius of 405 mm;
- 30% CF₃I / 70% CO₂ mixture at 0.6 MPa, GIL external radius of 325 mm;
- 70% R12 / 30% air mixture at 0.4 MPa, GIL external radius of 250 mm;
- 80% R134 / 20% N₂ mixture at 0.4 MPa, GIL external radius of 250 mm;
- 80% R410A / 20% CO₂ mixture at 0.4 MPa, GIL external radius of 250 mm.

These results underline several things, the first of which is that for most of the mixtures considered, with an appropriate choice of pressure and mixing ratio, there is no need to modify the standard geometrical dimensions related to the adoption of a 20% SF₆ / 80% N₂ mixture, as it can be noted looking at the value, common for nearly all the solutions, of 250 mm for the external enclosure radius.

The only exceptions are the mixtures containing C₅F₁₀O and CF₃I which, due to liquefaction concerns of the base gas, have mixing ratios and gas pressures that cannot respectively exceed 5% and 0.6 MPa in the case of C₅ and 30% and 0.6 MPa in the case of CF₃I, therefore they need bigger GIL absolute dimensions in order to obtain a critical electric field which can be supported by the insulating gas.

Conclusions

This project has focused on the research of an eco-friendly alternative capable of replacing the greenhouse SF₆ gas in high-voltage Gas-Insulated Transmission Lines. This has been done with the goal of reducing the environmental impact, maintaining the reference dielectric properties and guaranteeing a working temperature range which could be suitable for at least some specific applications.

In order to do that several gases, some of which just known for other uses, have been analyzed and compared.

Precisely, six gases have been studied: perfluoronitrile C₄F₇N, perfluoropentanone C₅F₁₀O, trifluoroiodomethane CF₃I, dichlorodifluoromethane CCl₂F₂ (R12), tetrafluoroethane C₂H₂F₄ (R134a) and a mixture of 50% CH₂F₂ / 50% C₂HF₅ (R410A).

In the pure form these gases result not to be suitable for insulating purposes due to their too high liquefaction temperature in comparison with SF₆ or, in some cases like R12, R134a and R410A, their too high GWP in relation to the fixed target, therefore mixtures with some other buffer gases like CO₂, N₂, O₂ or dry air have been considered.

C₄F₇N has been analyzed in mixtures with CO₂ and N₂ showing in both cases great dielectric properties but with a practical preference for the first one due to its highest chemical stability.

C₅F₁₀O has been studied admixed with dry air, N₂, CO₂ / O₂ and N₂ / O₂ demonstrating always good insulating performances but unfortunately liquefaction concerns have to be taken into account due to the really high boiling point of the pure gas.

CF₃I has been considered in combination with CO₂ and N₂ resulting in worse dielectric properties than the first two gases, but nevertheless acceptable dielectric properties

in comparison with the reference SF₆ mixture.

R12 has been studied in mixtures with dry air and N₂ underlining great dielectric potential at high mixing ratios and a wide low temperature application range.

R134a too has been considered mixed with dry air and N₂ showing similar properties to R12 mixtures but slightly higher working temperatures and a lower GWP.

R410A instead has been analyzed in mixtures with dry air and CO₂ highlighting good dielectric properties, low GWP but most of all very low working temperatures.

For each gas and mixture many parameters have been observed, reworked with MATLAB software and reported, including physicochemical properties, GWP, ODP, atmospheric lifetime, toxicity, liquefaction temperature, AC, DC, lightning impulse dielectric strength and, where available, partial discharge inception voltage.

In addition, net ionization and rate coefficients have been obtained through BOLSIG+ software and used to complete the dielectric properties analysis.

Finally, a very simplified GIL sizing has been performed through COMSOL Multiphysics 5.4a software, simulating the electric field distribution along the geometry of the 3D GIL model and therefore determining the optimum absolute GIL dimensions in dependence on the specific insulating gas mixture adopted.

In conclusion, six different optimized gas mixtures have been proposed as potential eco-friendly substitutes of SF₆ in high-voltage Gas-Insulated Transmission Lines, with the indication of GIL absolute dimensions related to the adoption of that specific combination.

These mixtures, for a 420 kV rated voltage GIL, are:

- 4% C₄F₇N / 96% CO₂ (GWP=300) at 0.6 MPa with a 500 mm GIL outer diameter and a minimum working temperature of -30 °C (standard);
- 5% C₅F₁₀O / 95% CO₂ (GWP<1) at 0.6 MPa with a 810 mm GIL outer diameter and a minimum working temperature of -5 °C (specific applications);
- 30% CF₃I / 70% CO₂ (GWP=1) at 0.6 MPa with a 650 mm GIL outer diameter and a minimum working temperature of -7 °C (specific applications);
- 70% R12 / 30% air (GWP=2200) at 0.4 MPa with a 500 mm GIL outer diameter

and a minimum working temperature of $-45\text{ }^{\circ}\text{C}$ (suitable for cold zones);

- 80% R134 / 20% N_2 (GWP=1200) at 0.4 MPa with a 500 mm GIL outer diameter and a minimum working temperature of $-40\text{ }^{\circ}\text{C}$ (suitable for cold zones);
- 80% R410A / 20% CO_2 (GWP=1500) at 0.4 MPa with a 500 mm GIL outer diameter and a minimum working temperature of $-60\text{ }^{\circ}\text{C}$ (suitable for very cold zones).

This work is thought as a starting point for further investigations which might lead to experimental verifications of these proposals and then to the possibility of testing these gas mixtures on a real HV Gas-Insulated Transmission Line.

Bibliography

- [1] Koch, Hermann. *Gas-Insulated Transmission Lines (GIL)*. John Wiley & sons, 2011
- [2] Haddad, Amy and Haddad, Manu and Warne, DF and Warne, Doug. *Advances in high voltage engineering*. IET, 2004
- [3] Rycroft, Mike. "Gas-insulated transmission lines: the next generation of power transmission". *Energize*, 2015
- [4] Kuchler, Andreas. *High Voltage Engineering: Fundamentals-Technology-Applications*. Springer, Schweinfurt, 2017
- [5] Tognon, A. *AC Discharge Characteristics of Environmentally-Friendly Insulation Gases*. Master thesis, University of Padua, 2019
- [6] Tian, Shuangshuang and Zhang, Xiaoxing and Cressault, Yann and Hu, Juntao and Wang, Bo and Xiao, Song and Li, Yi and Kabbaj, Narjisse. "Research status of replacement gases for SF₆ in power industry". *AIP Advances*, 10(5), 2020, pp. 050702(1)-050702(34)
- [7] Camilli, G and Chapman, JJ. "Gaseous insulation for high-voltage apparatus". *Transactions of the American Institute of Electrical Engineers*, 66(1), 1947, pp. 1463-1470
- [8] Wang, Yong and Huang, Danqing and Liu, Jing and Zhang, Yaru and Zeng, Lian. "Alternative Environmentally Friendly Insulating Gases for SF₆". *Processes*, 7(4), 2019, pp. 216(1)-216(14)

- [9] Beroual, Abderrahmane and Haddad, Abderrahmane Manu. "Recent advances in the quest for a new insulation gas with a low impact on the environment to replace sulfur hexafluoride (SF_6) gas in high-voltage power network applications". *Energies*, 10(8), 2017, pp. 1216
- [10] Purohit, Pallav and Høglund-Isaksson, Lena. "Global emissions of fluorinated greenhouse gases until 2050: technical mitigation potentials and costs". *EGUGA*, 2016, pp. 4108
- [11] Grubb, Michael and Vrolijk, Christiaan and Brack, Duncan. *Routledge Revivals: Kyoto Protocol (1999): A Guide and Assessment*. Routledge, 2018
- [12] Mantilla, JD and Gariboldi, N and Grob, S and Claessens, M. "Investigation of the insulation performance of a new gas mixture with extremely low GWP". *2014 IEEE Electrical Insulation Conference (EIC)*, 2014, pp. 469-473
- [13] Yu, Xiaojuan and Hou, Hua and Wang, Baoshan. "Prediction on dielectric strength and boiling point of gaseous molecules for replacement of SF_6 ". *Journal of computational chemistry*, 38(10), 2017, pp. 721-729
- [14] Rokunohe, Toshiaki and Yagihashi, Yoshitaka and Endo, Fumihiko and Oomori, Takashi. "Fundamental insulation characteristics of air; N_2 , CO_2 , N_2 / O_2 , and SF_6 / N_2 mixed gases". *Electrical Engineering in Japan*, 155(3), 2006, pp. 9-17
- [15] Zhang, LC. "Study on insulation characteristics of $c-C_4F_8$ and its gas mixtures substituting SF_6 ". *Shanghai Jiao Tong University: Shanghai, China*, 2007
- [16] Koch, Myriam and Franck, CM. "High voltage insulation properties of $HFO1234ze$ ". *IEEE Transactions on Dielectrics and Electrical Insulation*, 22(6), 2015, pp. 3260-3268
- [17] Li, Yi and Zhang, Xiaoxing and Chen, Qi and Fu, Mingli and Zhuo, Ran and Xiao, Song and Chen, Dachang and Tang, Ju. "Study on the dielectric properties of C_4F_7N / N_2 mixture under highly non-uniform electric field". *IEEE Access*, 6, 2018, pp. 42868-42876

-
- [18] Kieffel, Yannick. "*Characteristics of g^3 - an alternative to SF_6* ". *2016 IEEE International Conference on Dielectrics (ICD)*, 2, 2016, pp. 880-884
- [19] Wang, Guoming and Kim, Woo-Hyun and Kil, Gyung-Suk and Kim, Sung-Wook and Jung, Jae-Ryong. "*Green gas for a grid as an eco-friendly alternative insulation gas to SF_6 : From the perspective of partial discharge under AC*". *Applied Sciences*, 9(4), 2019, pp. 651(1)-651(10)
- [20] Pan, Baofeng and Wang, Guoming and Shi, Huimin and Shen, Jiahua and Ji, Hong-Keun and Kil, Gyung-Suk. "*Green Gas for Grid as an Eco-Friendly Alternative Insulation Gas to SF_6 : A Review*". *Applied Sciences*, 10(7), 2020, pp. 2526(1)-2526(13)
- [21] Zhang, Xiaoxing and Li, Yi and Chen, Dachang and Xiao, Song and Tian, Shuangshuang and Tang, Ju and Zhuo, Ran. "*Reactive molecular dynamics study of the decomposition mechanism of the environmentally friendly insulating medium C_3F_7CN* ". *RSC advances*, 7(80), 2017, pp. 50663-50671
- [22] Li, Yi and Zhang, Xiaoxing and Chen, Qi and Zhang, Ji and Li, Yalong and Xiao, Song and Tang, Ju. "*Influence of oxygen on dielectric and decomposition properties of $C_4F_7N / N_2 / O_2$ mixture*". *IEEE Transactions on Dielectrics and Electrical Insulation*, 26(4), 2019, pp. 1279-1286
- [23] Nechmi, Housseem Eddine and Beroual, Abderrahmane and Girodet, Alain and Vinson, Paul. "*Fluoronitriles / CO_2 gas mixture as promising substitute to SF_6 for insulation in high voltage applications*". *IEEE Transactions on Dielectrics and Electrical Insulation*, 23(5), 2016, pp. 2587-2593
- [24] Zhang, Boya and Uzelac, Nenad and Cao, Yang. "*Fluoronitrile / CO_2 mixture as an eco-friendly alternative to SF_6 for medium voltage switchgears*". *IEEE Transactions on Dielectrics and Electrical Insulation*, 25(4), 2018, pp. 1340-1350
- [25] Wang, Cong and Cheng, Yi and Tu, Youping and Chen, Geng and Yuan, Zhikang and Xiao, Ang and Owens, John and Zhang, Agnes and Mi, Nathan.

- "Characteristics of C_3F_7CN / CO_2 as an alternative to SF_6 in HVDC-GIL systems". *IEEE Transactions on Dielectrics and Electrical Insulation*, 25(4), 2018, pp. 1351-1356
- [26] Wang, Guoming and Shen, Jiahua and Liu, Demao and Sung-Wook, Kim and Kil, Gyung-Suk. "Green gas for grid as an eco-friendly alternative insulation gas to SF_6 : from the perspective of PD initiated by metallic particles under DC". *Journal of Electrical Engineering*, 1(71), 2020, pp. 43-48
- [27] Sulbaek Andersen, Mads P and Kyte, Mildrid and Andersen, Simone Thirstrup and Nielsen, Claus J and Nielsen, Ole John. "Atmospheric Chemistry of $(CF_3)_2CFCN$: A Replacement Compound for the Most Potent Industrial Greenhouse Gas, SF_6 ". *Environmental science & technology*, 51(3), 2017, pp. 1321-1329
- [28] Zhang, Yue and Zhang, Xiaoxing and Li, Yi and Li, Yalong and Chen, Qi and Zhang, Guozhi and Xiao, Song and Tang, Ju. "AC breakdown and decomposition characteristics of environmental friendly gas $C_5F_{10}O / Air$ and $C_5F_{10}O / N_2$ ". *IEEE Access*, 7, 2019, pp. 73954-73960
- [29] Zhang, Yue and Zhang, Xiaoxing and Li, Yi and Li, Yalong and Chen, Qi and Zhang, Guozhi and Xiao, Song and Tang, Ju. "Effect of oxygen on power frequency breakdown voltage and decomposition characteristics of the $C_5F_{10}O/N_2 / O_2$ gas mixture". *RSC advances*, 9(33), 2019, pp. 18963-18970
- [30] Zhong, Linlin and Rong, Mingzhe and Wang, Xiaohua and Wu, Junhui and Han, Guiquan and Han, Guohui and Lu, Yanhui and Yang, Aijun and Wu, Yi. "Compositions, thermodynamic properties, and transport coefficients of high-temperature $C_5F_{10}O$ mixed with CO_2 and O_2 as substitutes for SF_6 to reduce global warming potential". *Aip Advances*, 7(7), 2017, pp. 075003
- [31] Kamarudin, MS and Chen, L and Widger, P and Elnaddab, KH and Albano, M and Griffiths, H and Haddad, A. " CF_3I gas and its mixtures: potential

- for electrical insulation". Proceedings of the CIGRE Session, 45, 2014, pp. 309(1)-309(9)*
- [32] Jamil, Mohamad Kamarol Mohd and Ohtsuka, Shinya and Hikita, Masayuki and Saitoh, Hitoshi and Sakaki, Masayuki. "Gas by-products of CF_3I under AC partial discharge". *Journal of Electrostatics*, 69(6), 2011, pp. 611-617
- [33] Zhang, Xiaoxing and Tian, Shuangshuang and Xiao, Song and Li, Yi and Deng, Zaitao and Tang, Ju. "Experimental studies on the power-frequency breakdown voltage of $CF_3I / N_2 / CO_2$ gas mixture". *Journal of Applied Physics*, 121(10), 2017, pp. 103303
- [34] Chen, Lujia and Griffiths, Huw and Haddad, Abderrahmane and Kamarudin, MS. "Breakdown of CF_3I gas and its mixtures under lightning impulse in coaxial-GIL geometry". *IEEE Transactions on Dielectrics and Electrical Insulation*, 23(4), 2016, pp. 1959-1967
- [35] Zhang, Xiaoxing and Tian, Shuangshuang and Xiao, Song and Li, Yi and Deng, Zaitao and Tang, Ju. "Experimental studies on the power-frequency breakdown voltage of $CF_3I / N_2 / CO_2$ gas mixture". *Journal of Applied Physics*, 121(10), 2017, pp. 103303
- [36] Kasuya, H and Katagiri, H and Kawamura, Y and Saruhashi, D and Nakamura, Y and Mizoguchi, H and Yanabu, S. "Measurement of decomposed gas density of CF_3I-CO_2 mixture". *Proceedings of the 16th International Symposium on High Voltage Engineering (ISH 2009), South African Inst. of Electrical Engineers, Cape Town, South Africa, 2009, pp. 24-28*
- [37] Xiao, Song. *Research on insulation performance of SF_6 substitute CF_3I / CO_2 under power frequency voltage and the influence of micro-moisture on CF_3I* . Ph.D. dissertation, University of Toulouse, 2016
- [38] Xiao, Song and Li, Yi and Zhang, Xiaoxing and Tang, Ju and Tian, Shuangshuang and Deng, Zaitao. "Formation mechanism of CF_3I discharge

- components and effect of oxygen on decomposition*". *Journal of Physics D: Applied Physics*, 50(15), 2017, pp. 155601
- [39] De Urquijo, J and Juárez, AM and Basurto, E and Hernández-Avila, JL. "Electron impact ionization and attachment, drift velocities and longitudinal diffusion in CF_3I and CF_3I-N_2 mixtures". *Journal of Physics D: Applied Physics*, 40(7), 2007, pp. 2205
- [40] Ullah, Rahmat and Rashid, Abdur and Rashid, Arooj and Khan, Faisal and Ali, Amjad. "Dielectric characteristic of dichlorodifluoromethane (R12) gas and mixture with N_2 / air as an alternative to SF_6 gas". *High voltage*, 2(3), 2017, pp. 205-210
- [41] Ullah, Rahmat and Ullah, Zahid and Haider, Aun and Amin, Salman and Khan, Faisal. "Dielectric properties of tetrafluoroethane (R134) gas and its mixtures with N_2 and air as a sustainable alternative to SF_6 in high voltage applications". *Electric Power Systems Research*, 163, 2018, pp. 532-537
- [42] Khan, Bakhtiar and Saleem, Jawad and Khan, Faisal and Faraz, Gul and Ahmad, Rizwan and Rehman, Naveed Ur and Ahmad, Zahoor. "Analysis of the dielectric properties of R410A Gas as an alternative to SF_6 for high-voltage applications". *High Voltage*, 4(1), 2019, pp. 41-48